

LARGE DEVIATIONS AND DYNAMICAL PHASE TRANSITIONS FOR QUANTUM MARKOV PROCESSES

MERLIJN VAN HORSSSEN, MMATH



The University of
Nottingham

THESIS SUBMITTED TO THE UNIVERSITY OF NOTTINGHAM
FOR THE DEGREE OF DOCTOR OF PHILOSOPHY

DECEMBER 2014

Do I dare
Disturb the universe?
In a minute there is time
For decisions and revisions which a minute will reverse.

— T.S. Eliot, *The Love Song of J. Alfred Prufrock*

In humble dedication to the loving memory of my mother, Els, and
my father, Jan.

ABSTRACT

Quantum Markov processes are widely used models of the dynamics open quantum systems, a fundamental topic in theoretical and mathematical physics with important applications in experimental realisations of quantum systems such as ultracold atomic gases and new quantum information technologies such as quantum metrology and quantum control. In this thesis we present a mathematical framework which effectively characterises dynamical phase transitions in quantum Markov processes, using the theory of large deviations, by combining insights developed in non-equilibrium dynamics with techniques from quantum information and probability.

We provide a natural decomposition for quantum Markov chains into phases, paving the way for the rigorous treatment of critical features of such systems such as phase transitions and phase purification (Ch. 4). A full characterisation of dynamical phase transitions beyond properties of the steady state is described in terms of a dynamical perspective through critical behaviour of the quantum jump trajectories (Ch. 5).

We extend a fundamental result from large deviations for classical Markov chains, the Sanov theorem, to a quantum setting; we prove this Sanov theorem for the output of quantum Markov chains Ch. 6, a result which could be extended to a quantum Donsker-Varadhan theory.

In Ch. 7 we perform an in-depth analysis of the atom maser, an infinite-dimensional quantum Markov process exhibiting various types of critical behaviour: for certain parameters it exhibits strong intermittency in the atom detection counts, and has a bistable stationary state. We show that the atom detection counts satisfy a large deviations principle, and therefore we deal with a phase cross-over rather than a genuine phase transition, although the latter occurs in the limit of infinite pumping rate. As a corollary, we obtain the Central Limit Theorem for the counting process.

Supervisor: Dr. Madalin Guta

Examiners: Dr. Ivette Fuentes

Dr. Fernando Brandao

PUBLICATIONS

Some ideas and figures have appeared previously in the following publications: [1, 2, 3]. An article based on Chs. 4 and 6 is currently in preparation.

So it goes.

— Kurt Vonnegut, *Slaughterhouse-Five*

ACKNOWLEDGMENTS

I am grateful to Madalin Guta, who has been my supervisor for the past four years; he has offered the patience and encouragement to help me find my own way in research.

The later years of my PhD involved an ongoing collaboration with Juan Garrahan and Igor Lesanovsky, and I would like to thank them for all the fruitful discussions.

This page would not be complete without acknowledging the friends I have made during the four years of my PhD. In particular, I would like to thank KS for keeping me sane and for introducing me to the amazing postgraduate theatre group.

I thank the wonderful SM, without whose patience, understanding and support writing this thesis would have seemed an insurmountable task.

Finally, words cannot express the gratitude I owe to my father, who regrettably passed away in April 2013. My arrival in the United Kingdom eight years ago, to study mathematics, would not have been possible without him.

Nottingham, December 2013

This thesis is typeset using the `classicthesis` package by A. Miede.
Figures use colours specified by `linspecer.m` by J.C. Lansey.

CONTENTS

List of Figures ix

I	BACKGROUND	1
1	INTRODUCTION	2
2	LARGE DEVIATIONS	4
2.1	Introduction	4
2.2	Large deviations: basic results	5
2.2.1	Cramér theorem	5
2.2.2	Sanov theorem for the empirical measure	7
2.2.3	Sanov theorem for the pair empirical measure	10
2.3	Large deviations principle: Gärtner-Ellis theorem	11
2.4	Rate functions and the classical Perron-Frobenius theorem	13
2.5	Large deviations for Markov processes	14
2.6	Large deviations and statistical mechanics	17
2.6.1	Curie-Weiss model: introduction	17
2.6.2	Curie-Weiss model: large deviations	18
2.7	Review of statistical mechanics of trajectories	20
3	QUANTUM MARKOV PROCESSES	23
3.1	Introduction	23
3.1.1	Notation and mathematical background	23
3.1.2	Completely positive maps and Kraus operators	24
3.2	Discrete time: quantum Markov chains	25
3.2.1	Schrödinger picture	26
3.2.2	Heisenberg picture	27
3.2.3	State of output chain	28
3.2.4	Quantum jump trajectories in discrete time	28
3.3	Continuous time: quantum Markov processes	29
3.3.1	Lindblad generator	29
3.3.2	Quantum dynamical semigroups	30
3.3.3	Dilation and QSDE	31
3.3.4	Counting in continuous time	34
3.4	s-ensembles and quantum dynamical phase transitions	36

3.5	Non-commutative Perron-Frobenius theory	40
3.6	The atom maser	42
3.6.1	Atom maser	43
3.6.2	The counting process	47
3.7	Review of large deviations in quantum systems	51
II	RESULTS	54
4	PHASE PURIFICATION	55
4.1	Introduction	55
4.2	Structure of discrete-time quantum Markov chains	55
4.2.1	Recurrent subspace	56
4.2.2	Structure	56
4.2.3	Dephasing and equivalences	57
4.2.4	Stationary states	59
4.2.5	Measurement and trajectories	60
4.2.6	Purification of phases	61
4.2.7	Large deviations and phase transitions	62
4.2.8	Phase transition as change in phase structure	64
4.3	Continuous-time phase structure	65
4.4	Examples	66
4.4.1	Example 1: intermittency and purification	66
4.4.2	Example 2: four-level system	68
4.4.3	Example 3: ‘symmetry breaking’ from perturbation: $XX0$ interaction	74
4.5	Conclusion	80
5	CHARACTERIZATION OF DYNAMICAL PHASE TRANSITIONS IN QUANTUM JUMP TRAJECTORIES	81
5.1	Introduction	81
5.2	Preliminaries and formalism	83
5.3	Three-level system	85
5.4	Other models	86
5.4.1	Dissipative Ising model	86
5.4.2	Dissipative quantum glass	87
5.4.3	Atom maser	87
5.5	Entanglement entropy	88
5.6	Conclusion	90
6	SANOV THEOREM FOR QUANTUM MARKOV CHAINS	91
6.1	Introduction	91

6.2	Background	92
6.3	Result	94
6.4	Conclusion	98
7	LARGE DEVIATIONS AND DYNAMICAL PHASE TRANSITIONS FOR THE ATOM MASER	99
7.1	Introduction	99
7.2	Main result	100
7.3	Details of proof	104
7.4	Dynamical phase transitions	109
7.5	Conclusion	113
8	CONCLUSION	115
8.1	Summary	115
8.2	Outlook	116
	BIBLIOGRAPHY	118

LIST OF FIGURES

Figure 2.1	Coin toss: typical trajectory (with sample mean converging to $1/2$) and rare trajectory	5
Figure 2.2	Coin toss rate function $I(z)$, $0 \leq z \leq 1$; note that $I(z)$ is convex and minimal at $\mathbb{E}(X) = 1/2$ (highlighted)	6
Figure 2.3	Curie-Weiss model: rate function $I_\beta(x)$ for various β including $\beta_c = 1$, showing multiple minima for $\beta > \beta_c$	19
Figure 2.4	Curie-Weiss model: ‘phase diagram’ of the rate function $I_\beta(x)$, with the minimal values (white line) showing the phase transition as a splitting at $\beta = \beta_c$	19
Figure 2.5	Rate function $I_\beta(x)$ (blue) and the rate function from the Gärtner-Ellis theorem (red), for $\beta = 1.2$. For $\beta > \beta_c$, I_β is non-convex and the Gärtner-Ellis theorem fails to give the correct rate function: it gives us the convex envelope of the actual rate function.	20
Figure 3.1	Diagram of a quantum Markov chain (see text)	26
Figure 3.2	Atoms enter a cavity, which is in contact with a thermal bath, in the excited state; the cavity state $ n\rangle$ gains energy from interaction with the atom	43
Figure 3.3	Mean photon number (black line) and photon number distribution (background) in the stationary state ρ_{ss} as function of $\alpha = \sqrt{N_{ex}}\phi$	46
Figure 3.4	The birth (blue) and death rates as functions of ϑ for different values of α . The intersection points correspond to minima and maxima of the stationary distribution.	48

- Figure 3.5 Rescaled potentials $U(n)/N_{\text{ex}}$ as function of n/N_{ex} , for various finite N_{ex} converge to a limit potential for $N_{\text{ex}} \rightarrow \infty$. For $\alpha < 1$ the potential is minimum at zero; for $1 < \alpha < 4.6$ it has a unique minimum away from $n = 0$; for $4.6 < \alpha < 7.8$ there are two local minima which become equal at $\alpha \approx 6.66$. 49
- Figure 3.6 Sample trajectories for cavity state (top) and output paths Λ_t (bottom) with $N_{\text{ex}} = 50$, corresponding to stationary state distribution (center) showing large variance at $\alpha \approx 1$ (red) and bistability at $\alpha \approx 6.66$ (green) 51
- Figure 3.7 Examples of quantum jump trajectories showing intermittency (taken from Sec. 4.4) 52
- Figure 4.1 Different rate functions for the phases (red and green) lead to the rate function for the combined system (blue) exhibiting a jump in the first derivative (cf. Fig. 4.7b below) 63
- Figure 4.2 Sample trajectories with the perturbed Kraus operators showing intermittency and no long-time purification 67
- Figure 4.3 Sample trajectories with the perturbed Kraus operators showing purification without intermittency 68
- Figure 4.4 Derivatives of the rate functions associated to the Kraus operators from Fig. 4.2 without purification (blue), and those from Fig. 4.3 with purification (red), showing that the rate function with purification is non-analytic at $s = 0$. 68
- Figure 4.5 Top four eigenvalues of master operator \mathcal{L} with $\Omega_1 = \Omega_2 = 1$. Note $\lambda_1 = 0$ is doubly degenerate for $\Lambda > 0$, and quadruply degenerate for $\Lambda = 0$. 69
- Figure 4.6 Activity $K(\Lambda, s)$ for equal $\Omega_1 = \Omega_2$, showing a smooth first derivative $K(\Lambda, s) = \partial_s \lambda(\Lambda, s)$ of the rate function 70

Figure 4.7	$K(\Lambda, s)$ for $\Omega_1 \neq \Omega_2$, showing a jump at $\Lambda = 0$; this is a dynamical phase transition in s , or a quantum phase transition in the limit $\Lambda \rightarrow 0$ 70
Figure 4.8	Top four eigenvalues of master operator \mathcal{L} with $\Omega_1 = 1, \Omega_2 = 2$. Note $\lambda_1 = 0$ is doubly degenerate only for $\Lambda = 0$. 71
Figure 4.9	Phase weight $\text{Tr}_1 \rho$ of representative trajectories (blue) near $\Lambda = 0$; fidelity F of moving average with the stationary phases $\rho_{ss,1}, \rho_{ss,2}$ (red and green) with $\Omega_1 = 1$ and $\Omega_1 = 1.15$. 73
Figure 4.10	Representative trajectories showing dramatic variation in behaviour. The critical points are $\omega = 0$ and $\omega = \pi/2$; other parameters as in Fig. 4.12. 74
Figure 4.11	Sample trajectory with events associated to different levels. 75
Figure 4.12	Sanov level 1 and 2 spectral radii and their derivatives for the XX0 model ($t = [t, -t]$ for level 1 and $t = [t, -t; -t, t]$ for level 2). Initial atom state angle $\pi/4$ and phase π . 76
Figure 4.13	Spectrum of transition operator (real and imaginary parts) showing 4-fold degeneracy at $\omega = 0$ and 2-fold degeneracy at $\omega = \pi$ 76
Figure 4.14	Expectations of Pauli operators σ_i in the 'XX ϵ ' model at $\omega = \pi$ critical point (note different scales) 77
Figure 4.15	Expectations of Pauli operators σ_i in the 'XX ϵ ' model at $\omega = 0$ critical point 78
Figure 4.16	Jump in the stationary state ρ_{ss} at $\omega = \pi$ with $J = [\omega, \omega - g, 0]$ 78
Figure 4.17	Expectation values of σ_y and σ_z with parametrisation $J = [\pi + \delta, \pi + \epsilon, 0]$ (change of coordinates from Fig. 4.16 (b).) 79
Figure 4.18	Expectation values of σ_y and σ_z along trajectories for varying ϵ in the δ, ϵ parametrisation 79
Figure 5.1	Three-level system 85
Figure 5.2	Sample jump trajectories 86
Figure 5.3	Atom maser, stationary properties 88

Figure 6.1	Derivatives of Sanov level 1 and 2 spectral radii for the XX0 model, see Fig. 4.12	98
Figure 7.1	$\lambda'(s)$ and the spectral gap $g(s)$ of L_s as functions of s and $\alpha = \phi/\sqrt{N_{\text{ex}}}$ (after Fig. 3 in [4]).	110
Figure 7.2	Phase boundaries at the $s = 0, \alpha \approx 6.66$ crossover with $N_{\text{ex}} = 75, 100$ and 125 .	111
Figure 7.3	Rescaled stationary state mean photon numbers, $\langle \rho_{\text{ss}} \rangle / N_{\text{ex}}$ for increasing N_{ex} , showing phase transition becomes sharp as $N_{\text{ex}} \rightarrow \infty$.	111
Figure 7.4	Spectrum of semigroup generator for $N_{\text{ex}} = 150$	112
Figure 7.5	Variance of stationary state (left) and variance of counting process (right), rescaled by factors of N_{ex}^{-1} and $N_{\text{ex}}^{-1.6}$, respectively	112

Part I

BACKGROUND

I thought of a labyrinth of labyrinths, of one sinuous
spreading labyrinth that would encompass the past and
the future and in some way involve the stars.

— Jorge Luis Borges, *The Garden of Forking Paths*

INTRODUCTION

This thesis is, in essence, about the connection between rare events and critical behaviour in quantum systems. The theory of large deviations is a probabilistic framework for establishing how unlikely rare events are. Intuitively speaking, if we flip a coin many times, it would be an unlikely event for it to come up heads each time. Indeed, if we imagine continuing this Sisyphean task ad infinitum, we would imagine it increasingly unlikely to only see the one side of the coin. Large deviations aims to answer the following question: with what rate does the probability of such unlikely events decay to zero? In Ch. 2 we will introduce the ideas and results of large deviations in detail.

The other main topic in this thesis is the identification of quantum phase transitions in a class of dynamical systems called quantum Markov processes; in Ch. 3 we will introduce quantum Markov processes in discrete and continuous time. The topics of large deviations and quantum phase transitions are connected through a shared language of statistical mechanics. In Sec. 2.6 and Sec. 2.7 we explain that large deviations is a natural way of looking at systems in classical statistical mechanics; meanwhile, in Sec. 3.4 and Sec. 3.7 we will see how the concept of quantum jump trajectories leads to a non-equilibrium statistical mechanics point of view in quantum systems.

These two background chapters make up the first part of the thesis; in the second part, consisting of Chs. 4 - 7, we will present our results. In Ch. 4 we show how a natural algebraic structure arises from a quantum Markov chain; we use this structure to obtain a decomposition into blocks, which we call *phases*. This allows us to rigorously define a type of phase transition, and we state and prove a result concerning purification towards such phases. We also explain how large deviations rate functions exhibit indications of phase transitions and phase purification. We look at several examples that illustrate these ideas.

In Ch. 5 we look at how phase transitions may be characterised, not only in terms of properties of the stationary state, but also through the behaviour of the trajectories. As will be shown in four examples, intermittency and jumps in the trajectories are typical of systems near critical points.

The shorter Ch. 6 contains a more technical result, which we refer to as the Sanov theorem for quantum Markov chains. This result extends a fundamental result in large deviations to the output of a quantum Markov chain. The ‘higher-level’ rate function associated with this result could serve as a more advanced indicator of phase transitions, in cases where the usual rate function is unable to uncover critical behaviour.

The final chapter, Ch. 7, is an in-depth study of a particular quantum Markov process, the atom maser. We discuss features of the stationary state and the trajectories that indicate possible critical behaviour and phase transitions. We show that a large deviations principle holds for the rate function associated to a counting process for the output of the atom maser; this means that a phase transition in one strict sense, failure of the rate function to be a smooth function, is only present in a limit of infinite pump rate.

LARGE DEVIATIONS

2.1 INTRODUCTION

We are studying the behaviour of quantum dynamical systems in the framework of large deviations. This is a wide-ranging topic in probability theory; in the book by den Hollander [5] we find a concise description:

Large deviation theory is a part of probability theory that deals with the description of events where a sum of random variables deviates from its mean by more than a “normal” amount, i.e., beyond what is described by the central limit theorem.

To get an idea of what is meant by large deviations, consider the following simple example. Suppose X_1, X_2, \dots is a sequence of real-valued i.i.d. (independent and identically distributed) random variables with distribution \mathbb{P} . Then the sequence S_1, S_2, \dots of partial sums $S_n = X_1 + \dots + X_n$ has its ‘normal’ behaviour described by the Strong Law of Large Numbers (SLLN) and the Central Limit Theorem (CLT.) These state, respectively, that

$$\frac{1}{n}S_n \rightarrow \mu \quad \text{almost surely w.r.t. } \mathbb{P}$$

and

$$\frac{1}{\sigma\sqrt{n}}(S_n - \mu n) \rightarrow Z \quad \text{in law w.r.t. } \mathbb{P}$$

where μ and σ are the mean and respective variance of \mathbb{P} and Z is a standard normal random variable. (Recall that a sequence of random variables X_n converges almost surely w.r.t. \mathbb{P} to X if

$$\mathbb{P}\left(\lim_{n \rightarrow \infty} X_n = X\right) = 1;$$

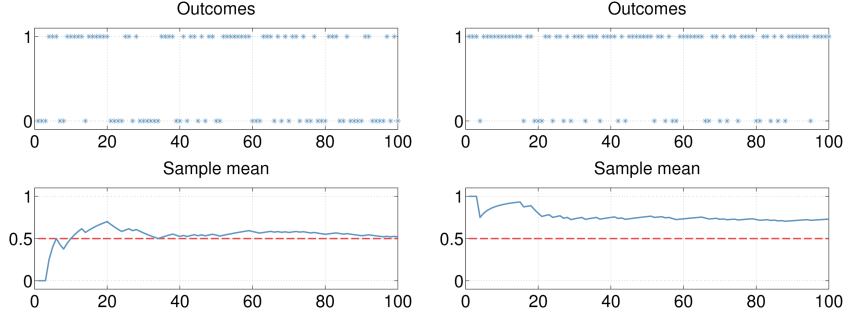


Figure 2.1: Coin toss: typical trajectory (with sample mean converging to $1/2$) and rare trajectory

X_n converges to X in law w.r.t. \mathbb{P} if the cumulative distribution functions of X_n converge to that of X . [6]) The SLLN tells us that the empirical average converges to μ , while the CLT gives us the probability that the empirical average differs from μ by an amount of order \sqrt{n} . Large deviations means asking about the probability of quantities, such as the empirical average, differing from their expected value by an amount of order n .

2.2 LARGE DEVIATIONS: BASIC RESULTS

Large deviations can be considered for any sequence of random variables. Exhaustive treatments of the classical theory of large deviations may be found in the books [7, 5, 8]. In the following section we review large deviations for independent and identically distributed (i.i.d.) random variables, and for Markov chains.

First we look at the important results for i.i.d. random variables: Cramér's theorem, which is a large deviations principle for the empirical mean, and the Sanov theorem, which looks at large deviations for the empirical measure.

2.2.1 Cramér theorem

At the most basic level we can consider large deviations for the sample means of a sequence of i.i.d. random variables; a large deviations statement in this case is a measure of how unlikely it is that we find a sample mean different from that predicted by the SLLN.

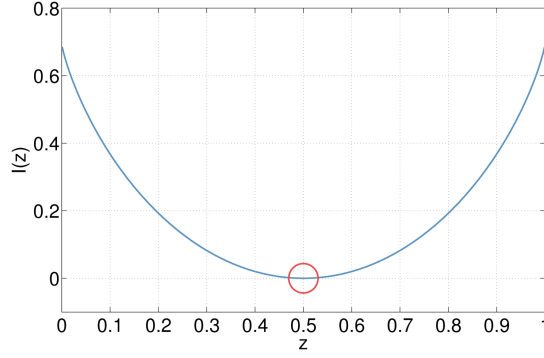


Figure 2.2: Coin toss rate function $I(z)$, $0 \leq z \leq 1$; note that $I(z)$ is convex and minimal at $\mathbb{E}(X) = 1/2$ (highlighted)

An intuitive understanding of the Cramér theorem may be gained by a simple example, namely a sequence of identical coin tosses (see Fig. 2.1). In this case, we have the i.i.d. random variables (X_i) with $\mathbb{P}(X_1 = 0) = \mathbb{P}(X_1 = 1) = \frac{1}{2}$. Setting $S_n = \sum_{i=1}^n X_i$ we get, for all $a > \frac{1}{2}$,

$$\lim_{n \rightarrow \infty} \frac{1}{n} \log \mathbb{P}(S_n \geq an) = -I(a)$$

where the rate function is given by

$$I(z) = \log 2 + z \log z + (1 - z) \log(1 - z) \quad (2.1)$$

if $z \in [0, 1]$ and ∞ otherwise.

Cramér's Theorem is about the large deviation behaviour of the *empirical average* $\frac{1}{n}S_n$.

Theorem 2.1 (Cramér's Theorem). Let (X_i) be i.i.d. \mathbb{R} -valued random variables satisfying

$$\varphi(t) = \mathbb{E}(e^{tX_1}) < \infty \quad \forall t \in \mathbb{R}.$$

Let $S_n = \sum_{i=1}^n X_i$. Then, for all $a > \mathbb{E}(X_1)$,

$$\lim_{n \rightarrow \infty} \frac{1}{n} \log \mathbb{P}(S_n \geq an) = -I(a),$$

where

$$I(z) = \sup_{t \in \mathbb{R}} [zt - \log \varphi(t)].$$

The proof of Cramér's Theorem consists of showing that the \limsup (\liminf) of $\frac{1}{n} \log \mathbb{P}(S_n \geq 0)$ is bounded above (below) by the quantity $\log \rho$, where $\rho = \inf_{t \in \mathbb{R}} \varphi(t)$. The \limsup bound follows from a result

called the exponential Chebyshev inequality, but the \liminf is more difficult. In particular, the lower bound is shown using a technique called the *Cramér transform* (or *Cramér tilting*); this is a change of probability measure, which effectively makes rare events become regular events. 2

The function $I(z)$ is called the *rate function* and it satisfies some nice properties; in particular, we have $I(z) \geq 0$ with equality if and only if $z = \mu$; $I''(\mu) = 1/\sigma^2$; and I is smooth and strictly convex (roughly speaking) whenever it is finite. Note that I is the *Legendre transform* of the logarithm of the *moment generating function* φ .

There are some technical points in the book [5] which allow us to loosen the hypothesis of the above theorem, but we skip these for now.

Finally, note that we can rewrite the result of Cramér's Theorem as

$$\lim_{n \rightarrow \infty} \frac{1}{n} \log \mathbb{P} \left(\frac{1}{n} S_n \in A \right) = - \inf_{z \in A} I(z)$$

where $A = [a, \infty)$, $a \geq \mu$. This paves the way for generalizations to other subsets A of \mathbb{R} , and besides leads to the following adage:

Any large deviation is done in the least unlikely of all the unlikely ways.

2.2.2 Sanov theorem for the empirical measure

The next step is to generalize Cramér's Theorem. The first way in which we will generalize that result is by looking at large deviations not just for the average of a sequence of i.i.d. random variables X_1, X_2, \dots , but for the frequency at which they take on certain values. We assume that X_1 takes on finitely many values in the set $\Gamma = \{1, \dots, r\}$; the distribution of X_1 is determined by

$$\mathbb{P}(X_1 = s) = \rho_s > 0$$

for all $s \in \Gamma$.

We define the *empirical measure* L_n^X associated to the process $X = (X_1, \dots, X_n)$ by

$$L_n^X = \frac{1}{n} \sum_{i=1}^n \delta_{X_i}$$

where, for $s \in \Gamma$, $\delta_{X_i}(s) = 1$ if $X_i = s$ and 0 otherwise. This is a probability measure on Γ : in particular, for $s \in \Gamma$,

$$L_n^X(s) = \frac{1}{n} \# \{i \in \{1, \dots, n\} : X_i = s\} \in [0, 1]$$

which is the empirical frequency of the event s . However, L_n^X is a *random* probability measure (in the literature referred to as a *point process*) since it depends on the random process (X_i) . Each realisation $x = (x_1, x_2, \dots, x_n) \in \Gamma^n$ defines (up to permutations) a probability measure $L_n^x \in L^1(\Gamma)$.

Note that the space of probability measures $L^1(\Gamma)$ is in one-to-one correspondence with the *probability simplex* $m_1(\Gamma)$ defined as

$$m_1(\Gamma) = \left\{ \nu = (\nu_1, \dots, \nu_r) \in [0, 1]^r : \sum_{s=1}^r \nu_s = 1 \right\};$$

in particular, to L_n is associated the element $(L_n(1), \dots, L_n(r)) \in m_1(\Gamma)$. This probability simplex can be given a topology from the *total variational distance*

$$d(\mu, \nu) = \frac{1}{2} \sum_{i=1}^r |\mu_s - \nu_s|$$

which allows us to consider convergence of L_n . Using the SLLN, we have that

$$\lim_{n \rightarrow \infty} d(L_n, \rho) = 0 \text{ } \mathbb{P} - \text{a.s.}$$

The CLT gives us, for each $s \in \Gamma$,

$$\lim_{n \rightarrow \infty} \frac{\sqrt{n}}{\sigma} (L_n(s) - \rho_s) \sim \mathcal{Z}(0, 1)$$

where

$$\sigma^2 = \text{Var}(\delta_{X_1}(s)) = \rho_s(1 - \rho_s).$$

So we are able to describe the ‘normal’ behaviour of S_n , but what about the large deviations behaviour? We know that the probability of L_n *not* converging to ρ goes to zero with n , but at what rate? This is what Sanov’s Theorem tells us: the probability of L_n staying outside of some ball around ρ .

Theorem 2.2 (Sanov’s Theorem for the empirical measure). Let (X_i) be i.i.d. random variables taking values in $\Gamma = \{1, \dots, r\}$ with probability $\mathbb{P}(X_1 = s) = \rho_s > 0$. Then, with L_n as above, for all $\alpha > 0$,

$$\lim_{n \rightarrow \infty} \frac{1}{n} \log \mathbb{P}(L_n \in B_\alpha^c(\rho)) = - \inf_{\nu \in B_\alpha^c(\rho)} I_\rho(\nu)$$

where $B_\alpha^c(\rho)$ is the open ball of radius α around ρ ,

$$B_\alpha^c(\rho) = \{\nu \in m_1(\Gamma) : d(\nu, \rho) < \alpha\},$$

and $I_\rho(\nu)$ is the *relative entropy* $H(\nu|\rho)$ of ν with respect to ρ ,

$$I_\rho(\nu) = \sum_{s=1}^r \nu_s \log \left(\frac{\nu_s}{\rho_s} \right).$$

2.2.2.1 Example: fair q -sided die

To illustrate Sanov's theorem for the empirical measure, consider the following example [9, Ex. 2.3]. In the first example we showed how the empirical mean of a sequence of fair coin tosses satisfies a large deviation principle; in this example we now consider repeated rolls of a fair q -sided die, and look at the large deviations mean of the *empirical measure*.

Suppose we roll a fair q -sided die n times and record the outcomes in a sequence $\omega = \omega_1, \dots, \omega_n$. Then we can use ω to work out the empirical measure for this process: denote by π_1, \dots, π_q how often each of the q possible outcomes $1, \dots, q$ appears in ω . Then the empirical measure is the vector $L^n(\omega) = (\pi_1, \dots, \pi_q)$. Intuitively, we expect that as $n \rightarrow \infty$, the empirical measure gets closer to the vector $\mu := (1/q, \dots, 1/q)$. The Sanov theorem for the empirical measure is a way of making this observation into a rigorous statement, using a large deviations principle for L^n .

For each $n \in \mathbb{N}$ the space of outcomes is $\Omega_n = \{1, 2, \dots, q\}^n$; for every $\omega \in \Omega_n$ we define for $i = 1, \dots, q$ the random variable

$$L_i^n(\omega) = \frac{1}{n} \sum_{j=1}^n \delta_{\omega_j}(i)$$

where $\delta_{\omega_j}(i)$ is 1 if $\omega_j = i$ and 0 otherwise. Then the empirical measure is given by $L^n(\omega) = (L_1^n(\omega), \dots, L_q^n(\omega))$. For any subset $A \subset \Omega_n$ define the probability

$$P_n(A) = \sum_{\omega \in A} \frac{1}{q^n}.$$

Then the law of large numbers states that $L^n - \mu \rightarrow \infty$ in law wrt. P_n as $n \rightarrow \infty$. The Sanov theorem gives us information about the large deviations behaviour of L^n , which means the rate of decay of the probability that L^n *stays away* from μ . To make this precise, [9, Thm. 2.4], for any subset $A \subset m_1(\Gamma)$ we have

$$\lim_{n \rightarrow \infty} \frac{1}{n} \log P_n(L^n \in A) = -\min_{\nu \in A} I(\nu|\mu)$$

where I denotes the relative entropy

$$I(\nu|\mu) = \sum_{i=1}^q \nu_i \log(\nu_i q).$$

2.2.3 Sanov theorem for the pair empirical measure

In order to study Markov chains, in which case the process X_1, X_2, \dots is generally not i.i.d., we now turn to *pair* empirical measures. With the process (X_i) as before, these are measures L_n^2 defined by

$$L_n^2 = \frac{1}{n} \sum_{i=1}^n \delta_{(X_i, X_{i+1})}$$

where $X_{n+1} = X_1$. Then for $(s, t) \in \Gamma \times \Gamma$ we have

$$L_n^2(s, t) = \frac{1}{n} \# \{i \in \{1, \dots, n\} : X_i = s, X_{i+1} = t\}$$

so $L_n^2(s, t)$ gives the empirical frequency of the subsequent events (s, t) . Then L_n^2 is a random probability measure on $\Gamma \times \Gamma$; in particular, it is an element of the set

$$\tilde{m}_1(\Gamma \times \Gamma) = \left\{ \nu = (\nu_{st}) \in m_1(\Gamma \times \Gamma) : \sum_t \nu_{st} = \sum_t \nu_{ts} \forall s \right\}$$

due to the periodic boundary condition. With the total variation distance from before

$$d(\mu, \nu) = \frac{1}{2} \sum_{s,t} |\mu_{st} - \nu_{st}|$$

we can use the SLLN to get

$$d(L_n^2, \rho \times \rho) \rightarrow 0 \text{ } \mathbb{P} - \text{a.s.}$$

For large deviations away from $\rho \times \rho$ we then have the following theorem.

Theorem 2.3 (Sanov's Theorem for the pair empirical measure). Let (X_i) be i.i.d. random variables as before, and L_n^2 as above. Then for all $\alpha > 0$,

$$\lim_{n \rightarrow \infty} \frac{1}{2} \log \mathbb{P}(L_n^2 \in B_\alpha^c(\rho \times \rho)) = - \inf_{\nu \in B_\alpha^c(\rho \times \rho)} I_\rho^2(\nu)$$

where the open ball B_α is

$$B_\alpha(\rho \times \rho) = \{\nu \in \tilde{m}_1(\Gamma \times \Gamma) : d(\nu, \rho \times \rho) \leq \alpha\}$$

and the rate function I_ρ^2 is

$$I_\rho^2(\nu) = \sum_{s,t} \nu_{st} \log \left(\frac{\nu_{st}}{\bar{\nu}_s \rho_t} \right)$$

where $\bar{\nu}_s = \sum_t \nu_{st}$.

We skip the proof; it is similar to the previous Sanov's Theorem, but more complicated due to the combinatorics involved. In Ch. 6 we will consider the Sanov theorem for the empirical measure, the pair empirical measure and the empirical measure for longer sequences for quantum Markov processes.

2.3 LARGE DEVIATIONS PRINCIPLE: GÄRTNER-ELLIS THEOREM

In this section we state an important result, the Gärtner-Ellis theorem; it is a generalisation of Cramér's theorem which no longer requires the sequence of random variables to be independent. The Gärtner-Ellis theorem gives a sufficient condition for the existence of a large deviations principle. Before we state the theorem, we introduce a rigorous definitions of the large deviations principle. Abstractly speaking, the large deviations principle characterises the limiting behaviour, as $n \rightarrow \infty$, of a family of probability measures $\{\mu_n\}$ on a topological space $(\mathcal{X}, \mathcal{B})$ in terms of a *rate function*.

Definition 2.1 (Rate function [8], p. 4). A (good) rate function I is a lower semicontinuous function $I : \mathcal{X} \rightarrow [0, \infty]$ (that is, for all $\alpha \in [0, \infty)$, the level set $\{x \in \mathcal{X} : I(x) \leq \alpha\}$ is a closed (compact) subset of \mathcal{X}). The domain of I is the set of points in \mathcal{X} for which the rate function I is finite.

The limiting behaviour of the probability measures $\{\mu_n\}$ is characterised in terms of asymptotic upper and lower bounds on the values that μ_n assigns to measurable subsets $\Gamma \in \mathcal{B}$.

Definition 2.2. (Large deviation principle [8, p. 5]). The sequence of probability measures $\{\mu_n\}$ satisfies a large deviation principle with a rate function I if, for all $\Gamma \in \mathcal{B}$,

$$-\inf_{x \in \Gamma^0} I(x) \leq \liminf_{n \rightarrow \infty} \frac{1}{n} \log \mu_n(\Gamma) \leq \limsup_{n \rightarrow \infty} \frac{1}{n} \log \mu_n(\Gamma) \leq -\inf_{x \in \bar{\Gamma}} I(x) \quad (2.2)$$

where Γ^0 and $\bar{\Gamma}$ denote the interior and closure of Γ , respectively.

The sentence “ μ_n satisfies the LDP” is used as shorthand for “ $\{\mu_n\}$ satisfies the large deviation principle with rate function I .” Loosely speaking, the above chain of inequalities may be summarised [10, p. 120] by the notation

$$\mu_n(dx) \approx e^{-nI(x)} dx \quad (2.3)$$

which is the informal idea behind the large deviation principle. We now state the Gärtner-Ellis theorem. Different versions of the theorem generally only differ by technicalities; we follow one of the main references to large deviations [8].

The Gärtner-Ellis theorem relies on technical details from convex analysis, which we will first introduce. Let Λ be a convex function on \mathbb{R}^d and let $\mathcal{D}_\Lambda = \{\lambda \in \mathbb{R}^d : \Lambda(\lambda) < \infty\}$. Then Λ is called *essentially smooth* [8, Df. 2.3.4] if the interior \mathcal{D}_Λ^0 is nonempty, Λ is differentiable on \mathcal{D}_Λ^0 , and Λ is *steep*: $|\nabla \Lambda(\lambda_n)| \rightarrow \infty$ for any sequence $(\lambda_n) \subset \mathcal{D}_\Lambda^0$ converging to a boundary point of \mathcal{D}_Λ^0 . The function Λ is called *lower semi-continuous* if for any $\alpha \geq 0$ the level set $\{x \in \mathbb{R}^d : \Lambda(x) \leq \alpha\}$ is a closed subset of \mathbb{R}^d . For example, any function which is differentiable on \mathbb{R}^d is lower-semicontinuous and essentially smooth.

Theorem 2.4 (Gärtner-Ellis theorem [8], pp. 44-55). Let (Z_n) be a sequence of random variables in \mathbb{R}^d with laws μ_n . Suppose that the logarithmic moment generating function

$$\Lambda(\lambda) = \lim_{n \rightarrow \infty} \frac{1}{n} \log \mathbb{E} \left[e^{\langle n\lambda, Z_n \rangle} \right], \quad \lambda \in \mathbb{R}^d \quad (2.4)$$

exists as an extended real number and is finite in a neighbourhood of the origin, and let Λ^* denote the Fenchel-Legendre transform of Λ , given by

$$\Lambda^*(x) = \sup_{\lambda \in \mathbb{R}^d} \{\langle \lambda, x \rangle - \Lambda(\lambda)\}. \quad (2.5)$$

If Λ is an essentially smooth, lower semicontinuous function then (Z_n) satisfies a LDP with good rate function Λ^* , that is, for any $F \in \mathcal{B}(\mathbb{R}^d)$,

$$-\inf_{x \in F^o} \Lambda^*(x) \leq \liminf_{n \rightarrow \infty} \frac{1}{n} \log \mu_n(F) \quad (2.6)$$

$$\leq \limsup_{n \rightarrow \infty} \frac{1}{n} \log \mu_n(F) \leq -\inf_{x \in \bar{F}} \Lambda^*(x). \quad (2.7)$$

Note that the original statement of the Gärtner-Ellis theorem formulates a weaker form of the LDP consisting of upper and lower bounds when the smoothness assumptions are dropped. This theorem contains Cramér's theorem as a special case, obtained by setting Z_n to be the sample mean $(X_1 + \dots + X_n)/n$ of a sequence (X_n) of i.i.d. random vectors with finite moment generating functions ([9, p. 115]). The function $\Lambda(\lambda)$ then equals $\log \mathbb{E} [e^{\langle t, X_1 \rangle}]$ with corresponding rate function Λ^* the same as in Cramér's theorem.

2.4 RATE FUNCTIONS AND THE CLASSICAL PERRON-FROBENIUS THEOREM

The Perron-Frobenius Theorem is an important step in proving any large deviations principle for classical processes, as the asymptotic behaviour of eigenvectors plays a key role in determining the existence of a rate function. Transition matrices, such as those characterising Markov chains, are *stochastic* matrices; that is, their elements are all non-negative and the rows sum to 1. For details on the concept of irreducibility for non-negative matrices we refer the reader to [11]; we briefly review the main definitions and theorems following [12] (Ch. 8).

A non-negative matrix X is called *irreducible* [8] if for all pairs of indices (i, j) there exists $n \in \mathbb{N}$ such that $[X^n]_{i,j} > 0$. The *spectral circle* of a matrix X consists of those eigenvalues λ of X satisfying $\lambda = \rho(X)$, where $\rho(X)$ is the *spectral radius* of X . The Perron-Frobenius theorem for such irreducible non-negative matrices considers the multiplicity of $\rho(X)$ and the positive eigenvectors of X .

The classical Perron-Frobenius theorem for irreducible (finite-dimensional) matrices says that the spectral radius is an eigenvalue with a positive eigenvector, and establishes invariance of the entire spectrum with respect to rotations of the complex plane.

Theorem 2.5 (Perron-Frobenius [13], p. 27-32). Let A be a positive irreducible matrix.

1. The spectral radius $r = r(A)$ is strictly positive, and r is a simple eigenvalue;
2. The matrix A has a strictly positive eigenvector x corresponding to r and any positive eigenvector of A is a multiple of x ;
3. If A has h eigenvalues of the same modulus, say

$$\lambda_0 = re^{i\theta_0}, \lambda_1 = re^{i\theta_1}, \dots, \lambda_{h-1} = re^{i\theta_{h-1}}, \quad (2.8)$$

$$0 = \theta_0 < \theta_1 < \dots < \theta_{h-1} < 2\pi \quad (2.9)$$

then these eigenvalues are simple and are the distinct roots of $\lambda^h - r^h = 0$;

4. The spectrum of A is invariant under a rotation of the complex plane by $2\pi/h$.

Note that this result does not exclude the possibility of finding other eigenvalues on the spectral circle. An irreducible non-negative matrix X is called *primitive* if it has only one eigenvalue on the spectral circle, namely the spectral radius itself. In other words, a matrix T is primitive if and only if it is irreducible and *aperiodic*.

An irreducible matrix which is not primitive has $h > 1$ eigenvalues on its spectral circle, and as such is *periodic* with period h . A result of Frobenius characterises primitive matrices, and can be used as a definition: a non-negative matrix X is called *primitive* if there exists $m \in \mathbb{N}$ such that $[X^m]_{i,j} > 0$ for all indices i, j .

In the following section, we will see how the Perron-Frobenius theorem plays a vital role in proving large deviation principles for non-i.i.d. stochastic processes.

2.5 LARGE DEVIATIONS FOR MARKOV PROCESSES

We noted in Sec. 2.3 that the Gärtner-Ellis theorem generalises Cramér's theorem to non-i.i.d. sequences of random variables. We will now see an application of the Gärtner-Ellis theorem by proving a large deviations principle for a class of non-i.i.d. processes, namely Markov chains. A sequence of random variables Y_1, Y_2, \dots taking values in a finite set Σ is called a *Markov chain* if, given the value of Y_m at some time m , for any $n > 0$ the probability distribution of Y_{m+n} is completely determined. In particular, the *transition probabilities*

$$\pi(i, j) = \mathbb{P}(Y_{m+1} = j | Y_m = i)$$

completely characterise the process; we denote by $\Pi = [\pi(i, j)]$ the *transition matrix* of the Markov process.

The Cramér theorem can be generalised to a Markov chain (Y_i) with transition matrix Π taking values in a finite set Σ . In order to define an empirical mean, we need to map the random variables Y_i to an additive space via a deterministic function $f : Y_i \mapsto X_i = f(Y_i) \in \mathbb{R}^d$. The empirical mean is then given by $S_n = \sum_{i=1}^n f(Y_i)$. In particular [8, p. 76], suppose we take f as an indicator function of the form $f(Y) = (1_1(Y), \dots, 1_{|\Sigma|}(Y))$. Then S_n is the empirical measure for the Markov chain, and we obtain the Sanov theorem for this measure by the following Cramér theorem.

It is also possible to use Cramér's theorem for Markov chains to prove an analogue of the Sanov theorem for the pair empirical measure. This is done by defining a new process Z_i consisting of the pairs $Z_i = (Y_i, Y_{i+1})$. This is itself a Markov chain, to which the Sanov theorem for the empirical measure can be applied; at the level of the process Y_i , this translates to the pair empirical measure (in this case, the rate function may be expressed as a relative entropy [8, p. 79]).

This is of particular interest for the results discussed in Ch. 6 where we state and prove a Sanov theorem (for the empirical measure, the pair empirical measure, and longer sequences of outcomes). Our proof also relies on the construction of a new process; in our case, this involves constructing a transition operator for a new quantum Markov process, on a larger space of outcomes. (In general, this approach of considering large deviation principles on all different levels, i.e. sample means, empirical measures (for the mean, pairs, etc.) and *empirical processes*, is referred to as *Donsker-Varadhan theory*.)

Note that *irreducibility* plays an important role in defining a large deviations principle for Markov chains; a reducible Markov chain may lead to non-analyticities in the LD rate function [14].

Theorem 2.6. (Cramér theorem for Markov chains [8, p. 74]). Let (Y_i) be a Markov chain, with finite state space Σ and irreducible transition matrix $\Pi = [\pi(i, j)]$. Define the empirical mean S_n in terms of a given deterministic function $f : \Sigma \rightarrow \mathbb{R}^d$ as

$$S_n = \frac{1}{n} \sum_{i=1}^n f(Y_i).$$

Denote by P_σ^π the probability measure associated to the Markov chain defined by

$$P_\sigma^\pi(y_1, \dots, y_n) = \pi(\sigma, 1) \pi(1, 2) \cdots \pi(n-1, n).$$

Then for any subset $\Gamma \subset \mathbb{R}^d$ and any initial state $\sigma \in \Sigma$,

$$\begin{aligned} - \inf_{z \in \Gamma^o} I(z) &\leq \liminf_{n \rightarrow \infty} \frac{1}{n} \log P_\sigma^\pi(S_n \in \Gamma) \\ &\leq \limsup_{n \rightarrow \infty} \frac{1}{n} \log P_\sigma^\pi(S_n \in \Gamma) \leq - \inf_{z \in \bar{\Gamma}} I(z) \end{aligned}$$

where the rate function I is given by the Legendre transform of the logarithm of the Perron-Frobenius eigenvalue of the deformed transition matrix Π_λ ,

$$I(z) = \sup_{\lambda \in \mathbb{R}^d} [\langle \lambda, z \rangle - \log \rho(\Pi_\lambda)]$$

where we define the deformed matrix elements

$$\pi_\lambda(i, j) = \pi(i, j)e^{\langle \lambda, f(j) \rangle}, \quad \lambda \in \mathbb{R}^d; \quad (2.10)$$

that is, S_n satisfies a large deviation principle with good rate function I .

Proof. The proof of this theorem relies on the Gärtner-Ellis theorem; since this way of proving that an LDP holds is quite general (in fact, it is how we approach our Sanov theorem in Ch. 6) we briefly sketch the proof. For $\lambda \in \mathbb{R}^d$ define the sequence of logarithmic moment generating functions

$$\Lambda_n(\lambda) = \log \mathbb{E} \left[e^{\langle \lambda, S_n \rangle} \right].$$

Then the limit (cf. Eq. 2.4)

$$\Lambda(\lambda) = \lim_{n \rightarrow \infty} \frac{1}{n} \Lambda_n(n\lambda)$$

satisfies the conditions of the Gärtner-Ellis theorem: in particular, Λ is finite and differentiable on \mathbb{R}^d . To see why, note that

$$\begin{aligned} \Lambda_n(n\lambda) &= \log \mathbb{E} \left[e^{\langle \lambda, \sum_{i=1}^n f(Y_i) \rangle} \right] \\ &= \log \sum_{y_1, \dots, y_n=1}^{|\Sigma|} \mathbb{P}_\sigma(Y_1 = y_1, \dots, Y_n = y_n) \prod_{k=1}^n e^{\langle \lambda, f(y_k) \rangle} \\ &= \log \sum_{y_n=1}^{|\Sigma|} \Pi_\lambda^n(\sigma, y_n) \end{aligned}$$

using the Markov property and the definition of π_λ in Eq. 2.10. Since Π_λ is irreducible and positive, the Perron-Frobenius theorem applies, and we conclude that the dominating term in Π_λ^n is the spectral radius $\rho(\Pi_\lambda)$, and

$$\Lambda(\lambda) = \log \rho(\Pi_\lambda).$$

Because $\rho(\Pi_\lambda)$ is a simple eigenvalue, we may conclude that it is positive, finite and differentiable, and so the large deviation principle follows. \square

As we will see in the next chapters, the perturbed transition operator obtained by rescaling its matrix elements plays a central role, both in classical and quantum applications of large deviations.

2.6 LARGE DEVIATIONS AND STATISTICAL MECHANICS

As we will explained below, the use of large deviations in quantum systems has its roots partially in statistical mechanics [9]. It is in this context that phase transitions are traditionally studied, and it is therefore instructive to take some time to consider the developments that lead to the formulation of quantum phase transitions. We suggest [15] for a reference on classical thermodynamics. The review article [9] offers a very good overview of large deviations and its connection to statistical mechanics; in this section we will only consider one example from this article.

We will look at the Curie-Weiss model, in which we consider the sample means (using Cramér's theorem) for the magnetisation. This model is a particular type of ferromagnetic model on a lattice, which is a larger class of spin systems including the Curie-Weiss-Potts model and the Ising model. *Dynamical phase transitions* arise from two competing microscopic effects: attractive forces of interaction, ordering the system (measured in *energy*), and thermal excitations, randomising the system (measured in *entropy*). In phase transitions at sufficiently low temperatures, energy effects predominate.

2.6.1 Curie-Weiss model: introduction

The Curie-Weiss model is a spin system defined on an increasing sequence of subsets of \mathbb{N} given by $\Lambda_n = \{1, 2, \dots, n\}$. The configuration space of this model is $\Omega_n = \{-1, 1\}^{\Lambda_n}$; a sequence $\omega \in \Omega_n$ represents the values of the *spin* at each of the n sites. We assign a probability 2^{-n} to each sequence, which extends to a probability measure P_n on Ω_n . We define a function $H_n : \Omega_n \rightarrow \mathbb{R}$ called the *Hamiltonian*, given by

$$H_n(\omega) = -\frac{n}{2} \left(\frac{1}{n} \sum_{i=1}^n \omega_i \right)^2.$$

The state of the system is described by a probability measure on the set $\{\Lambda_n : n \in \mathbb{N}\}$ called the *finite-volume Gibbs state*; this state is defined by a probability measure $P_{n,\beta}$ on each Λ_n , and is parametrised by the *inverse absolute temperature* $\beta > 0$. The probability measure $P_{n,\beta}$ is defined for $\omega \in \Omega_n$ as

$$P_{n,\beta}(\omega) = \frac{1}{Z_n(\beta)} \exp[-\beta H_n(\omega)] P_n(\omega)$$

where the normalisation factor $Z_n(\beta)$, called the *partition function*, is defined by

$$Z_n(\beta) = \int_{\Omega_n} \exp[-\beta H_n(\omega)] P_n(d\omega).$$

2.6.2 Curie-Weiss model: large deviations

Usually in statistical mechanics, large deviations are considered for a *macroscopic observable*: by this, we mean a sequence of random variables (Y_n) such that $Y_n/|\Lambda_n|$ has a limit as $n \rightarrow \infty$. In this example we consider the magnetisation, which is defined as the average spins per site S_n/n where

$$S_n = \sum_{i=1}^n \omega_i.$$

In particular, the sequence $\{P_{n,\beta}(S_n/n \in dx) : n \in \mathbb{N}\}$ satisfies a large deviation principle [9, Thm. 9.1] on \mathbb{R} with rate function

$$I_\beta(x) = I(x) - \frac{\beta}{2}x^2 - \inf_{y \in \mathbb{R}} \left\{ I(y) - \frac{\beta}{2}y^2 \right\}$$

shown in Fig. 2.3. Here I is the rate function for fair coin tossing (cf. Eq. 2.1) given by

$$I(x) = \frac{1-x}{2} \log(1-x) + \frac{1+x}{2} \log(1+x)$$

for $|x| \leq 1$ and ∞ otherwise. The rate function I_β reflects two competing effects: there is a thermal effect, randomisation, coming from the $I(x)$ term, while there is an ordering effect from the quadratic term.

Notice that the Hamiltonian is minimal when the system is in a configuration where all spins have the same sign (denoted by ω^+ and ω^-). The Gibbs state assigns larger probabilities to configurations where more sites agree in sign (which is why the Gibbs state models a *ferromagnet*.) For $\beta = 0$ the probability measure $P_{n,\beta}$ becomes the fair coin tossing measure discussed before; we know this satisfies a law of large numbers and a large deviations principle. On the other hand, as $\beta \rightarrow \infty$, the probability measure $P_{n,\beta}$ becomes the sum of two Dirac delta measures on the extremal configurations ω^+ and ω^- : as $n \rightarrow \infty$,

$$\lim_{\beta \rightarrow \infty} P_{n,\beta} = \frac{1}{2}(\delta_{\omega^+} + \delta_{\omega^-})$$

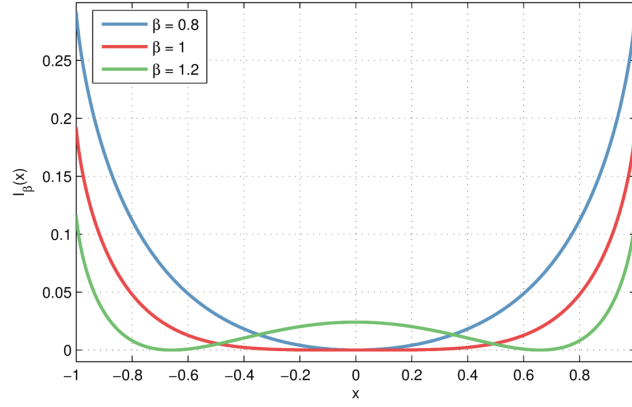


Figure 2.3: Curie-Weiss model: rate function $I_\beta(x)$ for various β including $\beta_c = 1$, showing multiple minima for $\beta > \beta_c$

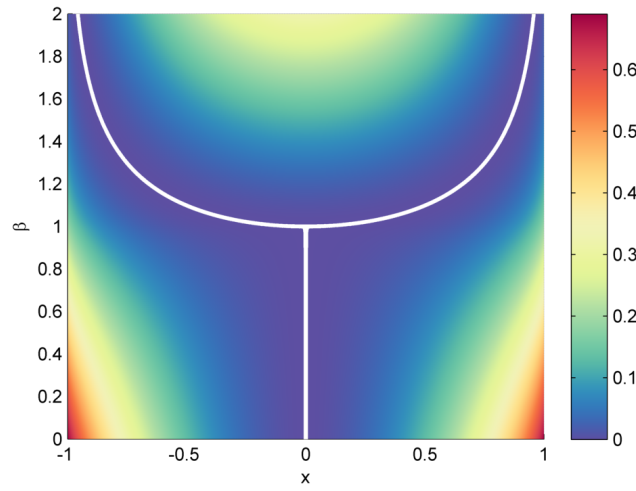


Figure 2.4: Curie-Weiss model: ‘phase diagram’ of the rate function $I_\beta(x)$, with the minimal values (white line) showing the phase transition as a splitting at $\beta = \beta_c$

for which the law of large numbers fails and the rate function becomes non-convex. We therefore expect there to be some critical temperature $\beta_c > 0$.

For $\beta \leq 1$ the rate function $I_\beta(x)$ attains its infimum 0 at the unique point $x = 0$, and I_β is strictly convex on the interval $[-1, 1]$. For $\beta > 1$ there is no longer a unique infimum: $I_\beta(x) = 0$ at some $m^+(\beta) \in (0, 1)$ and at $-m^+(\beta)$ and I_β is no longer convex (see Figs. 2.3 and 2.4)..

This behaviour at the critical inverse temperature $\beta_c = 1$ can be seen in a breakdown of the law of large numbers [9, Thm. 9.2]: if $\beta \leq 1$ we have the limit as $n \rightarrow \infty$

$$P_{n,\beta}(S_n/n \in dx) \rightarrow \delta_0$$

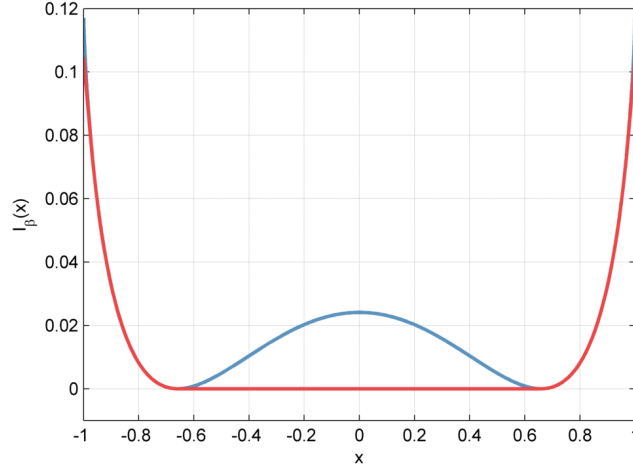


Figure 2.5: Rate function $I_\beta(x)$ (blue) and the rate function from the Gärtner-Ellis theorem (red), for $\beta = 1.2$. For $\beta > \beta_c$, I_β is non-convex and the Gärtner-Ellis theorem fails to give the correct rate function: it gives us the convex envelope of the actual rate function.

so a law of large numbers is valid; however, if $\beta > 1$ we have

$$P_{n,\beta}(S_n/n \in dx) \rightarrow \frac{1}{2} (\delta_{m^+(\beta)} + \delta_{-m^+(\beta)})$$

meaning the law of large numbers is no longer valid; this breaking down of the law of large numbers is called a *phase transition*. It is important to note that it is still possible (for example, in this case) for a large deviations principle to hold at such a phase transition; however, the Gärtner-Ellis theorem fails to give the correct rate function, as shown in Fig. 2.5. Using the Gärtner-Ellis theorem, by considering the non-analytic or non-convex behaviour of the rate function, to indicate phase transitions is something we will return to in Ch. 7.

2.7 REVIEW OF STATISTICAL MECHANICS OF TRAJECTORIES

Our treatment of large deviations in quantum systems is founded on a similar approach to large deviations in statistical mechanics, called the statistical mechanics (or thermodynamics) of trajectories. In this subsection we present a short literature review on the use of large deviations in statistical mechanics, focused on the development towards the formalism of thermodynamics of trajectories. The recent comprehensive review article [16] considers the connections between the theory of large deviations and equilibrium and non-equilibrium statist-

ical mechanics, including the ensembles of trajectories and phase transitions in non-equilibrium systems considered in this section.

Trajectories for a statistical mechanical model consist of realisations of the stochastic dynamics. For the Curie-Weiss model from the previous section, for example, one particular trajectory takes the form $\omega(t) = \omega_1(t), \omega_2(t), \dots$ of the spins on each site. The Curie-Weiss model features a phase transition at a critical point $\beta_C > 0$; at this point, trajectories show *intermittency* in time, coming from the competing order and disorder from the two phases. This is a feature of the thermodynamics of trajectories approach: phase transitions are indicated by intermittent behaviour of the trajectories.

The role played by large deviations in the thermodynamics of trajectories is the same, in spirit, as in the coin toss example at the beginning of this chapter: there, rare trajectories stayed away from the mean, and typical trajectories converge to the mean. Associating a probability measure to trajectories allows us to rigorously talk about ‘rare’ and ‘typical’ realisations. In particular, a large deviations parameter introduced as a field s which couples to one of the order parameters. Taking $s \neq 0$, the *master operator* of the dynamics then generates trajectories for which the rare realisations become typical [17].

The pair of articles [18, 19] play an important role in the development of the thermodynamics of trajectories formalism. The authors study the occurrence of phase transitions by considering ensembles of trajectories in the framework of large deviations: this is done by defining a large deviations rate function which encodes information about fluctuations around *typical* trajectories. The rate function depends on some order parameter s ; singularities near $s = 0$ correspond to transitions between phases of distinct *dynamical activity*. This rate function is obtained as the largest real eigenvalue of the superoperator associated to the Markov dynamics. (See also [20, 21] for a treatment of phase transitions between regions of differing dynamical activities.)

The influential article [22] introduces Ruelle’s thermodynamic formalism: here the large deviations rate function is identified as largest real eigenvalue of the master superoperator (sometimes referred to as the Lebowitz-Spohn operator [23]). Degeneracies in the largest real eigenvalue are shown to imply the existence of metastable phases in [24], an important relationship, which plays a role in our results.

A particular class of models in which the thermodynamics of trajectories approach has been applied successfully are kinetically constrained models [25] of slowly relaxing systems called *glasses* [26]. Again, trajectories are classified according to their dynamical activity [27] and phase transitions, called *glassy transitions* [28, 29, 30], are shown to occur. In terms of *trajectories*, coexistence of the phases is shown by the existence of large “bubbles” of low activity in the space-time trajectory. A probability density may be defined for the occurrence of such bubbles; larger (*mesoscopic*) bubbles are rare and dominate the non-Gaussian (exponential tail) of the “magnetisation” (or activity) distribution [31, 32]. This non-traditional phase transition is characterised in [33, 34] using a field s that couples to the activity.

In Ch. 5 we will consider quantum analogues of statistical mechanical models, and see how phase transitions appear in their trajectories.

QUANTUM MARKOV PROCESSES

3.1 INTRODUCTION

In this chapter we first introduce the necessary background to quantum Markov processes, in discrete time and in continuous time. We briefly review existing prior work on the use of large deviations in quantum systems and outline the framework of thermodynamics of quantum trajectories.

Real quantum systems are "open" in the sense that they interact with their environment, which leads to an irreversible loss of coherence and to energy dissipation. In many cases, the dynamics can be well described by the Markov approximation in which the environment possesses no memory and interacts weakly with the system. The joint unitary evolution of the system and environment can be described through the input-output formalism [35] using quantum stochastic calculus [36]. In this framework, the Markov semigroup can be seen as the average of a stochastic quantum trajectories arising from continuous-time measurements performed in the environment. Since in many experiments the system is not directly accessible, its (conditional) evolution is inferred from the detection trajectories via stochastic Schrödinger (or filtering) equations [37, 38]. In the next two sections we will introduce quantum Markov processes in discrete and continuous time; in part this follows the treatment of this topic found in [39].

3.1.1 *Notation and mathematical background*

We briefly review some mathematical background used in the description of quantum systems; we refer the reader to e.g. [40] for a complete introduction. Pure states of a quantum system are unit vectors in some

Hilbert space \mathfrak{h} (i.e. a complete inner product space \mathfrak{h}), and observables are self-adjoint operators acting on \mathfrak{h} . If \mathfrak{h} is finite-dimensional, $\mathfrak{h} \equiv \mathbb{C}^d$, say, the set of all linear combinations of observables on \mathfrak{h} is equivalent to the space M_d of complex $d \times d$ matrices; we refer to M_d as the algebra of observables associated to the quantum system. (In this context, an algebra is simply a vector space on which multiplication is defined.)

If \mathfrak{h} is infinite-dimensional, the algebra of observables associated to the system is given by the set $\mathcal{B}(\mathfrak{h})$ of all bounded operators on \mathfrak{h} . In the finite-dimensional case, $\mathcal{B}(\mathbb{C}^d)$ coincides with the matrix algebra M_d . (For later reference, we note that the algebra $\mathcal{B}(\mathfrak{h})$ is a C^* -algebra, and specifically, a von Neumann algebra.)

If the quantum system is in a pure state $\psi \in \mathfrak{h}$ we compute expectation values of observables $X \in \mathcal{B}(\mathfrak{h})$ as the inner product $\langle \psi, X\psi \rangle$. More generally, a state on $\mathcal{B}(\mathfrak{h})$ is defined by a positive[†] operator $\rho \in \mathcal{B}(\mathfrak{h})$ with unit trace, called a density operator; any such density operator ρ may be expressed as a convex linear combination of pure states by writing $\rho = \sum_i p_i |\psi\rangle\langle\psi|$. Such a state is called a mixed state, and expectation values of $X \in \mathcal{B}(\mathfrak{h})$ are computed as the trace $\text{Tr}[\rho X]$.

3.1.2 Completely positive maps and Kraus operators

In the following sections we will consider time evolution of quantum systems. If the time evolution is a reversible change of the state of the system (that is, there is an operation which takes us back to the original state) it is described by a unitary operator $U \in \mathcal{B}(\mathfrak{h})$ (i.e. $U^*U = UU^* = \mathbf{1}_{\mathfrak{h}}$) defining a change to the state $\rho \mapsto U\rho U^*$. (We note that this is a description of the change in the Schrödinger picture, describing the way states change; dual to this is the Heisenberg picture, in which states are fixed and observables change.) More generally, irreversible changes to a quantum system are described by completely positive maps, which are the most general description of any change, dynamical or otherwise, to a quantum system.

A map T on an operator algebra $\mathcal{B}(\mathfrak{h})$ is called *positive* if it leaves invariant the set of all positive elements in $\mathcal{B}(\mathfrak{h})$; T is called *completely positive* if

$$T \otimes \text{Id} : \mathcal{B}(\mathfrak{h}) \otimes M_n \rightarrow \mathcal{B}(\mathfrak{h}) \otimes M_n$$

[†] An operator $X \in \mathcal{B}(\mathfrak{h})$ is called positive, denoted $X \geq 0$, if $\langle X\psi, \psi \rangle \geq 0$ for all $\psi \in \mathfrak{h}$.

is a positive map for all $n \in \mathbb{N}$. In the section on Perron-Frobenius theory below we will discuss more notions of positivity.

Completely positive maps satisfy an abstract result called the Stinespring representation theorem [41], from which we obtain the following *Kraus form*. T is a completely positive map on a finite-dimensional algebra $\mathcal{B}(\mathfrak{h})$ if and only if there exists a family of *Kraus operators* V_1, \dots, V_k in $\mathcal{B}(\mathfrak{h})$ such that, in the Heisenberg picture,

$$T(X) = \sum_{i=1}^k V_i^* X V_i \quad (3.1)$$

for all $X \in \mathcal{B}(\mathfrak{h})$; T is identity preserving if and only if $\sum_{i=1}^k V_i^* V_i = \mathbf{1}$ (and in this case, T is also referred to as a channel). Clearly the dual (Schrödinger picture) map T_* satisfies

$$T_*(\rho) = \sum_{i=1}^k V_i \rho V_i^*$$

for all density operators $\rho \in \mathcal{B}(\mathfrak{h})$.

3.2 DISCRETE TIME: QUANTUM MARKOV CHAINS

We first consider quantum Markov processes in discrete time; in this case, we refer to them as quantum Markov chains. Intuitively speaking, a quantum Markov chain is a family of states $(\rho(0), \rho(1), \rho(2), \dots)$ where each state at time t , $\rho(t)$, is obtained from the state at the preceding time $t - 1$ by some transition operator T_* ,

$$\rho(t) = T_*(\rho(t - 1)).$$

Note that this is analogous to a classical Markov chain, where the probability distribution (state) at a time t is obtained by applying the transfer matrix to the state at the previous time $t - 1$. Replacing the probability distribution by a density matrix, and the transfer matrix by a completely positive trace-preserving map called the transition operator, we arrive at a *quantum* Markov chain.

A quantum Markov chain is constructed as the state of a system which repeatedly interacts with identical copies of an auxiliary system (sometimes referred to as the environment). The *Markov approximation*, which lets us conclude that at any given time t , the state of the system only depends on the state at the previous time $t - 1$, limits our choice for stating how the system interacts with each auxiliary system.

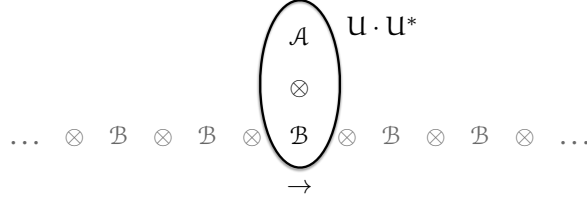


Figure 3.1: Diagram of a quantum Markov chain (see text)

3.2.1 Schrödinger picture

Suppose the system is described by an algebra \mathcal{A} and each auxiliary system is described by an algebra \mathcal{B} . Note that \mathcal{A} and \mathcal{B} can be regarded as algebras of bounded operators on some Hilbert spaces $\mathfrak{h}_{\mathcal{A}}$ and $\mathfrak{h}_{\mathcal{B}}$, respectively.

Let the initial state of \mathcal{A} be $\rho(0)$, and (as the auxiliary systems are identically prepared) let the initial state of each \mathcal{B} be a mixed state represented by a density matrix φ . We consider what happens during a single time step of this quantum Markov chain; that is, we will obtain an expression for $\rho(1)$ in terms of a transition operator applied to $\rho(0)$. First, the chain of auxiliary systems moves one place to the right, and the current copy of \mathcal{B} couples to \mathcal{A} (see Fig. 3.1).

This means we have a joint system $\mathcal{A} \otimes \mathcal{B}$ whose state is $\rho(0) \otimes \varphi$. Next, the coupled systems interact: since we are considering only the closed system $\mathcal{A} \otimes \mathcal{B}$ this interaction is described by some unitary operator $U \in \mathcal{A} \otimes \mathcal{B}$, and the joint state after this interaction is $U \rho(0) \otimes \varphi U^*$. Finally, the auxiliary system decouples: the resulting state of the system is $\rho(1)$, and is given by the partial trace over the auxiliary system:

$$\rho(1) = \text{Tr}_{\mathcal{B}} (U \rho(0) \otimes \varphi U^*).$$

Note that in the above equation each of the above steps is clearly reflected: coupling with the auxiliary system, unitary evolution, partial trace. Moreover, the composition of these three operations is itself a completely positive trace preserving map $T_* : \mathcal{A} \rightarrow \mathcal{A}$, referred to as the Schrödinger picture transition operator. This one time-step can be applied to the state at any time, and we arrive at the desired relation

$$\rho(n+1) = T_*(\rho(n)) \tag{3.2}$$

$$= \text{Tr}_{\mathcal{B}} (U \rho(n) \otimes \varphi U^*). \tag{3.3}$$

It is clear that the transition operator T_* , and therefore the quantum Markov chain, is completely specified by a unitary operator, U , and the initial state for the auxiliary system, φ ; that is,

$$T_*(\rho) = \text{Tr}_{\mathcal{B}} (U \rho \otimes \varphi U^*). \quad (3.4)$$

The *Markov property* means that repeated applications of the map T can be represented as powers of T_* . For example, we compute the state $\rho(n+2)$ by tracing over \mathcal{B} one at a time as

$$\begin{aligned} \rho(n+2) &= \text{Tr}_{\mathcal{B} \otimes \mathcal{B}} (U_2 (U_1 \rho(n) \otimes \varphi U_1^*) \otimes \varphi U_2^*) \\ &= \text{Tr}_{\mathcal{B}} (U_2 T_*(\rho(n)) \otimes \varphi U_2^*) \\ &= T_*^2(\rho(n)), \end{aligned}$$

and in general, $\rho(n+m) = T_*^m(\rho(n))$.

3.2.2 Heisenberg picture

In the Heisenberg picture the transition operator is denoted by T ; this linear map is composed of the maps dual to the maps that make up T_* . The maps T_* and T satisfy the duality relation

$$\text{Tr} [X T_*(\rho)] = \text{Tr} [T(X) \rho]$$

for all $X \in \mathcal{A}$ and all density operators $\rho \in \mathcal{A}_*$. This allows us to derive an explicit form for T ,

$$\begin{aligned} \text{Tr} [T(X) \rho] &= \text{Tr}_{\mathcal{A}} [X \text{Tr}_{\mathcal{B}} (U \rho \otimes \varphi U^*)] \\ &= \text{Tr}_{\mathcal{A}, \mathcal{B}} [U^* X \otimes \mathbf{1} U \rho \otimes \varphi] \\ &= \text{Tr}_{\mathcal{A}} [P_{\varphi} (U^* X \otimes \mathbf{1} U) \rho] \end{aligned}$$

where P_{φ} is a *conditional expectation* [41]. This means that P_{φ} is a map $\mathcal{A} \otimes \mathcal{B} \rightarrow \mathcal{A}$ such that for any $Z \in \mathcal{A} \otimes \mathcal{B}$,

$$\text{Tr}_{\mathcal{A}} [P(Z) \rho] = \text{Tr}_{\mathcal{A}, \mathcal{B}} [Z \rho \otimes \varphi];$$

in other words, it is a map dual to the map $\rho \mapsto \rho \otimes \varphi$. In conclusion, this allows us to write the Heisenberg picture transition operator T as

$$T(X) = P_{\varphi} (U^* X \otimes \mathbf{1} U). \quad (3.5)$$

3.2.3 State of output chain

Although we will go in more detail when we prove results in the following chapters, we will briefly make some helpful observations now.

Since any finite-dimensional algebras \mathcal{A} are composed of matrix algebras, we can find a concrete expression for the Kraus operators. Let the system algebra be M_d and suppose that each auxiliary algebra is isomorphic to M_k , and for simplicity assume that the initial state for each auxiliary system is a pure state $|\varphi\rangle \in \mathbb{C}^k$. If the system is also in a pure state, say $|\psi\rangle$, we can write the action of U on the joint state $|\psi\rangle \otimes |\varphi\rangle$ as

$$U(|\psi\rangle \otimes |\varphi\rangle) = \sum_{i=1}^k V_i |\psi\rangle \otimes |b_i\rangle.$$

Here $\{|b_i\rangle\}$ is a basis for \mathbb{C}^k , associated to which is the set of Kraus operators $\{V_i\} \subset M_d$, which are obtained from U as $V_i = \langle b_i|U|\varphi\rangle$. In this thesis we are interested in the output of such quantum Markov chains; especially in Ch. 6 where we consider the statistics of the output from a large deviations point of view. With this in mind, the basis $\{|b_i\rangle\}$ is usually chosen as a basis of eigenvectors of some observable on the output sites.

Suppose we keep the assumption from above that the initial states for the system and environment are pure. The product structure, due to the Markov property, is clear in the total state after n steps, which is the state given by

$$\sum_{i_1, \dots, i_n=1}^k V_{i_n} \cdots V_{i_1} |\psi\rangle \otimes |b_{i_1}, \dots, b_{i_n}\rangle. \quad (3.6)$$

If we measure the state of the system and find the state $|\psi_F\rangle$, say, then the resulting state on the output chain is the (unnormalised) matrix product state (MPS)

$$\sum_{i_1, \dots, i_n=1}^k \langle \psi_F | V_{i_n} \cdots V_{i_1} | \psi \rangle |b_{i_1}, \dots, b_{i_n}\rangle;$$

we will return to this idea in Sec. 5.2.

3.2.4 Quantum jump trajectories in discrete time

Suppose we have an output chain of length n and measure the same observable X simultaneously on each site; if we obtain the outcomes

$X^{(1)} = i_1, \dots, X^{(n)} = i_n$ then the state on the output chain will be $|b_{i_1}, \dots, b_{i_n}\rangle$. If we consider the state of the system conditioned on these outcomes, we obtain a *realisation* of the quantum Markov chain. This means that the unnormalised state of the system has followed the evolution

$$|\psi\rangle \mapsto V_{i_n} \cdots V_{i_1} |\psi\rangle;$$

we refer to this as the *quantum jump trajectory* associated to the quantum Markov chain (also referred to as an *unravelling* of the system state). It is our knowledge of the state of the system after n steps, given that measuring the output chain resulted in the values i_1, \dots, i_n .

If the initial state of the system is not a pure state, the unravelling of the dynamics takes the following form. To each of the k Kraus operators V_i we may associate a *jump operator* T_i such that

$$T_{*,i}(\rho) = V_i \rho V_i^*.$$

Then the unravelling of the transition operator is given by

$$T_*(\rho) = \sum_{i=1}^k T_{*,i}(\rho) \quad (3.7)$$

and the conditional state of the system, after having measured the outcomes $\omega = (\lambda_{i_1}, \dots, \lambda_{i_n})$ on the output chain, is given by

$$\rho_n(\omega) = Z^{-1} T_{i_n,*} \circ \cdots \circ T_{i_1,*}(\rho) \quad (3.8)$$

where Z is a normalisation factor.

3.3 CONTINUOUS TIME: QUANTUM MARKOV PROCESSES

The quantum Markov chain, as introduced in the previous section, is a discrete time process; as a result, it is easily described in terms of a repeated interaction scheme. If we move to continuous time it becomes less straightforward to find such an interpretation; however, the continuous time approach is far more general.

3.3.1 Lindblad generator

In the discrete time case we were able to work directly with a transition operator T (or T_*); in the case of continuous time, the most useful

description is the *quantum master equation*, which describes the time evolution of the state $\rho(t)$ as a differential equation

$$\frac{d\rho}{dt} = \mathcal{L}(\rho)$$

where \mathcal{L} is the *generator* of the continuous time dynamics. In particular, \mathcal{L} is the generator of a *quantum dynamical semigroup* $\{T_t\}_{t \geq 0}$ of transition operators: for all $t, s \geq 0$ we have

$$\rho(t+s) = T_t(\rho(s)).$$

As before, we denote the system algebra by \mathcal{A} . If \mathcal{A} is finite dimensional, any generator \mathcal{L} of a quantum dynamical semigroup on \mathcal{A} has a Lindblad (or GKSL) form [42, 43]

$$\mathcal{L}(\rho) = -i[H, \rho] + \sum_{i=1}^k \left(L_i \rho L_i^* - \frac{1}{2}(L_i^* L_i \rho + \rho L_i^* L_i) \right). \quad (3.9)$$

Here H is the Hamiltonian describing a free evolution of the system, while the jump operators L_i are associated to the possible ways the system can interact with the environment. In particular, if the system is closed, the master equation simply describes a unitary evolution.

3.3.2 Quantum dynamical semigroups

The Heisenberg picture Lindblad operator \mathcal{L} is the generator of a strongly continuous semigroup on $\mathcal{B}(\mathfrak{h})$ (cf. [44] for an introduction to the general theory.) This means that there exists a family $(\mathcal{T}(t))_{t \geq 0}$ of maps on $\mathcal{B}(\mathfrak{h})$ which satisfy the *semigroup property*

$$\begin{aligned} \mathcal{T}(t)\mathcal{T}(s) &= \mathcal{T}(t+s) \quad \text{for all } t, s \geq 0, \\ \mathcal{T}(0) &= I, \end{aligned}$$

such that $t \mapsto \mathcal{T}(t)(X)$ is norm continuous for all $X \in \mathcal{B}(\mathfrak{h})$. Moreover, $\mathcal{T}(t)$ is completely positive and unit preserving for all $t \geq 0$. In general, the Lindblad form in Eq. (3.9) is not valid when \mathfrak{h} is infinite-dimensional; the generator \mathcal{L} can be recovered by

$$\mathcal{L}(X) = \lim_{h \downarrow 0} \frac{1}{h} (\mathcal{T}(h)(X) - X),$$

for all X in the domain of \mathcal{L} . Although no simple expression exists for the operators $\mathcal{T}(t)$ in terms of the generator \mathcal{L} , it is helpful to think of $\mathcal{T}(t)$ as the exponential of the generator

$$\mathcal{T}(t)(X) = e^{t\mathcal{L}}(X), \quad (3.10)$$

especially from the point of view of relating spectral properties of \mathcal{L} to those of $\mathcal{T}(t)$, e.g. *spectral mapping theorems*. Eq. (3.10) is valid for finite-dimensional systems; for infinite-dimensional systems, it is more complicated. By definition, Eq. (3.10) does hold for analytic vectors of \mathcal{L} which form a core of its domain (for details, see proof of Lemma 7.1).

3.3.3 Dilation and QSDE

In the discrete time case we were able to write the transition operator as the composition of coupling to the environment, unitary evolution, and tracing out the environment (Eq. 3.2). We will now show how the continuous time case affords a very similar interpretation, which also allows us to sketch how the master equation is derived. As before, we couple the system to an auxiliary algebra, called the environment; the joint state is $\rho(0) \otimes \varphi$. We then apply a unitary operator, and trace out the environment (which is assumed to be in a vacuum state) to obtain the state of the system at some later time: for any $t \geq 0$,

$$\rho(t) = T_t(\rho(0)) \quad (3.11)$$

$$= \text{Tr}_{\text{env}}(U(t) \rho(0) \otimes \varphi U(t)^*). \quad (3.12)$$

The difference between the unitary operator defined in Eq. 3.2 and the continuous-time case here, is that we now have a continuous family of stochastic unitary operators $\{U(t)\}_{t \geq 0}$, whereas before we had a single fixed unitary generating the dynamics. In the discrete time setting, the unitary operator is generally defined by a Hamiltonian describing the interaction between the system and each copy of the environment. In the continuous time case, the unitary operator is found as a solution to a quantum stochastic differential equation (or *QSDE*), see [45, 46, 47]. This equation takes the form

$$dU(t) = \sum_{i=1}^k \left(L_i dA_{i,t}^* - L_i^* dA_{i,t} - \frac{1}{2} L_i^* L_i dt \right) U(t), \quad (3.13)$$

where the L_i are the jump operators, each of which couples to a pair of increments $dA_{i,t}, dA_{i,t}^*$ of creation and annihilation operators. Each of these operators $A_{i,t}^*$ represent the creation of an excitation in the bosonic field associated to the i th channel (see [36]).

We briefly discuss the *fundamental noises* which are a vital ingredient in QSDEs [48]. If we start with a Hilbert space \mathcal{H} , we may define the symmetric Fock space $\mathcal{F}(\mathcal{H})$ as

$$\mathcal{F}(\mathcal{H}) = \bigoplus_{n \geq 0} \mathcal{H}^{\otimes n};$$

the k th term in the direct sum is referred to as the k -particle subspace. The *vacuum state* is the vector $|\Phi\rangle = 1 \oplus 0 \oplus 0 \oplus \dots \in \mathcal{F}(\mathcal{H})$. In this sense, the Fock space describes an arbitrary number of particles. Associated to any $f \in \mathcal{H}$ we define the exponential vector $e(f) \in \mathcal{F}(\mathcal{H})$ by

$$e(f) = \bigoplus_{n \geq 0} \frac{1}{\sqrt{n!}} f^{\otimes n}.$$

For every $f \in \mathcal{H}$ we may then define the *Weyl operator* $W(f)$ on $\mathcal{F}(\mathcal{H})$ which acts on the dense subset $\mathcal{D} = \{e(f) : f \in \mathcal{H}\}$ as

$$W(f)e(g) = \exp\left(-\langle f, g \rangle - \frac{1}{2}\|f\|^2\right) e(f+g).$$

For each $f \in \mathcal{H}$, the set $\{W(tf) : t \in \mathbb{R}\}$ is a strongly continuous one-parameter group of unitary operators on $\mathcal{F}(\mathcal{H})$; by Stone's theorem there exists a selfadjoint generator for this group, denoted $B(f)$ - we refer to this as the *field operator* associated to f .

An important class of field operators is obtained by taking f to be an indicator function $\mathbf{1}_A$. In this case, the field operators $\{B(\mathbf{1}_{[0,t]}) : t > 0\}$ all commute with each other; they can be considered as classical random variables with respect to the vacuum state, distributed as Brownian motion. Specifically, we define the random variables $B_t = \langle \Phi | B(\mathbf{1}_{[0,t]}) | \Phi \rangle$; then the stochastic process $\{B_t\}_{t \geq 0}$ is a Brownian motion. Associated to this process are creation operators A_t^* and annihilation operators A_t defined by

$$\begin{aligned} A(t)^* &= \frac{1}{2} (B(i\mathbf{1}_{[0,t]}) + iB(\mathbf{1}_{[0,t]})) \\ A(t) &= \frac{1}{2} (B(i\mathbf{1}_{[0,t]}) - iB(\mathbf{1}_{[0,t]})). \end{aligned}$$

From the commutation relation for the field operators, $[B(f), B(g)] = 2i\text{Im}\langle f, g \rangle$ we derive the familiar canonical commutation relations (CCR) for the creation and annihilation operators,

$$[A(t), A(s)] = [A^*(t), A^*(s)] = 0, \quad [A(t), A^*(s)] = \min\{t, s\}.$$

Another operator associated to the QSDE is the counting operator $\Lambda(t)$, which counts how many particles there are in the interval $[0, t]$. This

$dX \setminus dY$	$dA(t)$	$d\Lambda(t)$	$dA(t)^*$	dt
$dA(t)$	0	$dA(t)$	dt	0
$d\Lambda(t)$	0	$d\Lambda(t)$	$dA(t)^*$	0
$dA(t)^*$	0	0	0	0
dt	0	0	0	0

Table 3.1: Quantum Itô table, specifying the products $dXdY$

self-adjoint operator on $\mathcal{F}(\mathcal{H})$ is implicitly defined, through Stone's theorem, as the generator of the strongly continuous one-parameter group of unitary operators $\{\Gamma(\exp[isP_t]) : s \in \mathbb{R}\}$. Here P_t is the projection $P(t)(f) = \mathbf{1}_{[0,t]}f$ and Γ is the *second quantisation* map defined by

$$\Gamma : \mathcal{B}(\mathcal{H}) \rightarrow \mathcal{B}(\mathcal{F}(\mathcal{H})) : X \mapsto \bigoplus_{n \geq 0} X^{\otimes n}.$$

Then the random variables $\Lambda_t = \langle \Phi | \Lambda(t) | \Phi \rangle$ form a Poisson process $\{\Lambda_t\}_{t \geq 0}$.

To summarise, we have defined the *fundamental martingales*: these are the Brownian motion $\{B_t\}_{t \geq 0}$ and the Poisson process $\{\Lambda_t\}_{t \geq 0}$. Associated to these are the three fundamental operator-valued processes $A(t), A(t)^*, \Lambda(t)$. Without going into the details, we state a fundamental result in the theory of QSDEs, which is the quantum Itô calculus satisfied by the increments of these processes. In particular, we wish to compute the increment of a product $d(X_t Y_t)$ where X_t and Y_t can be any of the four aforementioned processes. Then the quantum Itô rules say that

$$d(X_t Y_t) = X_t dY_t + dX_t Y_t + dX_t dY_t$$

where the final term is given in the quantum Itô table (Table 3.1).

The QSDE formalism allows us to derive the continuous time master equation. This is done by taking the derivative of Eq. (3.12) to obtain $d\rho(t)$ and using the expression for $dU(t)$ in Eq. (3.13); working out the Itô rules then gives

$$\lim_{dt \rightarrow 0} \frac{d\rho(t)}{dt} = \mathcal{L}(\rho(t)),$$

where \mathcal{L} is as in Eq. 3.9. Note that the evolution of the state of the system,

$$T_t : \rho(0) \mapsto \rho(t)$$

is usually irreversible: if the inverse exists T_t^{-1} exists, it is not a completely positive, trace-preserving map. However, on the combined algebra of the system and the auxiliary space, the evolution is unitary and therefore reversible. This construction, going from an irreversible evolution to a reversible unitary one, is called a *dilation*. The dilation is an abstract approach to quantum dynamical semigroups, and a more physical derivation of a master equation is possible in specific cases by taking a quantum Markov limit, see e.g. [35].

3.3.4 Counting in continuous time

In the previous section, we explained how measurements performed on the output of a quantum Markov chain allows us to construct a conditional evolution for the state of the system; we referred to this as the quantum jump trajectory, or unravelling. Now we will perform an analogous construction in the continuous time case. The theory underlying continuous-time measurements in quantum systems is deep and we will only skim the surface in this section; for an approachable introduction to the topic we refer the reader to [48].

In Eq. 3.7 we presented an unravelling of the discrete time dynamics. We will now define an analogous concept in continuous time. The continuous time dynamics is governed by the QSDE in Eq. 3.13; the changes that occur in the system are due to the coupling between the jump operators L_i and the increments $dA_{i,t}$.

The *input-output* formalism allows us to express the *output* of a continuous time quantum Markov process in terms the increments of counting operators associated to the L_i . In particular, we denote by $\Gamma_{i,t}$ and $\Lambda_{i,t}$ the counting operator in the i th input field and the i th output field, respectively. These two operators are related by the evolution equation

$$\Lambda_{i,t} = U(t)^* (\mathbf{1} \otimes \Gamma_{i,t}) U(t) \quad (3.14)$$

where $U(t)$ is a solution to the QSDE 3.13. Excitations are created in the output fields as a result of interaction with the system, and the family of k equations in Eq. 3.14 provides the total counting statistics of the output fields.

Suppose for simplicity that $k = 1$, that is, there is a single jump operator $L_1 = L$, and we are interested in the distribution of the output

field counting operator $\Lambda_{i,t} = \Lambda_t$ at some time $t > 0$. This is equivalent to solving the problem in the Schrödinger picture of finding the conditional state at time t given that we have recorded n counts in the output field (in short, $\Lambda_t = n$).

In this case, we may suppose that counts have occurred at times $t \geq t_n > \dots > t_1 \geq 0$. This means that the evolution of the system state has undergone jumps due to L at these times, while the evolution in between jumps was a coherent evolution. This is what we understand by *unravelling* of the master equation in continuous time: we write the generator \mathcal{L} from Eq.3.9 as a sum

$$\mathcal{L} = \mathcal{L}_0 + \mathcal{J} \quad (3.15)$$

where \mathcal{L}_0 is the generator of the smooth evolution between jump events

$$\mathcal{L}_0(\rho) = -i[H, \rho] - \frac{1}{2}(L^*L\rho + \rho L^*L)$$

and \mathcal{J} is the instantaneous jump operator $\mathcal{J}(\rho) = L\rho L^*$. (Note that \mathcal{L}_0 can be seen as a generalisation of the effective Hamiltonian $H + \frac{i}{2}L^*L$ to the evolution of mixed states.)

In a continuous-time measurement, we record the jumps due to \mathcal{J} up to some time $t > 0$. If we know that n jumps have occurred, the space of outcomes is the set

$$\Omega_n([0, t]) = \{(t_1, \dots, t_n) : t > t_n > \dots > t_1 \geq 0\}.$$

If we do not know how many jumps have occurred, the space of outcomes $\Omega([0, t])$ is the union of all $\Omega_n([0, t])$

$$\Omega([0, t]) = \bigcup_{n=0}^{\infty} \Omega_n([0, t]); \quad (3.16)$$

this space $\Omega([0, t])$ is referred to as the *Guichardet space*.

Now that we have the necessary tools, the unravelling (3.15) and the Guichardet space of outcomes (3.16), we can write down the state of the system after performing a measurement, using an approach due to Davies [49, 50]. Given a sequence of outcomes $\omega = (t_1, \dots, t_n) \in \Omega([0, t])$ and an initial state ρ we can write the (unnormalised) conditional state of the system as

$$\tilde{\rho}_t(\omega) = \mathcal{T}_0(t - t_n)\mathcal{J}\mathcal{T}_0(t_n - t_{n-1})\mathcal{J}\cdots\mathcal{J}\mathcal{T}_0(t_2 - t_1)\mathcal{J}\mathcal{T}_0(t_1)(\rho)$$

where $(\mathcal{T}_0(t))_{t \geq 0}$ is the semigroup generated by \mathcal{L}_0 .

We are interested in the conditional state given that we have recorded n jumps; in terms of the conditional state $\tilde{\rho}_t(\omega)$ we can write this as an integral

$$\rho_n(t) = \int_{\Omega_n([0,t])} \tilde{\rho}_t(d\omega) \mu(d\omega)$$

where μ is a natural probability measure on $\Omega([0,t])$. As the details of μ are not important for our purposes, we note an equivalent, perhaps more intuitive way of expressing $\rho_n(t)$ as an integral. We may use the unravelling (3.15) to integrate over all possible time intervals between jumps and obtain the *Dyson expansion* [51]

$$\rho_n(t) = \int_{t_n}^t \int_{t_{n-1}}^{t_n} \cdots \int_0^{t_1} \mathcal{T}_0(t-t_n) \mathcal{J} \mathcal{T}_0(t_n-t_{n-1}) \mathcal{J} \cdots \mathcal{J} \mathcal{T}_0(t_1)(\rho) dt_1 \cdots dt_n.$$

The state of the system evolves according to the semigroup $(\mathcal{T}(t))_{t \geq 0}$, but we may also obtain the state of the system at time t by taking the average of the conditional states $\rho_n(t)$. We therefore end up with

$$\rho(t) = \sum_{n \geq 0} \rho_n(t) = \mathcal{T}(t)(\rho),$$

which relates the two approaches to continuous time measurements: the unravelling and the quantum dynamical semigroup.

The unravelling takes different forms depending on whether we are working in discrete or continuous time. In Ch. 5 we will consider a discretisation scheme which bridges the gap between the two unravellings. We also note that we have only considered unravellings based on counting statistics; other unravellings are possible, such as homodyne detection [48].

3.4 S-ENSEMBLES AND QUANTUM DYNAMICAL PHASE TRANSITIONS

Recall that in Ch. 2, we considered the relation between large deviations and phase transitions in statistical mechanical systems. In the following two sections we will see that such a relation also exists between large deviations and phase transitions for quantum systems.

The example in Sec. 2.6, the Curie-Weiss model, showed a phase transition in the thermodynamic limit for a macroscopic observable of the system. Specifically, the law of large numbers for the average spin broke down at a critical value β_c of the inverse absolute temperature.

This was reflected in the large deviation rate function I_β for the average spin, which went from being convex with a unique infimum for $\beta < \beta_c$, to having two different infima for $\beta > \beta_c$.

For closed systems, quantum phases transitions are generally studied in terms of the ground states and spectra of the Hamiltonians governing the dynamics [52]. In open quantum systems, dynamical phase transitions are also often (but not always, as we discuss in Ch. 5) indicated by static quantities; in this case, spectral properties of the generator. However, a more interesting approach [53] lies in a dynamical view, which involves looking at phase transitions through the statistics of the output.

The vital observation in defining quantum phase transitions is that (quantum analogues of) macroscopic observables may be expressed as large deviations rate functions for some stochastic process associated to the system, usually statistics of some measurement.

As we have seen in Ch. 2, when considering large deviations for a stochastic process, moment generating functions play an important role (especially in Thm. 2.4, the Gärtner-Ellis theorem). In this section we will look at how moment generating functions are defined for quantum Markov processes.

In Sec. 3.2 we explained how trajectories are obtained for quantum Markov chains: measuring the same observable X on each of the n sites on the output chain results in a trajectory $X^{(1)} = i_1, \dots, X^{(n)} = i_n$ of outcomes. In terms of the unravelling of the dynamics from Eq. (3.7), the conditional state of the system corresponding to this jump trajectory is $T_{i_n,*} \circ \dots \circ T_{i_1,*}(\rho)$.

If we recall the example from Sec. 2.6, we found a phase transition in the Curie-Weiss model which was visible, through Crámer's theorem, on the level of the sample means (this was a simple example, and the analogy with quantum systems is with *non-equilibrium* statistical mechanics). The quantum analogue of a phase transition on this level involves looking at the trajectories of the system through this statistical mechanics framework: in short, the thermodynamics of quantum jump trajectories [53]. For related work on *ergodicity* of quantum trajectories see [54, 55, 56].

For simplicity, suppose that there are two possible outcomes λ_1, λ_2 to the measurement. Let Λ_n be the counting operator which tracks the number of times outcome λ_1 has been measured at time n . To com-

plete the analogy with the Curie-Weiss model, consider the following questions:

- does the quantity Λ_n/n satisfy a large deviations principle?
- does the associated rate function indicate phase transitions?

Both these questions will be answered in detail, for different models, in Chs. 5, 6 and 7, in discrete and continuous time (see below).

The moment generating function for Λ_n is given by

$$Z_n(s) = \sum_{k \geq 0} \mathbb{P}(\Lambda_n = k) e^{-sk},$$

where the probability $\mathbb{P}(\Lambda_n = k)$ is the trace of the unnormalised conditional state of the system $\rho_k(n)$ given that k jump events have occurred up to time n . Given an initial state ρ this conditional state is computed as a ‘sum over paths’ over all trajectories containing k jumps,

$$\rho_k(n) = \sum_{|\{j:i_j=1\}|=k} T_{i_n,*} \circ \cdots \circ T_{i_1,*}(\rho).$$

Then the moment generating function may be expressed as

$$Z_n(s) = \text{Tr} \left(\sum_{k \geq 0} \sum_{|\{j:i_j=1\}|=k} T_{i_n,*}^s \circ \cdots \circ T_{i_1,*}^s(\rho) \right); \quad (3.17)$$

here we introduce maps $T_1^s = e^{-s} T_1$ (and $T_2^s = T_2$) by modifying the maps T_1 and T_2 from the unravelling in Eq. (3.7). These new maps define a biased unravelling

$$T_{s,*}(\rho) = T_{1,*}^s(\rho) + T_{2,*}^s(\rho).$$

This allows us to write the moment generating function in the economical form [19, 32, 57]

$$Z_n(s) = \text{Tr} (T_{s,*}^n(\rho)). \quad (3.18)$$

It is important to note the similarity between the modified transition operator T_s defined here and the approach used in the proof of Cramér’s theorem for Markov chains (see Thm. 2.6), where a modified transition matrix was constructed.

Suppose that, in this simple case, there are two phases, characterised by a difference in the expectation value of Λ_n/n in the thermodynamic

limit $n \rightarrow \infty$; this means that the first moment, $Z'_n(s)$, is discontinuous at $s = 0$. In particular, suppose that in the limit $n \rightarrow \infty$

$$\lim_{s \rightarrow 0^-} Z'_n(s) < \lim_{s \rightarrow 0^+} Z'_n(s).$$

This discontinuity in the expected sample mean can be understood intuitively if we regard s as a field which couples to the counting field Λ_n . For $s < 0$, this forces the sample mean to be the lower of the two. In terms of the moment generating function $Z_n(s)$ in Eq. (3.17), we can see this as $s < 0$ increases the contribution of trajectories which are less active, that is, have fewer events of type λ_1 . On the other hand, if $s > 0$, this increases the contribution of trajectories which are more active in this sense. Thus we may interpret this type of phase transition as a transition between different *ensembles of trajectories*; this formulation is referred to as the s -ensemble. The development of this approach is outlined in section 3.7 below.

In the previous chapter, we saw that the Perron-Frobenius theorem plays an important role in establishing a large deviations principle; an approach similar to that used in the proof of Thm. 2.6 can be followed in the quantum setting. To show that the counting process Λ_n satisfies a large deviations principle, we use the Gärtner-Ellis theorem. Using Eq. (2.4) this means that the logarithmic moment generating function

$$Z(s) = \lim_{n \rightarrow \infty} \frac{1}{n} \log Z_n(s)$$

exists and is a smooth function of s . From Eq. (3.18) we see that (similar to the proof of Thm. 2.6)

$$Z(s) = \lim_{n \rightarrow \infty} \frac{1}{n} \log \text{Tr} (T_{s,*}^n(\rho)). \quad (3.19)$$

Under the right conditions, we are then able to write $Z(s) = \log \rho(T_s)$, where $\rho(T_s)$ is the spectral radius of T_s .

This is an important feature of large deviations for quantum Markov processes: we are able to express the rate function of some output statistics as the spectral radius of a perturbation of the transition operator, just as in the classical case. But the difference is that, in the classical case, this spectral radius had the desired properties due to the Perron-Frobenius theorem for transition *matrices*. Now we are in the quantum setting, and we need a Perron-Frobenius type result for transition *operators*. Such results will be studied in Sec. 3.5 below.

So far we have only discussed quantum phase transitions and large deviations in discrete time. The approach to the continuous time problem is similar, but requires a shift from looking at a perturbed transition operator T_s , to looking at a perturbed generator \mathcal{L}_s ; then \mathcal{L}_s generated a perturbed semigroup of transition operators. This approach will be used in detail in Ch. 7 below.

One aspect of quantum phase transitions that we will discuss in this thesis is the role played by *bistability* [58], or degeneracy of the stationary state, at critical points. In the stationary regime, intermittency of the trajectories (see Sec. 3.7 below) is caused by the existence of multiple stationary states - or being *close* to this degenerate situation. Such intermittency has recently been observed in experiments with quantum spin chains [59, 60].

3.5 NON-COMMUTATIVE PERRON-FROBENIUS THEORY

Our results depend on the transition operator T in question satisfying certain properties; in particular, we require that T is *irreducible*. Irreducibility for linear maps on finite-dimensional von Neumann algebras is defined in [61], from which we quote the following definitions.

A matrix $X \in M_n$ is called *strictly positive*, denoted $X > 0$, if X is positive and invertible (i.e. there exists $\epsilon > 0$ such that $X \geq \epsilon \mathbf{1}$). A linear map $T : M_n \rightarrow M_n$ is called *positive* if $T(X) \geq 0$ for all $X \geq 0$; T is called *strictly positive* if $T(X) > 0$ for all non-zero $X \geq 0$.

We say T is *reduced* by a projection $P \in M_n$ if there exists $\lambda > 0$ such that $T(P) \leq \lambda P$; T is said to be *irreducible* if it is not reduced by any non-trivial projections. The following characterisation (ibid., Lemma 2.1) is occasionally useful: a positive linear map T on M_n is irreducible if and only if $(\mathbf{1} + T)^{n-1} > 0$ (that is, $\mathbf{1} + T$ is *primitive*).

Irreducible positive maps form a useful class of operators; in particular, they satisfy the a quantum analog of the commutative Perron-Frobenius theorem, given below. As we noted in Sec. 3.1.1, it suffices to keep in mind a concrete algebra of bounded operators $\mathcal{B}(\mathfrak{h})$ for any von Neumann algebra considered in these results.

Definition 3.1 (Schwarz map). A linear map ϕ on a von Neumann algebra A is called a *Schwarz map* if $\phi(1) = 1$ and $\phi(x^*x) \geq \phi(x)^*\phi(x)$ for all $x \in A$.

The Schwarz property is stronger than positivity, but weaker than 2-positivity [62]. If we restrict ourselves to completely positive maps, the concept of irreducibility can be reformulated in terms of the associated Kraus operators [63]: the map is irreducible if and only if there are no nontrivial invariant subspaces for all of the Kraus operators.

We conclude this section with the following extension of the Perron-Frobenius theorem. The development of Perron-Frobenius theory for positive maps on operator algebras is an interesting topic [64, 65, 66, 67, 68, 69]; for our purposes, the following early formulation due to Evans [61] is instructive. This theorem applies to the Schwarz maps introduced above, which includes unital completely positive maps [70, Prop. 3.3].

Theorem 3.1. (Perron-Frobenius theorem for Schwarz maps [61, Thms. 4.3-4.4]) Let T be an irreducible Schwarz map on M_n and let $\sigma(T)$ denote the spectrum of T .

- The spectral circle $\Gamma = \{\lambda \in \sigma(T) : |\lambda| = 1\}$ of T is a discrete group (acting on $\sigma(T)$) of m elements generated by $\gamma = \exp(2\pi i/m)$; moreover, each eigenvalue in Γ is simple.
- The spectral circle is trivial, $\Gamma = \{1\}$, if and only if T^k is irreducible for all $k \geq 1$.
- The set of eigenvectors associated to the eigenvalues in Γ form an abelian group isomorphic to Γ ; we have

$$T(U^k) = \gamma^k U^k.$$

where the unitary matrix $U \in M_n$ has spectral decomposition

$$U = \sum_{k=0}^{m-1} \gamma^k P_k$$

with $T(P_k) = P_{k-1}$ (with $T(P_0) = P_{m-1}$).

This last statement has a dual interpretation in the Schrödinger picture; since T is irreducible, there is a unique faithful invariant state ω for T_* .

[†]A subset V of a Banach space X is called relatively compact if its closure is compact; V is called compact if, whenever the union of a family of subsets of X contains V , there is a finite number of elements in this family whose union also contains V .

The Krein-Rutman theorem is an extension of the Perron-Frobenius theorem to the infinite-dimensional setting of general Banach spaces (see [71] for a nice historical overview), which lacks any statements about invariance properties of the spectrum. (Recall that a Banach space is a complete normed vector space; in particular, any Hilbert space is a Banach space.) The following generalisation of the Krein-Rutman theorem to *ordered Banach spaces* will be used in Ch. 7. The abstract definition of a compact linear operator T on a Banach space X is that the image of any bounded set is relatively compact; in Ch. 7 we will need to prove compactness for a family of linear maps, and we refer to that chapter for discussion on compactness in terms of spectral properties of the map.

Theorem 3.2 (Krein-Rutman for Banach spaces [72]). Let X be a Banach space and $T : X \rightarrow X$ a compact linear operator that is positive with spectral radius $r(T) > 0$. Then $r(T)$ is an eigenvalue and there exists a non-zero $x \geq 0$ such that $Tx = r(T)x$. Moreover, $r(T^*) = r(T)$ is an eigenvalue of T^* .

Restricting [72] the compact operator T to be *strictly positive* means there are no other eigenvalues of the same modulus. This version of the Krein-Rutman theorem therefore coincides with the first part of the Perron-Frobenius theorem.

3.6 THE ATOM MASER

The topics covered in this chapter so far will be used in this section, as we introduce the atom maser and its Markov semigroup and the counting processes associated to the jump terms in the Lindblad generator. In the final chapter in this thesis, Ch. 7, we will return to this model as we prove a large deviations result and discuss the dynamical phase transitions that occur in a thermodynamic limit.

In the atom maser, two-level atoms pass successively through a cavity and interact resonantly with the electromagnetic field inside the cavity. The two-level atoms are identically and independently prepared in the excited state, and for simplicity we assume that only a single atom passes through the cavity at any time. In addition, the cavity is also coupled to a thermal bath which represents the interaction between the (non-ideal) cavity and the environment. The combined effects of the

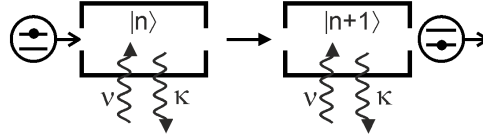


Figure 3.2: Atoms enter a cavity, which is in contact with a thermal bath, in the excited state; the cavity state $|n\rangle$ gains energy from interaction with the atom

interactions with the atoms and the environment changes the state of the cavity (see Fig. 3.2) whose time evolution is described by a *quantum Markov semigroup*, in a certain coarse grained approximation described below; see Refs. [73] and [74] for a mathematical overview, and [75] for the physical derivation of the master equation. In this section we give an intuitive description of the dynamics starting with a simplified discrete time model, with an emphasis on the statistics of measurements performed on the atoms.

3.6.1 Atom maser

The cavity is described by a one mode continuous variable system with Hilbert space $\mathfrak{h} = \ell^2(\mathbb{N})$ whose canonical basis vectors $(|e_n\rangle)_{n \geq 0}$ represent pure states of fixed number of photons. Therefore, if $|\psi\rangle \in \mathfrak{h}$ is a pure state, the *photon number distribution* of the cavity is given by $|\langle e_n, \psi \rangle|^2$. Mixed states are described by density operators, i.e. trace-class operators $\rho \in L^1(\mathfrak{h})$ which are positive and normalised to have unit trace, and the observables are represented by self-adjoint elements of the von Neumann algebra of bounded operators $\mathcal{B}(\mathfrak{h})$ whose predual is $L^1(\mathfrak{h})$. Recall that the *annihilation operator* a on \mathfrak{h} is defined by

$$a|e_n\rangle = \begin{cases} \sqrt{n}|e_{n-1}\rangle & \text{if } n > 0 \\ 0 & \text{if } n = 0 \end{cases};$$

its adjoint is the *creation operator* a^* , and $N = a^*a$ is the photon number operator such that $N|e_n\rangle = n|e_n\rangle$. The atom is modelled by a two-dimensional Hilbert space \mathbb{C}^2 with standard orthonormal basis $\{|0\rangle, |1\rangle\}$ consisting of the "ground" and "excited" states. We denote by σ^* and σ the corresponding raising and lowering operators (i.e. $\sigma^*|0\rangle = |1\rangle$ etc.).

The interaction between an atom and the cavity is described by the Jaynes-Cummings hamiltonian on $\mathbb{C}^2 \otimes \mathfrak{h}$

$$H_{\text{int}} = -g(\sigma \otimes a^* + \sigma^* \otimes a),$$

where g is the coupling constant which, for simplicity, is considered to be constant across the cavity. The free hamiltonian is

$$H_{\text{free}} = \omega \mathbf{1} \otimes a^* a + \omega \sigma^* \sigma \otimes \mathbf{1},$$

where ω is the frequency of the resonant mode; however by passing to the interaction picture the effect of the free evolution can be ignored. Therefore if the interaction lasts for a time t_0 , the joint evolution is described by the unitary operator $U := \exp(it_0 H_{\text{int}})$ whose action on a product initial state is

$$U : |k\rangle \otimes |1\rangle \mapsto \cos(\phi\sqrt{k+1})|k\rangle \otimes |1\rangle + \sin(\phi\sqrt{k+1})|k+1\rangle \otimes |0\rangle,$$

where $\phi := t_0 g$ is the *accumulated Rabi angle*. If a measurement is performed on the outgoing atom in the standard basis, then the cavity remains in state $|k\rangle$ with probability $\cos^2(\phi\sqrt{k+1})$ or gains an excitation with probability $\sin^2(\phi\sqrt{k+1})$. If we average over the outcomes, we obtain the cavity transfer operator $\mathcal{T}_* : L^1(\mathfrak{h}) \rightarrow L^1(\mathfrak{h})$

$$\mathcal{T}_*(\rho) = K_1 \rho K_1^* + K_2 \rho K_2^* = \mathcal{K}_1(\rho) + \mathcal{K}_2(\rho) \quad (3.20)$$

where the *Kraus operators* K_i are given by

$$K_1 = a^* \frac{\sin(\phi\sqrt{aa^*})}{\sqrt{aa^*}}, \quad K_2 = \cos(\phi\sqrt{aa^*}),$$

and \mathcal{K}_i are the corresponding jump operators on the level of density matrices. Since each atom interacts with the cavity only once, the state of the cavity after n such interactions is given by $\rho(n) = \mathcal{T}_*^n(\rho)$, which can be interpreted as a *discrete time* quantum Markov dynamics. Let us imagine that after the interaction, each atom is measured in the standard basis and found to be either in the excited or the ground state. The master dynamics can be unravelled according to these events as (cf. Eq. (3.15))

$$\mathcal{T}_*^n(\rho) = \sum_{\mathbf{i}=(i_1, \dots, i_n)} \mathcal{K}_{i_n} \dots \mathcal{K}_{i_1}(\rho). \quad (3.21)$$

Here each term of the sum represents the (unnormalised) state of the cavity after a certain sequence $\mathbf{i} = (i_1, \dots, i_n) \in \{e, g\}^n$ of measurement outcomes, whose probability is

$$\mathbb{P}(i_1, \dots, i_n) = \text{Tr}(\mathcal{K}_{i_n} \dots \mathcal{K}_{i_1}(\rho)).$$

If $\Lambda_n(\mathbf{i}) := \#\{j : i_j = g\}$ denotes the number of ground state atoms detected up to time n , we can use the previous relation to compute its moment generating function

$$\begin{aligned} \mathbb{E}(e^{s\Lambda_n}) &= \sum_{k \geq 0} \mathbb{P}(\Lambda_n = k) e^{sk} \\ &= \sum_{\mathbf{i}} e^{s\Lambda_n(\mathbf{i})} \text{Tr}(\mathcal{K}_{i_n} \dots \mathcal{K}_{i_1}(\rho)) = \text{Tr}(\mathcal{T}_{*s}^n(\rho)) \end{aligned} \quad (3.22)$$

where

$$\mathcal{T}_{*s}(\rho) = e^s \mathcal{K}_1(\rho) + \mathcal{K}_2(\rho)$$

is a "deformed" transfer operator, i.e. a completely positive but not trace preserving map on $L^1(\mathfrak{h})$. The relation (3.22) and its continuous time analogue (3.30) will be the key to analysing the large deviations properties of the counting process in terms of spectral properties of operators such as \mathcal{T}_s and \mathcal{L}_s below.

To make the model more realistic we will pass to a continuous time description in which the incoming atoms are Poisson distributed in time with intensity N_{ex} , and the cavity is in contact with a thermal bath. If one ignores the details of short term cavity evolution, the discrete time dynamics can be replaced by coarse grained *continuous time* Lindblad (master) equation [76]

$$\begin{aligned} \frac{d}{dt} \rho(t) &= \mathcal{L}_*(\rho(t)), \\ \mathcal{L}_*(\rho) &= \sum_{i=1}^4 \left(L_i \rho L_i^* - \frac{1}{2} \{L_i^* L_i, \rho\} \right) \\ &= \sum_{i=1}^4 L_i \rho L_i^* + \mathcal{L}_*^{(0)}(\rho) = \sum_{i=1}^4 \mathcal{J}_i(\rho) + \mathcal{L}_*^{(0)}(\rho) \end{aligned} \quad (3.23)$$

with jump operators L_i defined by

$$L_1 = \sqrt{N_{\text{ex}}} a^* \frac{\sin(\phi \sqrt{a a^*})}{\sqrt{a a^*}}, \quad (3.24)$$

$$L_2 = \sqrt{N_{\text{ex}}} \cos(\phi \sqrt{a a^*}), \quad (3.25)$$

$$L_3 = \sqrt{\gamma + 1} a, \quad (3.26)$$

$$L_4 = \sqrt{\gamma} a^*. \quad (3.27)$$

As before, the operators L_1 and L_2 are associated to the detection of an atom in the ground and excited state, respectively. The emission and absorption of photons due to contact with the bath is represented by

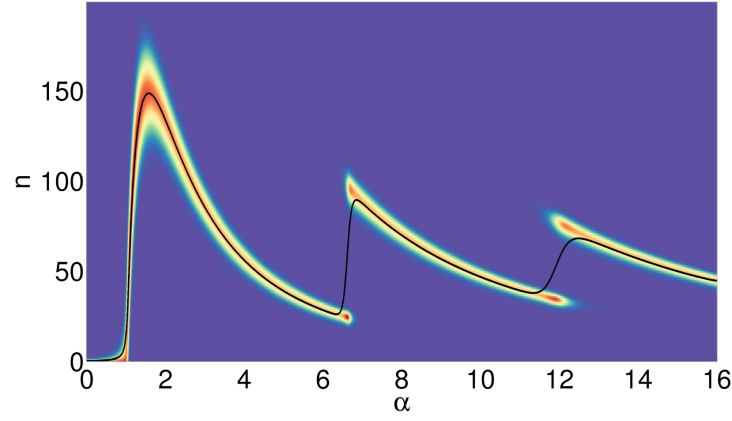


Figure 3.3: Mean photon number (black line) and photon number distribution (background) in the stationary state ρ_{ss} as function of $\alpha = \sqrt{N_{ex}}\phi$

operators L_3 and L_4 , respectively. As explained in Sec. 3.3, the Heisenberg picture Lindbladian \mathcal{L} is the generator of a strongly continuous semigroup $(\mathcal{T}(t))_{t \geq 0}$ on $\mathcal{B}(\mathfrak{h})$ which described the time evolution of the system state $\rho(t+s) = \mathcal{T}(t)(\rho(s))$.

The Markov semigroup $(\mathcal{T}(t))_{t \geq 0}$ has a unique stationary state ρ_{ss} which has diagonal density matrix in the Fock (photon number) basis with entries

$$\rho_{ss}(n) := \rho_{ss}(0) \prod_{k=1}^n \left(\frac{\nu}{\nu+1} + \frac{N_{ex}}{\nu+1} \frac{\sin^2(\phi\sqrt{k})}{k} \right) \quad (3.28)$$

equal to the probabilities of finding n photons in the cavity, with $\rho_{ss}(0)$ taken such that $\text{Tr}(\rho_{ss}) = 1$. Moreover, the Markov semigroup is ergodic, in the sense that any initial states ρ converges to the stationary state [77]

$$\lim_{t \rightarrow \infty} \mathcal{T}_*(t)(\rho) = \rho_{ss}.$$

The dependence of the stationary mean photon number and photon number distribution on the "pumping parameter" $\alpha := \sqrt{N_{ex}}\phi$ is shown in Fig. 3.3, for $\nu = 0.15$ and $N_{ex} = 150$. We note two interesting features in this figure: first, there is a sharp change in the mean photon number at $\alpha \approx 1$ followed by less pronounced jumps near $\alpha = 6.66$ and $\alpha = 12$. The other, related, feature to note is that the photon number distribution has a single peak for most values of α except in certain regions such as around the critical point $\alpha \approx 6.66$, where the stationary state has two local maxima. We will come back to these aspects in the next section.

3.6.2 The counting process

In Sec. 3.3.4 we introduced the counting processes associated to the unraveling of continuous-time quantum Markov processes. To better understand the behaviour of the stationary state illustrated in Figure 3.3, we unravel the Markov semigroup $\mathcal{T}_*(t)$ with respect to the four counting processes associated to the jump terms (3.24 - 3.27), each of them corresponding to a counting measurement of the quantum output process. If ρ is the initial state of the cavity, then $\rho(t) := \mathcal{T}_*(t)$ is the evolved state at time t which (in analogy to Eq.(3.21)) can be seen as an average over all possible counting events in the environment

$$\rho(t) := \mathcal{T}_*(t) = \sum_{k \geq 0} \sum_{i_1, \dots, i_k=1}^4 \int \dots \int_{0 \leq t_1 \leq \dots \leq t_k \leq t} \rho(t; t_1, i_1, \dots, t_k, i_k) dt_1 \dots dt_k \quad (3.29)$$

where the integrand

$$\rho(t; t_1, i_1, \dots, t_k, i_k) := e^{(t-t_k)\mathcal{L}_*^{(0)}} \mathcal{J}_{i_k} \dots e^{(t_2-t_1)\mathcal{L}_*^{(0)}} \mathcal{J}_{i_1} e^{t_1\mathcal{L}_*^{(0)}}(\rho),$$

is the unnormalised state of the cavity given that detections of type $i_1, \dots, i_k \in \{1, 2, 3, 4\}$ have occurred at times $0 \leq t_1 \leq \dots \leq t_k \leq t$, and no other counting events happened in the meantime. From the four counting processes we focus on the first one associated with the detection of an atom in the ground state and simultaneous absorption of a photon by the cavity. We denote by Λ_t the total number of such atoms detected up to time t . Similarly to the discrete case, by using the above unravelling we can show that the moment generating function of Λ_t is given by

$$\mathbb{E}(e^{s\Lambda_t}) = \text{Tr}(\mathcal{T}_{*s}(t)(\rho)) = \text{Tr}(\rho \mathcal{T}_s(t)(\mathbf{1})). \quad (3.30)$$

where $(\mathcal{T}_{*s}(t))_{t \geq 0}$ is the completely positive semigroup on $L^1(\mathfrak{h})$ with generator

$$\mathcal{L}_{*s}(\rho) = e^s \mathcal{J}_1(\rho) + \sum_{j=2}^4 \mathcal{J}_j(\rho) + \mathcal{L}_*^{(0)}(\rho) = (e^s - 1) \mathcal{J}_1(\rho) + \mathcal{L}_*(\rho), \quad (3.31)$$

and $(\mathcal{T}_s(t))_{t \geq 0}$ is the dual semigroup on $\mathcal{B}(\mathcal{H})$. Equation (3.30) plays a central role in our treatment of the atom maser in Ch. 7; we will use it to formulate a large deviations principle for the counting process Λ_t , and in particular, to relate the moment generating function of Λ_t to

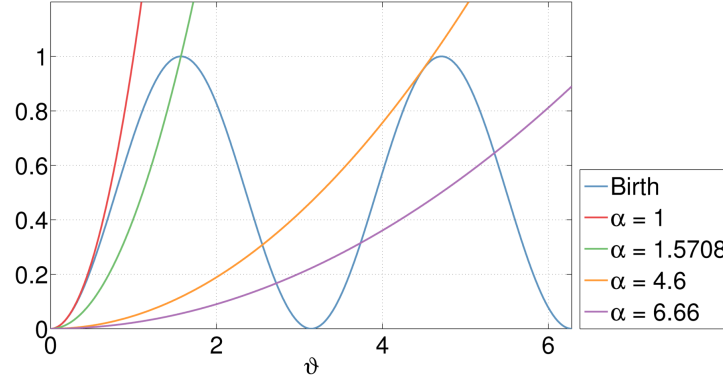


Figure 3.4: The birth (blue) and death rates as functions of ϑ for different values of α . The intersection points correspond to minima and maxima of the stationary distribution.

the spectral properties of \mathcal{L}_s . Note that \mathcal{L}_s differs from the Lindblad generator by the factor e^s multiplying the jump term associated to the detection of a ground state atom. It is still the generator of a completely positive semigroup, but it is no longer identity preserving, and therefore does not represent a physical evolution except for $s = 0$.

The unravelling (3.29) allows for a classical interpretation of the cavity dynamics. Indeed, the semigroup generated by \mathcal{L} (and \mathcal{L}_s) leaves invariant the commutative subalgebra $\mathcal{N} \subset \mathcal{B}(\mathfrak{h})$ generated by the number operator N , and the restriction of $(\mathcal{T}(t))_{t \geq 0}$ to the diagonal algebra is the dynamical semigroup of a classical *birth-death process* on the state space $\{0, 1, 2, \dots\}$, with rates

$$\begin{aligned} \lambda_k^2 &:= N_{\text{ex}} \sin(\phi \sqrt{k+1})^2 + \nu(k+1), \quad k \geq 0 \\ \mu_k^2 &:= (\nu+1)k, \quad k \geq 1 \end{aligned} \quad (3.32)$$

and stationary distribution $\pi_{\text{ss}}(n) = \rho_{\text{ss}}(n)$. Figure 3.4 shows the birth and death rates (minus the common factor νk) as functions of the parameter $\vartheta := \sqrt{(k+1)/N_{\text{ex}}} \alpha$ in the limit $N_{\text{ex}} \rightarrow \infty$. The intersection points correspond to minima and maxima of the stationary distribution [76] as suggested by the following argument. For $\alpha < 1$ the death rate is always larger than the birth rate and the distribution is maximum at the vacuum state. For $1 < \alpha < 4.6$ there is a single non-trivial intersection point such that the birth rate is larger to its left and smaller to its right, and therefore corresponds to the maximum of the stationary distribution. Similarly, when $4.6 < \alpha < 7.8$ the rates intersect in three points, the first and last are located at local maxima while the middle point is a local minimum, so we deal with a bimodal distribution.

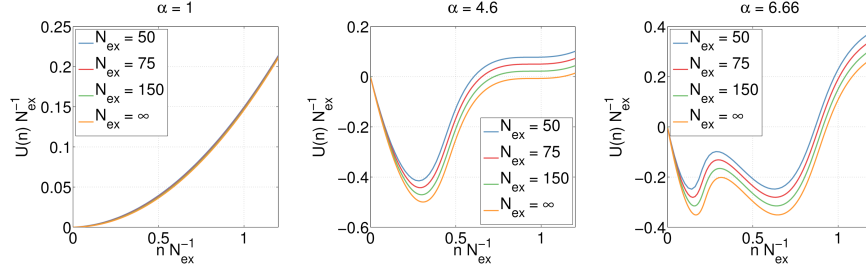


Figure 3.5: Rescaled potentials $U(n)/N_{\text{ex}}$ as function of n/N_{ex} , for various finite N_{ex} converge to a limit potential for $N_{\text{ex}} \rightarrow \infty$. For $\alpha < 1$ the potential is minimum at zero; for $1 < \alpha < 4.6$ it has a unique minimum away from $n = 0$; for $4.6 < \alpha < 7.8$ there are two local minima which become equal at $\alpha \approx 6.66$.

bution. However, while this analysis clarifies the emergence of multimodal distributions, it does not explain the sudden jump of the mean photon number at $\alpha \approx 6.66$.

This feature can be intuitively understood by appealing to the effective potential model [78]. If we think of the photon number as a continuous variable and introduce a fictitious potential U defined by

$$\rho_{ss}(n) = \rho_{ss}(0)e^{-U(n)}, \quad (3.33)$$

then the photon number distribution appears as the thermal equilibrium distribution of a particle moving in the potential U (with $k_B \cdot T = 1$), see Figure 3.5. When the potential has a single local minimum (for $0 < \alpha < 4.6$), the stationary distribution is unimodal and concentrates around this point. The cavity state fluctuates around the mean, and Λ_t increases steadily with average rate. When there are two (or more) local minima of different height, the higher minimum corresponds to a metastable phase from which the system eventually escapes due to thermal fluctuations. The rate of return to the metastable phase is typically much lower due to the larger potential barrier that needs to be climbed. The point $\alpha \approx 6.66$ where the two local minima are equal plays the role of a "phase transition", and corresponds roughly to the point where the mean photon number changes abruptly. Here the cavity spends long periods of time around the two local maxima with rare but quick transitions between them. The change from the low energy to the high energy mode is accompanied by a clear change in the slope of the counting process Λ_t

$$\frac{\mathbb{E}(\Lambda_t)}{t} = N_{\text{ex}} \sum_n \rho_{\text{ss}}(n) \sin^2(\phi \sqrt{n+1}) = N_{\text{ex}} \left(\sum_n n \rho_{\text{ss}}(n) - \nu \right).$$

Unlike the "first order transition occurring at $\alpha = 6.66$, a "second order transition occurs at $\alpha \approx 1$. Here the first derivative of the mean photon number has a jump in the limit of $N_{\text{ex}} \rightarrow \infty$. This and the scaling of the potential U with N_{ex} will be discussed in Sec. 7.4.

The statistics of the trajectories are therefore closely related to the dynamics of the cavity and consequently with its stationary state. The next step is to think of the time trajectories as "configurations" of stochastic system draw from ideas in non-equilibrium statistical mechanics and large deviations theory to study their phases and phase transitions. Here the idea is to identify *dynamical phase transitions* of the open system, by analysing the statistics of jump trajectories in the long time (stationary) regime. The trajectories play an analogous role to the configurations of a statistical mechanics model at equilibrium.

In this analogy, the parameter s of the moment generating function (3.30) can be seen as a "field" which biases the distribution of trajectories in the direction of active or passive trajectories by effectively changing the probability of a trajectory $\omega := (i_1, t_1, \dots, i_n, t_n)$ by a factor $\exp(s\Lambda_t(\omega))$.

When α is such that the stationary distribution is unimodal, the trajectories' distribution changes smoothly from passive ones for $s < 0$ to active ones for $s > 0$. However, near $\alpha \approx 6.66$ (corresponding to the jump in the mean photon number) there is a steep change in the counting rates around $s = 0$. The active trajectories are associated to periods when the cavity is in the higher, excited phase while the passive trajectories are connected to the lower phase. Since the cavity makes very rare transitions between the phases, any trajectory – when followed for long but finite periods of time – falls typically into one of the two distinct categories (see Figure 3.6). Our goal is to investigate whether this distinction survives the infinite time limit, in which case we would deal with a dynamical phase transition characterised by the non-analyticity of a certain large deviations rate function. We will show that this is not the case, but rather we deal with a *cross-over* behaviour; that is, the count rate does not jump but has a very steep change around $s = 0$, which appears to become a jump in the limit of infinite pumping rate $N_{\text{ex}} \rightarrow \infty$ (see Sec. 7.4).

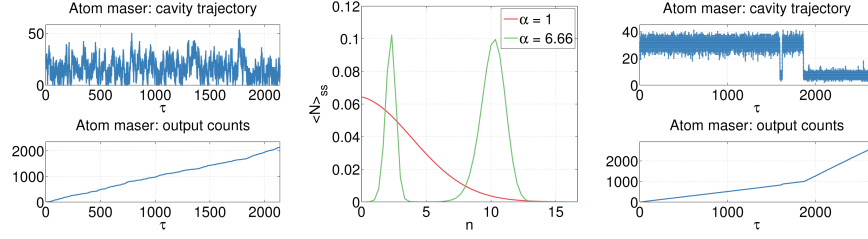


Figure 3.6: Sample trajectories for cavity state (top) and output paths Λ_t (bottom) with $N_{\text{ex}} = 50$, corresponding to stationary state distribution (center) showing large variance at $\alpha \approx 1$ (red) and bistability at $\alpha \approx 6.66$ (green)

3.7 REVIEW OF LARGE DEVIATIONS IN QUANTUM SYSTEMS

Our approach to large deviations in quantum systems is based on the thermodynamics of quantum trajectories framework. This is not the first time that the theory of large deviations has been used to study quantum systems: large deviations has natural applications in the theory of estimation and quantum hypothesis testing [79, 80, 81, 82, 83, 84, 85, 86]. There are also many results on the large deviations for (finitely correlated or KMS) states on quantum spin chains [87, 88, 89, 90, 91, 92, 93, 94] as well as a generalised theory of quantum statistical mechanics and entropic functionals [95, 96, 97, 98, 99, 100]. Finally, some approaches consider large deviations behaviour not for measurement outcomes but for operators themselves [101, 102].

In [53] a new perspective was put forward, which looks at quantum jumps from the viewpoint of non-equilibrium statistical mechanics [103] (see also [104]). For recent work on quantum dynamical phase transitions we refer to [53, 32, 34, 33, 105, 4]. In [87] (see also [89]) a large deviation principle is shown to hold for correlated states on quantum spin chains; large deviations for quantum Markov semigroups are studied in [102]. Metastable behaviour in a different atom maser has been investigated in [106]. More broadly, there is a large body of large deviations work in quantum systems [107, 87, 92, 93, 108, 84].

The use of quantum trajectories (or *quantum-jump approach*) in quantum optics is studied in the review article [38]; as we will be using the quantum trajectories framework in most of what follows, we refer the reader to this article for more information. We also note [109] as an important article in the development of quantum trajectories. The ap-

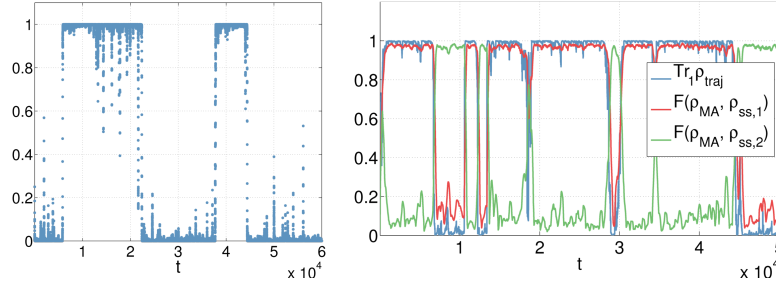


Figure 3.7: Examples of quantum jump trajectories showing intermittency (taken from Sec. 4.4)

proach involves obtaining quantum trajectories by performing measurements on the output fields of an open quantum system [38]. The three-level system and atom maser, which we consider below, are studied using quantum trajectories; the authors note the intermittency visible in the trajectories, showing *bright* and *dark* periods in the emission events (see also [110] for a treatment of such phenomena with experiments in mind).

The use of large deviations to study open quantum systems in terms of thermodynamics of ensembles of quantum jump trajectories was started in [53] (see also *Viewpoint* commentary in [104]). The systems studied all have in common that they undergo *quantum jumps* of some type which allows defining *ensembles of trajectories* defined by some *activity*. The LD approach involves a biased master operator (corresponding to different ensembles of trajectories) whose largest real eigenvalue corresponds to the LD function. Singularities in the phase diagram for the micromaser corresponds to *space-time* phase transitions between different *dynamical activities*.

The thermodynamic formalism for quantum jump trajectories in dissipative systems is related to large deviations in [53] (see also [4, 111, 112, 113, 105, 114, 115]), where (dissipative) quantum *non-equilibrium* systems are studied using the large deviations method. The systems examined all have in common that they undergo *quantum jumps* of some type which allows defining *ensembles of trajectories* defined by some *activity*. Examples considered are the driven two-level system, the three-level system (*electron shelving*) and the atom maser (studied in detail below). This article introduces some important features: singularities in the phase diagram for corresponds to phase transitions between different *dynamical activities*, much like in (classical) statistical

mechanics; biased trajectories give rise to the LD function as largest eigenvalue of biased master operator.

Part II

RESULTS

Time passes and the constants stay.

— James Blake, *Overgrown*

PHASE PURIFICATION

4.1 INTRODUCTION

In this chapter we show how a natural decomposition for the space associated to a discrete-time quantum Markov chain may be found by considering the algebraic structure of the commutant of Kraus operators. Using this decomposition, we are able to define phases, what it means to purify towards such phases in terms of measurement trajectories; we refer to this as phase purification.

We will also clarify the meaning of phase transitions in this context and connect these notions of phase purification and phase transitions to the behaviour of large deviations rate functions.

In the continuous-time setting we will connect our findings to a result due to [116]; we finish the chapter with several illustrative examples.

4.2 STRUCTURE OF DISCRETE-TIME QUANTUM MARKOV CHAINS

In this section we introduce a structure theorem which describes the state space of discrete-time quantum Markov chains; we will use this structure theorem to carefully define the notion of *phases* for quantum Markov processes.

In classical Markov processes, the state space can generally be decomposed into *transient* and *recurrent* components, characterised by the asymptotic behaviour of the process. The set of recurrent states are the states in which the process will end up almost surely. Conversely, the transient states are those states whose probability of being visited vanishes in the asymptotic limit.

4.2.1 Recurrent subspace

The first step in the structure theorem is the quantum analogue of a decomposition into recurrent and transient states. Suppose that the dynamics takes place on the algebra of operators on some finite-dimensional Hilbert space $\mathcal{H} = \mathbb{C}^n$: then using the definitions from Ch. 3 we have a transition operator T which is a completely positive, identity preserving map

$$T : M_n \rightarrow M_n.$$

In general, any identity-preserving completely positive map T on M_n can be decomposed into a recurrent and transient part as follows. The recurrent projection P_0 of T is found by taking the projection onto the maximal range of all positive matrices that remain invariant under T ; then T is said to be *recurrent* if $P_0 = \mathbf{1}$.

The restriction T_0 to the *recurrent subalgebra* $P_0 M_n P_0$ is again a trace-preserving positive map, and T_0 is recurrent with respect to this restriction. Conversely, the *transient subalgebra* $P_0^\perp M_n P_0^\perp$ (or *decaying subspace* [116]), is obtained by taking the restriction of T to the subspace $P_0^\perp \mathcal{H}$. This subspace is characterised by [61, Thm. 3.3]

$$\lim_{k \rightarrow \infty} P_0^\perp T_*^k(\rho) P_0^\perp = 0 \quad \text{for all } \rho \in \mathcal{S}(M_n).$$

Note that this definition applies to discrete and continuous time quantum Markov processes; the only difference is that in the continuous time case, we take the limit $t \rightarrow \infty$ for the elements of the semigroup $T_{*,t}$.

The upshot of these definitions is that, given the transition operator T for a quantum Markov process, we can always define its recurrent restriction T_0 which is itself a quantum Markov process. For this reason, we will in the following assume for simplicity that the quantum Markov process is already recurrent.

4.2.2 Structure

Our treatment of the structure of quantum Markov chains starts with the Kraus decomposition introduced in Eq. (3.1): for all states ρ the transition operator T_* takes the form

$$T_*(\rho) = \sum_{i=1}^k V_i \rho V_i^*$$

where the Kraus operators are denoted by V_1, \dots, V_k . We start with considering the *commutant* of the Kraus operators, denoted by \mathcal{A} : this is the set of all elements in M_n that commute with all of the Kraus operators,

$$\begin{aligned}\mathcal{A} &= \{V_1, \dots, V_k\}' \\ &= \{X \in M_n : [V_i, X] = 0 \text{ for all } i = 1, \dots, k\}.\end{aligned}$$

Then \mathcal{A} is a subalgebra of M_n , and we may write \mathcal{A} in the form [117]

$$\mathcal{A} = \bigoplus_{\alpha} \mathcal{B}(\mathcal{K}_{\alpha}) \otimes \mathbf{1}_{\mathcal{H}_{\alpha}}$$

corresponding to a decomposition of the original Hilbert space $\mathcal{H} = \mathbb{C}^n$ of the type

$$\mathcal{H} = \bigoplus_{\alpha} \mathcal{K}_{\alpha} \otimes \mathcal{H}_{\alpha}. \quad (4.1)$$

Here $\{\mathcal{K}_{\alpha}\}$ and $\{\mathcal{H}_{\alpha}\}$ are all finite-dimensional Hilbert spaces; we denote by P_{α} the orthogonal projection onto the subspace $\mathcal{K}_{\alpha} \otimes \mathcal{H}_{\alpha}$. Each \mathcal{K}_i is the *multiplicity space* associated to \mathcal{H}_i , accounting for the equivalences between copies of \mathcal{H}_i : in the notation of [116] we may write

$$\mathcal{K}_{\alpha} \otimes \mathcal{H}_{\alpha} = \mathbb{C}^{n(\alpha)} \otimes \mathcal{H}_{\alpha} \quad (4.2)$$

where $n(i)$ is the number of equivalent blocks \mathcal{H}_i . By definition of \mathcal{A} , the Kraus operators then have the decomposition

$$V_i = \bigoplus_{\alpha} \mathbf{1}_{\mathcal{K}_{\alpha}} \otimes V_i^{(\alpha)},$$

where $V_i^{(\alpha)} \in \mathcal{B}(\mathcal{H}_{\alpha})$.

This decomposition of M_n is the finest possible splitting in the following sense. Suppose $\psi \in \mathcal{K}_{\alpha}$ is a unit vector. Then the space $\mathcal{H}_{\psi}^{\alpha} := \psi \otimes \mathcal{H}_{\alpha}$ is a minimal invariant subspace for T , corresponding to a one-dimensional projection in the algebra $\mathcal{B}(\mathcal{K}_{\alpha}) \otimes \mathbf{1}_{\mathcal{H}_{\alpha}}$ and the restriction of T to $\mathcal{B}(\mathcal{H}_{\psi}^{\alpha})$ is an irreducible map (for a related decomposition, see *decoherence free subspaces* found in [118].)

4.2.3 Dephasing and equivalences

The next step in this decomposition is defining a notion of equivalence of diagonal blocks $P_{\alpha} M_n P_{\alpha}$. Note first that an important feature of this

decomposition is that T acts independently on the blocks $P_a M_n P_b$: that is, $T(P_a X P_b) = P_a T(X) P_b$ for all $X \in M_n$. We denote by $T_{a,b}$ the restriction of T to the block $P_a M_n P_b$.

Note that the spectrum of the restriction $\sigma(T_{a,b})$ is a subset of the spectrum of T ; as T is a contraction, $\sigma(T)$ is contained in the complex unit disc. Suppose first that all eigenvalues lie strictly within the unit disc; that is, for all $\lambda \in \sigma(T_{a,b})$ we have $|\lambda| < 1$. Then for any $Y \in P_a M_n P_b$

$$\lim_{n \rightarrow \infty} T_{a,b}^n(Y) = 0,$$

which means that the block $P_a M_n P_b$ shows *relative dephasing* between P_a and P_b .

The other possibility is that $T_{a,b}$ has an eigenvalue λ such that $\lambda = e^{i\varphi_a}$. In this case the Kraus operators associated to $T_{a,b}$ are related by the phase λ [119],

$$V_i^{(a)} = e^{i\varphi_a} V_i^{(b)}$$

and the block $P_a M_n P_b$ does not dephase: the eigenmatrices associated to eigenvalues on the unit circle show no decay.

Note that such equivalences are not the same as a unitary equivalence of the type $V_i^{(a)} = U V_i^{(b)} U^*$ where U is a unitary matrix; such equivalences are already accounted for in the original decomposition.

Our aim is to obtain a decomposition of \mathcal{H} such that off-diagonal blocks all exhibit dephasing. This is done by collecting blocks that have no relative dephasing, which takes the form of an equivalence relation on the indices with classes

$$\begin{aligned} [a] &= \{b : P_a M_n P_b \text{ shows no dephasing} \} \\ &= \{b : |\lambda| = 1 \text{ for some } \lambda \in \sigma(T_{a,b})\}. \end{aligned}$$

By collecting equivalent blocks in Eq. (4.1) we obtain the decomposition

$$\mathcal{H} = \bigoplus_{[a]} \left[\bigoplus_{b \in [a]} \mathcal{K}_b \otimes \mathcal{H}_b \right]$$

while the Kraus operators take the form

$$\begin{aligned} V_i &= \bigoplus_{[a]} \left[\bigoplus_{b \in [a]} e^{i\varphi_b} \mathbf{1}_{\mathcal{K}_b} \otimes V_i^{(a)} \right] \\ &= \bigoplus_{[a]} \left[U_{[a]} \otimes V_i^{(a)} \right]. \end{aligned}$$

In the last line we have introduced a unitary operator U_a , acting on $\bigoplus_{b \in [a]} \mathcal{K}_b$, given by

$$U_{[a]} = \bigoplus_{b \in [a]} e^{i\varphi_b} \mathbf{1}_{\mathcal{K}_b}.$$

Then the off-diagonal blocks associated to the equivalence classes all exhibit relative dephasing, as desired.

Definition 4.1 (Phases). The *phases* of a quantum Markov process on M_n are the diagonal blocks $P_{[a]} M_n P_{[a]}$ obtained by grouping together equivalent diagonal blocks in the decomposition Eq. (4.1).

We denote by $P_{[a]}$ the orthogonal projection onto the subspace

$$\bigoplus_{b \in [a]} \mathcal{K}_b \otimes \mathcal{H}_b,$$

which may be written as $P_{[a]} = \sum_{b \in [a]} P_b$.

4.2.4 Stationary states

The block structure we have identified carries over to the structure of stationary states of T . We first note that relative dephasing for states means that $P_{[a]} \rho(n) P_{[b]} \rightarrow 0$ as $n \rightarrow \infty$ for any $[a] \neq [b]$. If $\rho_{[a]}$ is a state supported by $P_{[a]}$ then its evolution takes the form

$$\rho_{[a]}(n) = U_{[a]}^n \otimes T_{[a]}^n(\rho_{[a]});$$

a unitary rotation supported on the multiplicity space $\bigoplus_{b \in [a]} \mathcal{K}_b$ and an evolution due to the Kraus operators, supported on $\bigoplus_{b \in [a]} \mathcal{H}_b$.

As a result of relative dephasing between the blocks, stationary states on \mathcal{H} are convex linear combinations of stationary states supported by blocks: we denote by $\mathcal{S}(\mathcal{H})$ the set of stationary states for T , then

$$\mathcal{S}(\mathcal{H}) = \left\{ \bigoplus_{[a]} \lambda_{[a]} \rho_{[a]} : \lambda_{[a]} \geq 0, \sum_{[a]} \lambda_{[a]} = 1, \rho_{[a]} \in \mathcal{S}_{[a]} \right\}. \quad (4.3)$$

Here $\mathcal{S}_{[a]}$ denotes the set of stationary states supported by $P_{[a]} \mathcal{H}$, given by convex combinations of the extremal points

$$\mathcal{S}_e(\mathcal{H}) = \{ |\psi\rangle\langle\psi| \otimes \sigma_{[a]} : |\psi\rangle \text{ is an eigenvector of } U_{[a]} \} \quad (4.4)$$

where $\sigma_{[a]}$ is the unique stationary state for $T_{[a]}$.

Note that, if $U_{[a]}$ has nondegenerate spectrum, $\mathcal{S}_{[a]}$ is a simplex generated by a finite set of extremal points. If $U_{[a]}$ has degenerate spectrum, the set $\mathcal{S}_{[a]}$ is more subtle; for example if $U_{[a]} = \mathbf{1}$ then the set of eigenvectors for $U_{[a]}$ is a complex projective space (e.g. the Bloch sphere in two dimensions).

We point out that it is possible, for restricted evolutions $T_{[a]}, T_{[b]}$, with $[a] \neq [b]$, to be unitarily equivalent in the sense

$$T_{[a]}(U\rho_{[a]}U^*) = UT_{[b]}(\rho_{[b]})U^*,$$

while there still is dephasing between blocks. This is unitary equivalence on the level of the transition operator T , which is different from unitary equivalence of Kraus operators (this can happen, for example, as a result of non-uniqueness of the Kraus decomposition).

4.2.5 Measurement and trajectories

The decomposition into phases can be related to the statistics of measurements on the output. For our convenience we will suppose that the dynamics decomposes into two phases; furthermore, we assume that the phases have no multiplicity space associated to them. This last assumption is justified as follows. Since we are interested in the measurement statistics in the stationary regime, the probability distribution of a sequence of outcomes from a particular phase is

$$\mathbb{P}_a^{ss}(i_1, \dots, i_n) = \text{Tr}(V_{i_1} \cdots V_{i_n} |\psi\rangle\langle\psi| \otimes \rho_{ss} V_{i_1}^* \cdots V_{i_n}^*).$$

By the previous discussion, $V_i = U_a \otimes V_i^{(a)}$ and $|\psi\rangle$ is an eigenvector of U_a . The above trace therefore simplifies to

$$\mathbb{P}_a^{ss}(i_1, \dots, i_n) = \text{Tr}(V_{i_1}^{(a)} \cdots V_{i_n}^{(a)} \rho_{ss} V_{i_1}^{(a)*} \cdots V_{i_n}^{(a)*}),$$

showing that a multiplicity space with unitary U_a does not change the stationary distributions.

In this setting of two phases without multiplicity space, the phase decomposition of \mathcal{H} takes the form $\mathcal{H} = \mathcal{H}_a \oplus \mathcal{H}_b$ and the Kraus operators are of the form

$$V_i = V_i^{(a)} \oplus V_i^{(b)}.$$

At this point we note that it is possible for the two phases to give the same measurement output distributions. For example, suppose that

$V_i = \sqrt{\lambda_i} U_i^{(a)} \oplus \sqrt{\lambda_i} U_i^{(b)}$ where $U_i^{(a)}$ and $U_i^{(b)}$ are unitary operators, and $\lambda_i \geq 0$, $\sum_{i=1}^k \lambda_i = 1$. Then the restricted transition operators are

$$\begin{aligned} T_{a,*}(\rho_a) &= \sum_{i=1}^k \lambda_i U_i^{(a)} \rho_a U_i^{(a)*} \\ T_{b,*}(\rho_b) &= \sum_{i=1}^k \lambda_i U_i^{(b)} \rho_b U_i^{(b)*}; \end{aligned}$$

then trajectories generated by T_a and T_b have the same distributions, namely i.i.d. outcomes with probabilities λ_i . However, this does not exclude the possibility that a different choice of measurement will be able to distinguish the two phases. In fact [119], two blocks in the decomposition Eq. (4.1) are *not* dephasing if and only if their stationary quantum output states are the same; therefore, the classical measurement distributions are equal for any choice of measurement. Therefore, by construction of the phases, this means that there exists a measurement that gives different distributions for the two phases.

Suppose now that the system starts in a superposition of two states $|\psi_a\rangle$ and $|\psi_b\rangle$, associated to phase a and b , respectively, with initial state $|\psi\rangle = \sqrt{\lambda}|\psi_a\rangle + \sqrt{1-\lambda}|\psi_b\rangle$. Then the probability distribution for trajectories coming from the total system is

$$\mathbb{P}^\psi(i_1, \dots, i_n) = \lambda \mathbb{P}_a^{\psi_a}(i_1, \dots, i_n) + (1-\lambda) \mathbb{P}_b^{\psi_b}(i_1, \dots, i_n);$$

in other words, the distribution \mathbb{P}^ψ of trajectories is a mixture of distributions $\mathbb{P}_a^{\psi_a}$ and $\mathbb{P}_b^{\psi_b}$ associated to the two phases, with weights given by the initial state weights. Asymptotically, due to decay of correlations, there will be no dependence on the initial states $|\psi_a\rangle$ and $|\psi_b\rangle$ within each phase; therefore in the stationary regime, the distribution is a similar mixture given by $\mathbb{P}^{ss} = \lambda \mathbb{P}_a^{ss} + (1-\lambda) \mathbb{P}_b^{ss}$.

4.2.6 Purification of phases

The discussion of phases so far has concerned itself mainly with the measurement output. We will now see how phases play a role in the conditional evolution of the state of the system. Associated to a trajectory of outcomes is the conditional state of the system; if we have obtained a measurement trajectory (i_1, \dots, i_n) then the conditional state of the system is (cf. Eq. (3.8))

$$\rho(i_1, \dots, i_n) = \frac{V_{i_n} \cdots V_{i_1} \rho_0 V_{i_1}^* \cdots V_{i_n}^*}{\text{Tr}(V_{i_n} \cdots V_{i_1} \rho_0 V_{i_1}^* \cdots V_{i_n}^*)},$$

where $\rho(0)$ is the initial state.

Definition 4.2 (Phase purification). Suppose $\mathcal{H} = \mathcal{H}_a \oplus \mathcal{H}_b$ is the decomposition of the system into two phases. Then the system exhibits *phase purification* if the conditional state becomes supported on one of the phases; that is, if

$$\lim_{n \rightarrow \infty} \text{Tr} [P_a \rho(i_1, \dots, i_n)] \in \{0, 1\},$$

almost surely with respect to the stationary probability distribution on trajectories.

It is vital to note that the notion of phase purification depends on the choice of measurement. In particular, suppose that the distributions associated to the phases are identical ($\mathbb{P}_a = \mathbb{P}_b$). This means that we cannot decide from looking at the trajectories whether the state of the system is in phase a or phase b, and so no purification occurs.

Phase purification is a statement about the *conditional state*, but it also appears in the stationary states. Suppose the initial state ρ_0 has weights $\lambda = \text{Tr} [P_a \rho_0]$ and $1 - \lambda = \text{Tr} [P_b \rho_0]$. Then the stationary state ρ_{ss} will take the form

$$\rho_{ss} = \lambda \rho_{ss}^{(a)} \oplus (1 - \lambda) \rho_{ss}^{(b)}, \quad (4.5)$$

where $\rho_{ss}^{(i)}$ is the unique stationary state in phase i. The ratio of initial weights λ gives the proportion of trajectories associated to phase a, versus those associated to phase b.

4.2.7 Large deviations and phase transitions

Large deviations rate functions may be used to show that phase purification should occur, for suppose that the stationary output distributions $\mathbb{P}_a, \mathbb{P}_b$ are not identical. Then, as we noted above, there is some local statistic on which the two distributions disagree (i.e., they have different means). Then the large deviations rate functions, say $\Lambda_a(\cdot)$ and $\Lambda_b(\cdot)$ associated to the phases are not the same.

Since the distribution of the trajectories from the total system is a mixture

$$\mathbb{P} = \lambda \mathbb{P}_a + (1 - \lambda) \mathbb{P}_b.$$

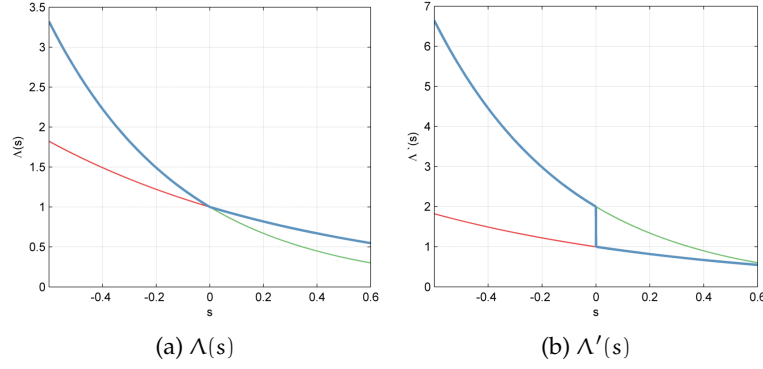


Figure 4.1: Different rate functions for the phases (red and green) lead to the rate function for the combined system (blue) exhibiting a jump in the first derivative (cf. Fig. 4.7b below)

The large deviation rate function for any stochastic process X_n associated to the output (for instance, the sample mean of counts) is

$$\begin{aligned}\Lambda(s) &= \lim_{n \rightarrow \infty} \frac{1}{n} \log (\lambda \mathbb{E}_a [e^{sX_n}] + (1 - \lambda) \mathbb{E}_b [e^{sX_n}]) \\ &= \max_{a,b} \{\Lambda_a(s), \Lambda_b(s)\}.\end{aligned}$$

Then, as shown in Fig. 4.1, this will lead to a non-analyticity at some s for the rate function $\Lambda(\cdot)$, although the individual rate functions are smooth.

For example, consider the simple case of the sample mean of the counting process associated to the output. It is possible for phase purification to occur, without this being visible in the distribution for the sample mean. In this case, the rate function for a higher level statistic is required to show phase purification. For more on higher level rate functions, see Ch. 6.

If the sample mean distributions are different, this does not necessarily happen for the first moments (i.e., the mean); rather, a higher moment such as the variance might be required to see the difference. This corresponds to a discontinuity at $s = 0$ appearing on a higher derivative of the rate function. Of course, taking a higher moment as the initial statistic causes the phase transition to appear at the level of the first moment of this new statistic.

The connection between the phase structure and the large deviations rate function may be summarised as follows. If there is a single phase, then the rate function is analytic, and there is no dynamical phase transition.

If there are two (or more) phases, there are the following two possibilities:

- A. the measurement processes have the same distribution (although the output quantum states are not identical) — equivalently, the phases are dephasing at the level of the master equation;
- B. the measurement processes have different distributions: in this case, it is possible for the rate function to be non-analytic (e.g. a jump in the first moment), and this is a dynamical phase transition associated to phase purification.

4.2.8 Phase transition as change in phase structure

So far we have discussed phase purification, where a dynamical phase transitions in the sense of a discontinuity of a rate function with respect to a large deviations parameter s . We can also look at phase transitions in a more general sense, and say that a phase transition occurs when the phase structure changes, as a result of a change in a parameter g of the system. In terms of phase purification this means, for example, that a critical point $g = g_0$ is a phase transition if there is no phase purification for $g < g_0$, while there is phase purification for $g \geq g_0$.

The distinction between non-analytic behaviour in s for some fixed g , and non-analytic behaviour in g itself, may be illustrated as follows. In terms of the large deviations rate function $\Lambda(s)$, this means that Λ is smooth for $g < g_0$ while Λ is non-analytic at $s = 0$ for $g \geq g_0$. This point of view allows us to track phase transitions by considering non-analytic behaviour in the two-variable function $\Lambda(s, g)$. The dependence on g may be visible in the output on higher level large deviations but not the first one, as in the third example below. This shows that the higher level large deviations contain more information than the first. The example discussed below has a smooth family of Kraus operators $\{V_i^g\}$ such that in the limit $g \rightarrow g_0^+$ the stationary state converges to ρ_s^1 and in the limit $g \rightarrow g_0^-$ the stationary state converges to ρ_s^2 , where both limiting stationary states are non-faithful (e.g. pure); in this case, $\Lambda(s, g)$ is non-analytic in g at g_0 but analytic in s .

4.3 CONTINUOUS-TIME PHASE STRUCTURE

For continuous-time processes, the discretisation scheme discussed in Sec. 5.2 can be employed to obtain an analogous discrete-time system described by a family of Kraus operators. To this system one can then apply the methods from the previous section.

An alternative approach is found in [116] (see also [120, 121]). The authors consider the structure of quantum dynamical semigroups in continuous time in terms of algebraic properties of the commutant $\mathcal{N} = \{H, L_k\}'$ of the Hamiltonian H and the jump operators $\{L_k\}$. This is done as follows: orthogonal projections P_i in \mathcal{N} correspond to *minimal collecting subspaces* $P_i M_n P_i$; these correspond precisely to the blocks in our decomposition.

As in our setting, off-diagonal blocks $P_i M_n P_j$ do not necessarily show dephasing; equivalent minimal collecting subspaces are grouped together to obtain projections Q_i . Then the blocks $Q_i M_n Q_j$ are relatively dephasing, and each such block $Q_i M_n Q_i$ consists of repetitions of unitarily equivalent blocks; the Hilbert space \mathcal{H} may be expressed as in Eq. (4.1) where $Q_i \mathcal{H} = \mathcal{K}_i \otimes \mathcal{H}_i$. The restricted evolution on a subspace $Q_i M_n Q_i$ is of the form $U_t \otimes T^{(i)}$, where $T^{(i)}$ has a unique stationary state and U_t is a fixed unitary on the multiplicity space.

In Eq. (4.3) we described the set of stationary states in the case of discrete time. In continuous time [116, Thm. 2 (3)], for all initial states ρ the time evolution $T_{t,*}(\rho)$ satisfies the asymptotic form

$$\lim_{t \rightarrow \infty} \left| T_{t,*}(\rho) - \bigoplus_{i=1}^N \lambda_i e^{-iH_i t} R_i e^{iH_i t} \otimes \rho_i \right| = 0 \quad (4.6)$$

where $0 \leq \lambda_i \leq 1$ with $\sum_{i=1}^N \lambda_i = 1$, and each $R_i \in M_{n(i)}$ is a positive matrix with trace one. The weights λ_i and the matrices R_i depend on the initial state ρ , and each ρ_i is a *unique* stationary state on \mathcal{H}_i .

This asymptotic form shows that, as we expect due to the dephasing condition introduced before, the state $\rho(t)$ becomes concentrated on the subspaces $Q_i M_n Q_i$. Eq. (4.6) shows that the time evolution in each block is reduced to a unitary (reversible) evolution on the multiplicity space with $U_{i,t} = \exp(iH_i t)$. As a direct corollary of this, the set of stationary states $\mathcal{S}_{ss}(M_n)$ consists of the states formed in Eq. (4.6) where each R_i commutes with the unitary $U_{i,t}$:

$$\mathcal{S}_{ss}(M_n) = \left\{ \bigoplus_{i=1}^N \lambda_i R_i \otimes \rho_i : [H_i, R_i] = 0, \lambda_i \geq 0, \sum_{i=1}^N \lambda_i = 1 \right\}.$$

Comparing with Eq. (4.3) shows the similarities between the continuous-time and discrete-time settings.

4.4 EXAMPLES

In this section, we will examine both discrete-time and continuous-time cases and see how the features discussed in the previous two sections appear in some basic models.

4.4.1 Example 1: intermittency and purification

The first example we consider is a discrete time quantum Markov chain on M_2 , which physically can be interpreted as a single qubit channel. Consider the dynamics given by the pair of Kraus operators

$$V_1 = a \begin{pmatrix} 1 & 0 \\ 0 & -1 \end{pmatrix}, \quad V_2 = b \begin{pmatrix} -1 & 0 \\ 0 & 1 \end{pmatrix}.$$

Then there is a single phase, with a two-dimensional multiplicity space: the phase decomposition is effectively given by $\mathbb{C} \oplus \mathbb{C}$ and the stationary states are of the form $\rho \otimes \sigma$ where ρ is unique and σ is in the space spanned by the eigenvectors of the unitary operator acting on the multiplicity space (as in Eq. (4.4)). The stationary phase is one-dimensional and there are two Kraus operators acting on it,

$$V_1^1 = a\mathbf{1}, \quad V_2^1 = -b\mathbf{1},$$

corresponding to a restriction of the original Kraus operators to the state $|0\rangle$; since the space is one-dimensional these can be thought of as a and $-b$, respectively. If instead we restrict the Kraus operators to the state $|1\rangle$ we obtain the same operators but with opposite minus sign,

$$V_1^2 = -a\mathbf{1}, \quad V_2^2 = b\mathbf{1},$$

These restricted Kraus operators can be considered simultaneously by writing

$$V_i = U \otimes V_i^1, \quad U = \begin{pmatrix} 1 & 0 \\ 0 & -1 \end{pmatrix}.$$

At this point, we do not observe any intermittency in the trajectories to indicate a phase transitions, since there is no sense in which the phase

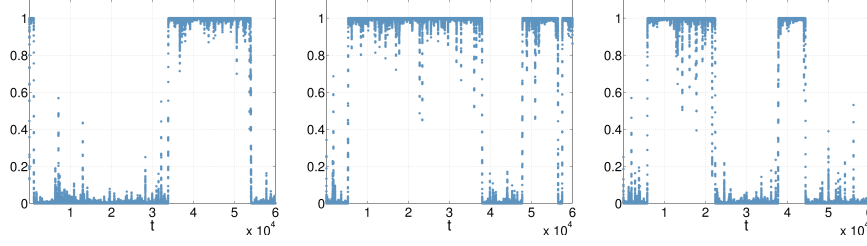


Figure 4.2: Sample trajectories with the perturbed Kraus operators showing intermittency and no long-time purification

splits into two separate phases for some value of the parameters a, b . The evolution of the state in this case will simply rotate with the unitary operator U on the multiplicity space.

So far, the one-dimensional phases are equivalent and therefore no phase purification occurs. Now we consider an extension of the model which lets us construct a point where the system goes from being degenerate to being nondegenerate. The Kraus operators are given by a perturbation of the previous ones,

$$V_1 = \begin{pmatrix} a_0 & \epsilon_1 \\ 0 & a_1 \end{pmatrix}, \quad V_2 = \begin{pmatrix} b_0 & 0 \\ \epsilon_2 & b_1 \end{pmatrix},$$

with $a_0 \neq a_1$, $b_0 \neq b_1$, and $\epsilon_i > 0$.

Previously there was a single phase with a multiplicity space of dimension two; if $a_0 \neq a_1$ and $\epsilon_1 = 0$ (and similar for V_2), we have i.i.d. measurements and phase purification occurs. If we are close to the Kraus operators from the last example (that is, $a_0 \approx a_1$, $b_0 \approx b_1$ and $\epsilon_i > 0$) we see intermittency in the trajectories; this is most visible by choosing the perturbation from the diagonal case an order of magnitude larger than ϵ_i . Purification comes from the phases having statistically different trajectories; intermittency comes from the off-diagonal ϵ_i allowing for transitions between phases. - For example, in Fig. 4.2 we show sample trajectories with the Kraus operators

$$V_1 = \begin{pmatrix} 0.77 & 0.01 \\ 0 & -0.63 \end{pmatrix}, \quad V_2 = \begin{pmatrix} -0.63 & 0 \\ -0.01 & 0.77 \end{pmatrix}.$$

These trajectories show jumps between the stationary states $|0\rangle$ and $|1\rangle$ of the unperturbed Kraus operators. For short timescales we see purification towards these eigenstates, but on longer timescales jumps between these phases due to the off-diagonal perturbation.

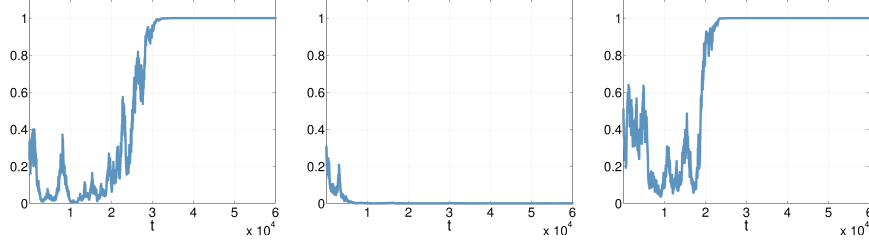


Figure 4.3: Sample trajectories with the perturbed Kraus operators showing purification without intermittency

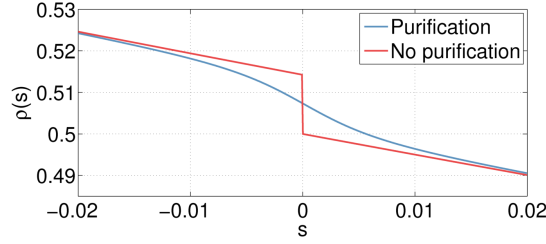


Figure 4.4: Derivatives of the rate functions associated to the Kraus operators from Fig. 4.2 without purification (blue), and those from Fig. 4.3 with purification (red), showing that the rate function with purification is non-analytic at $s = 0$.

We see purification towards the eigenstates without intermittency by removing the off-diagonal perturbations; in 4.3 we take

$$V_1 = \begin{pmatrix} 0.72 & 0 \\ 0 & -0.71 \end{pmatrix}, \quad V_2 = \begin{pmatrix} -0.70 & 0 \\ 0 & 0.71 \end{pmatrix}.$$

With no perturbation present to allow transitions between the phases, we see that the trajectories purify towards the eigenstates. In Fig. 4.4 we show the derivatives of the large deviations rate functions associated to the two cases. When there is purification, there is a discontinuity in the rate function at $s = 0$.

4.4.2 Example 2: four-level system

The next example is a continuous time quantum Markov process; we are looking at a four-level system with a single jump operator; this can be interpreted as a system composed of two interacting qubits. The four levels are denoted $\{|0\rangle, |0'\rangle, |1\rangle, |1'\rangle\}$; the Hamiltonian is

$$H = \Omega_1|0\rangle\langle 1| + \Omega_2|0'\rangle\langle 1'| + \Lambda|1\rangle\langle 1'| + \text{h.c.}$$

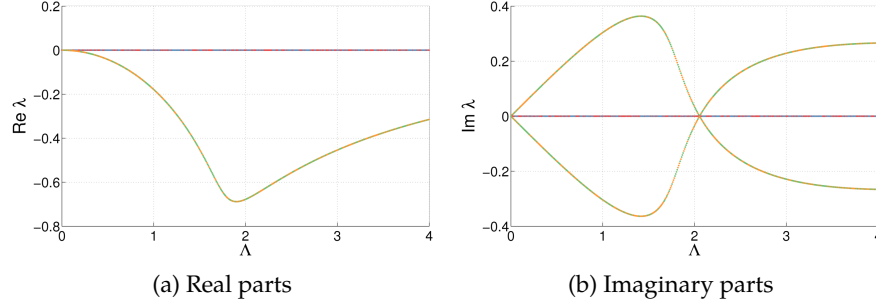


Figure 4.5: Top four eigenvalues of master operator \mathcal{L} with $\Omega_1 = \Omega_2 = 1$. Note $\lambda_1 = 0$ is doubly degenerate for $\Lambda > 0$, and quadruply degenerate for $\Lambda = 0$.

and the jump operator acts coherently (i.e. identically on the subsystems) as

$$L = \sqrt{\kappa} (|0\rangle\langle 1| + |0'\rangle\langle 1'|).$$

Time evolution of the density operator ρ is then given by the master operator

$$\mathcal{L}(\rho) = -i[H, \rho] + L\rho L^* - \frac{1}{2}\{L^*L, \rho\}.$$

We will initially consider the case where the subsystems have the same coupling $\Omega_1 = \Omega_2$ (so the dynamics is symmetric with respect to the interchange $0 \leftrightarrow 0', 1 \leftrightarrow 1'$). Coupling between the subsystems is governed by Λ ; when $\Lambda = 0$ the subsystems evolve independently. To investigate the possible occurrence of phase a dynamical phase transition at $\Lambda = 0$ we consider the following questions:

- Does the *activity* $K(\Lambda, s) = \partial_s \lambda(\Lambda, s)$ show any interesting behaviour around this critical point?
- Is the top eigenvalue of \mathcal{L} degenerate at $\Lambda = 0$ and does increasing Λ lift this degeneracy?
- Do the jump trajectories depend on Λ ? In particular, do they show intermittency near $\Lambda = 0$?
- What does the stationary state look like (can it be decomposed into states on the subsystems, or a tensor product with a symmetric or anti-symmetric state)?

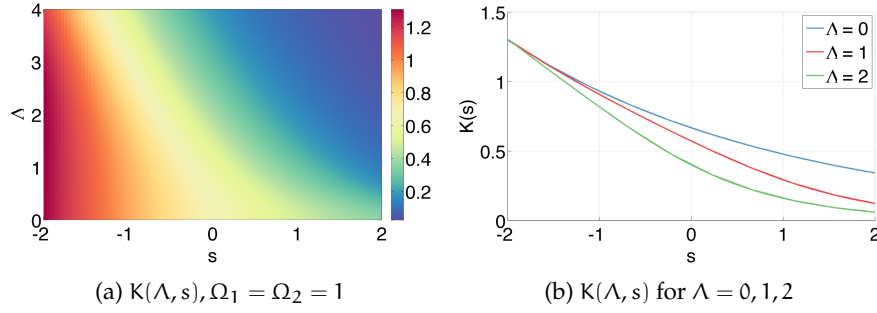


Figure 4.6: Activity $K(\Lambda, s)$ for equal $\Omega_1 = \Omega_2$, showing a smooth first derivative $K(\Lambda, s) = \partial_s \lambda(\Lambda, s)$ of the rate function

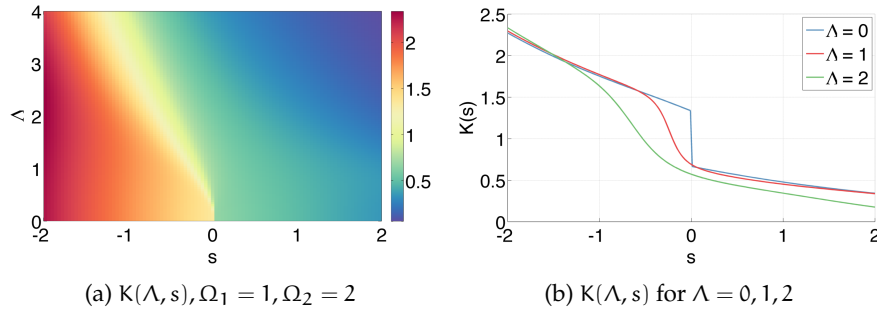


Figure 4.7: $K(\Lambda, s)$ for $\Omega_1 \neq \Omega_2$, showing a jump at $\Lambda = 0$; this is a dynamical phase transition in s , or a quantum phase transition in the limit $\Lambda \rightarrow 0$

The activity $K(\Lambda, s)$ is given by the derivative with respect to s of the top eigenvalue of the perturbed master operator $\mathcal{L}_s(\cdot)$

$$\mathcal{L}_s(\rho) = -i[H, \rho] + e^{-s} L \rho L^* - \frac{1}{2} \{L^* L, \rho\}.$$

In Fig. 4.6a the activity is shown as a function of Λ and s , while in Fig. 4.6b the activity is plotted for fixed values of Λ . The activity appears to be a smooth function of s for all values of the subsystem coupling Λ ; if there is indeed a phase transition, it is not indicated by this parameter. Note that when the symmetry is broken ($\Omega_1 \neq \Omega_2$) the activity shows a jump at $s = 0$.

Fig. 4.5 shows the four largest eigenvalues of \mathcal{L} (including degeneracies). At $\Lambda = 0$ the top eigenvalue $\lambda_1 = 0$ is quadruply degenerate. This degeneracy is partially lifted by increasing Λ , which introduces a complex conjugate pair $\lambda_2, \bar{\lambda}_2$ while the degeneracy of λ_1 is decreased to two.

The simplest scenario in this model is the choice of parameters $\Omega_1 = \Omega_2$ and $\Lambda = 0$. The initial state $|\psi\rangle$ determines the evolution (when

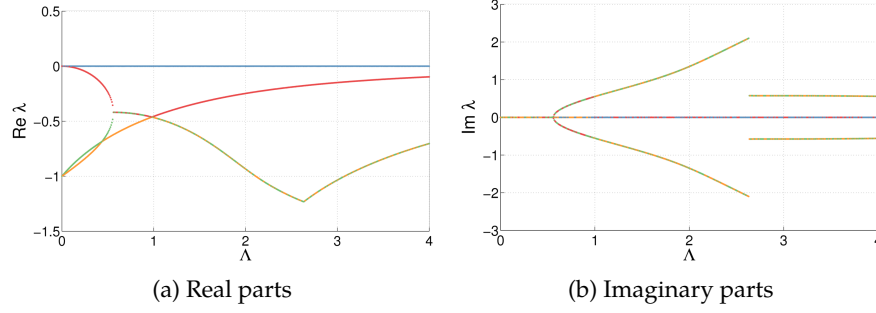


Figure 4.8: Top four eigenvalues of master operator \mathcal{L} with $\Omega_1 = 1, \Omega_2 = 2$. Note $\lambda_1 = 0$ is doubly degenerate only for $\Lambda = 0$.

$\Lambda = 0$). To see this, note that the Hilbert space decomposes into $\mathbb{C}^2 \otimes \mathbb{C}^2$ (one phase with two-dimensional multiplicity space) and any stationary state is of the form $P_{|\psi\rangle\langle\psi|} \otimes \rho_{ss}$ (see Eq. (4.4)). In particular, eigenmatrices of \mathcal{L} are given by $\rho_i = E_i \otimes \rho$ where

$$\rho = \begin{pmatrix} \frac{\kappa^2 + 4\Omega_1^2}{4\Omega_1^2} & \frac{\kappa i}{2\Omega_1} \\ -\frac{\kappa i}{2\Omega_1} & 1 \end{pmatrix}$$

and E_1, \dots, E_4 are the standard matrix units,

$$E_1 = \begin{pmatrix} 1 & 0 \\ 0 & 0 \end{pmatrix}, E_2 = \begin{pmatrix} 0 & 0 \\ 0 & 1 \end{pmatrix}, E_3 = \begin{pmatrix} 0 & 1 \\ 0 & 0 \end{pmatrix}, E_4 = E_3^*.$$

In this case, clearly ρ_1 and ρ_2 can be normalised to be valid density matrices $\tilde{\rho}_1, \tilde{\rho}_2$; ρ_3 and ρ_4 are neither self-adjoint nor can they be normalised. However, $\rho_3 = \rho_4^*$ so any stationary state is of the form

$$\rho_{ss} = t\tilde{\rho}_1 + (1-t)\tilde{\rho}_2 + z\rho_3 + \bar{z}\rho_4$$

where $0 \leq t \leq 1$ and $z \in \mathbb{C}$. This reflects the fact that the dynamics on the multiplicity space \mathbb{C}^2 is fully degenerate, meaning there is the entire Bloch sphere of stationary states on the multiplicity space.

We now move to a more complex model and take our parameters to be $\Omega_1 \neq \Omega_2$ and $\Lambda = 0$; the phase decomposition is now $\mathbb{C}^2 \oplus \mathbb{C}^2$, so there are two phases \mathbb{C}^2 with no multiplicity. This is most clearly seen in the nullspace of \mathcal{L} , which is now two-dimensional:

$$\rho_1 = \begin{pmatrix} \frac{\kappa^2 + 4\Omega_1^2}{4\Omega_1^2} & \frac{\kappa i}{2\Omega_1} & 0 & 0 \\ -\frac{\kappa i}{2\Omega_1} & 1 & 0 & 0 \\ 0 & 0 & 0 & 0 \\ 0 & 0 & 0 & 0 \end{pmatrix}, \rho_2 = \begin{pmatrix} 0 & 0 & 0 & 0 \\ 0 & 0 & 0 & 0 \\ 0 & 0 & \frac{\kappa^2 + 4\Omega_2^2}{4\Omega_2^2} & \frac{\kappa i}{2\Omega_2} \\ 0 & 0 & -\frac{\kappa i}{2\Omega_2} & 1 \end{pmatrix}.$$

As in the previous case, these may be normalised to obtain density operators $\tilde{\rho}_1, \tilde{\rho}_2$ and any stationary state is represented by a density matrix of the form

$$\rho_{ss} = t\tilde{\rho}_1 + (1-t)\tilde{\rho}_2$$

where $0 \leq t \leq 1$; this is exactly the situation described in Eq. 4.5 above, with the parameter t determined by the phase weight of the initial state. Rather than having a full Bloch sphere of all states on \mathbb{C}^2 , we are now restricted to convex combinations of two extremal states. Fig. 4.9b shows a trajectory corresponding to this choice of parameters, and we see that phase purification indeed occurs.

So far, the coupling Λ has been considered zero. The most interesting dynamics occur when the coupling parameter is taken to be non-zero. With $\Omega_1 = \Omega_2$ and $\Lambda > 0$ the nullspace is again two-dimensional, spanned by the matrices ρ_1 , given by

$$\begin{pmatrix} 0 & 1 & -\frac{\kappa^2+4\Lambda^2+4\Omega_1^2}{4\Lambda\Omega_1} & -\frac{\kappa i}{2\Lambda} \\ 1 & 0 & \frac{\kappa i}{2\Lambda} & -\frac{\Omega_1}{\Lambda} \\ -\frac{\kappa^2+4\Lambda^2+4\Omega_1^2}{4\Lambda\Omega_1} & -\frac{\kappa i}{2\Lambda} & 0 & 1 \\ \frac{\kappa i}{2\Lambda} & -\frac{\Omega_1}{\Lambda} & 1 & 0 \end{pmatrix}$$

and ρ_2 , given by

$$\begin{pmatrix} \frac{\kappa^2+4\Lambda^2+4\Omega_1^2}{4\Omega_1^2} & 0 & \frac{\kappa^3 i+4\kappa\Lambda^2 i+4\kappa\Omega_1^2 i}{8\Lambda\Omega_1^2} & -\frac{\kappa^2+4\Lambda^2}{4\Lambda\Omega_1} \\ -\frac{\kappa i}{\Omega_1} & 1 & \frac{\kappa^2-4\Lambda^2}{4\Lambda\Omega_1} & \frac{\kappa i}{2\Lambda} \\ \frac{\kappa(\kappa^2+4\Lambda^2+4\Omega_1^2) i}{8\Lambda\Omega_1^2} & -\frac{\kappa^2+4\Lambda^2}{4\Lambda\Omega_1} & \frac{\kappa^2+4\Lambda^2+4\Omega_1^2}{4\Omega_1^2} & 0 \\ \frac{\kappa^2-4\Lambda^2}{4\Lambda\Omega_1} & \frac{\kappa i}{2\Lambda} & -\frac{\kappa i}{\Omega_1} & 1 \end{pmatrix}.$$

Since

$$\rho_2^* = \frac{i\kappa}{\Omega_1}\rho_1 + \rho_2$$

we have $\mathcal{L}(\rho_2^*) = 0$ and we obtain a stationary state $\tilde{\rho}$ from normalisation of $\rho_2 + \rho_2^*$. Since ρ_1 is traceless and self-adjoint, the general stationary state is of the form

$$\rho_{ss} = \tilde{\rho} + t\rho_1$$

where $t \in \mathbb{R}$. Since this family of stationary states is fully supported, there can be no dephasing: there are no stationary states which are located only in either one of the phases.

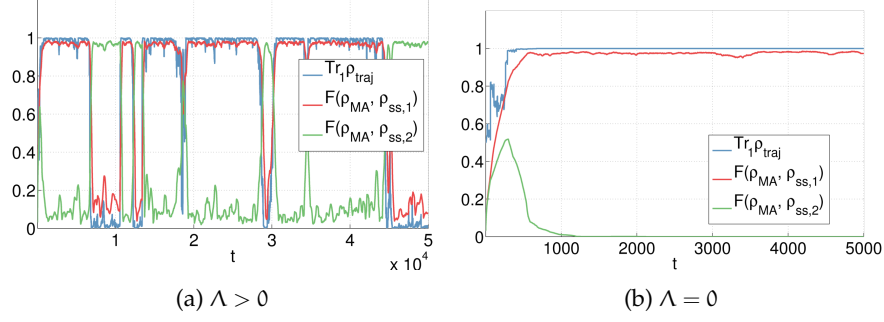


Figure 4.9: Phase weight $\text{Tr}_1 \rho$ of representative trajectories (blue) near $\Lambda = 0$; fidelity F of moving average with the stationary phases $\rho_{ss,1}, \rho_{ss,2}$ (red and green) with $\Omega_1 = 1$ and $\Omega_1 = 1.15$.

With $\Omega_1 \neq \Omega_2, \Lambda > 0$ the nullspace of \mathcal{L} is one-dimensional, with a unique stationary state ρ_{ss} ; again, no dephasing occurs. We conclude that whenever $\Lambda > 0$, there is only a single phase, with no multiplicity in this last case. Fig. 4.9a shows a trajectory corresponding to these parameters. Over short timescales, phase purification occurs, with trajectories moving towards one phase or the other. However, on longer timescales, intermittency plays a role, since we now have communication between the two phases; long-term purification is not possible.

4.4.2.1 Phase transitions

In the case of a single (coherent) jump, the most interesting behaviour is near $\Lambda = 0$ with Ω_1 slightly different from Ω_2 . As seen in Fig. 4.8a and the discussion above, when $\Lambda \rightarrow 0$ the unique eigenvector ‘decouples’ into a direct sum of eigenvectors $\rho_{ss,1} \oplus \rho_{ss,2}$ supported in the subspaces $\{|0\rangle, |1\rangle\}$ and $\{|0'\rangle, |1'\rangle\}$ respectively.

For $\Lambda = 0$ and $\Omega_1 \neq \Omega_2$ the stationary state ρ_{ss} may be expressed as a convex combination of the stationary states ρ_a, ρ_b corresponding to the separate two-level systems (or *phases*),

$$\rho_{ss} = \lambda \rho_a + (1 - \lambda) \rho_b, \quad 0 \leq \lambda \leq 1.$$

The simulations 4.9 show that, although theoretically any of the above convex combinations ρ_{ss} are valid stationary states, the system always ends up in either ρ_a or ρ_b . This is exactly the phase purification we discussed in the previous section.

The quantum phase transition occurs in the limit $\Lambda \rightarrow 0$; for any $\Lambda > 0$ the system has no dephasing, and the multiplicity components

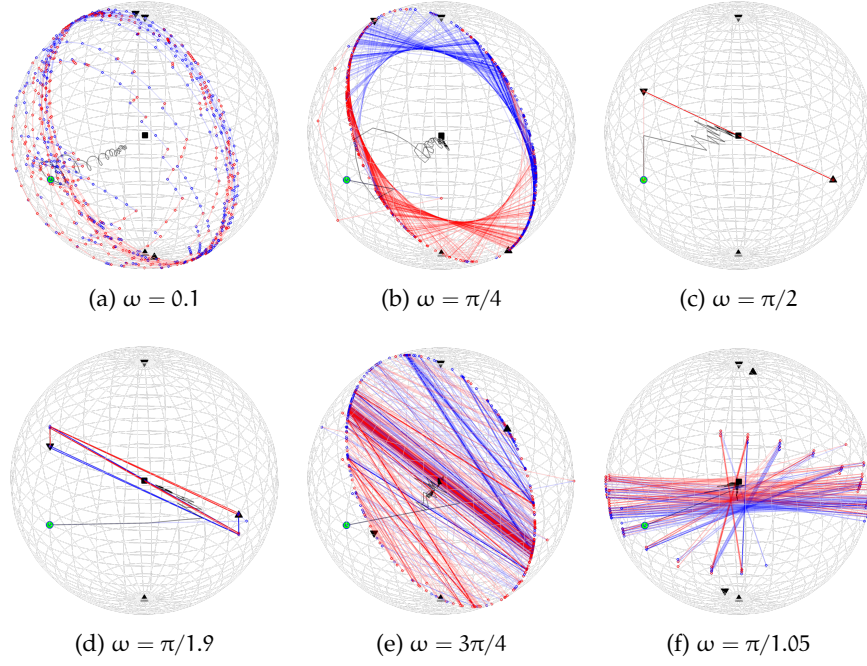


Figure 4.10: Representative trajectories showing dramatic variation in behaviour. The critical points are $\omega = 0$ and $\omega = \pi/2$; other parameters as in Fig. 4.12.

are trivial: the phase decomposition is simply \mathbb{C}^4 . At the point $\Lambda = 0$ this phase structure changes into $\mathbb{C}^2 \otimes \mathbb{C}^2$ if the rates Ω_i are equal, and $\mathbb{C}^2 \oplus \mathbb{C}^2$ if the rates are different. In Fig. 4.7 the first derivative of the rate function shows a jump at $s = 0$ when $\Lambda \rightarrow 0$, indicating this phase transition.

4.4.3 Example 3: ‘symmetry breaking’ from perturbation: XX0 interaction

The final example is again a discrete time quantum Markov chain; this example could be seen as a generalisation of the first example. The interaction is given by the Heisenberg XYZ model, where $U = \exp(-iH)$ with

$$H = -\frac{1}{2} (J_x \sigma_x \sigma_x + J_y \sigma_y \sigma_y + J_z \sigma_z \sigma_z),$$

where σ_x, σ_y and σ_z are the standard Pauli operators. In particular, we are interested in the case where $J_x = J_y = \omega$ and $J_z = 0$, in which case the Kraus operators take the form

$$K_0 = \begin{pmatrix} \lambda & 0 \\ i\mu \sin \omega & \lambda \cos \omega \end{pmatrix}, \quad K_1 = \begin{pmatrix} \mu \cos \omega & i\lambda \sin \omega \\ 0 & \mu \end{pmatrix}$$

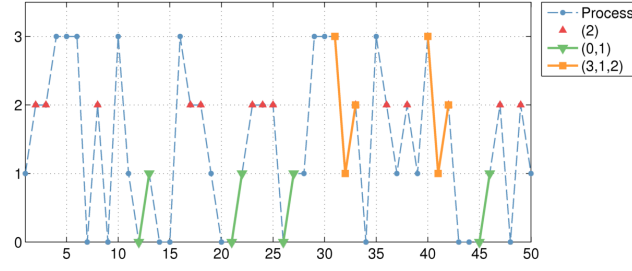


Figure 4.11: Sample trajectory with events associated to different levels.

where $\lambda = \cos \varphi_1$ and $\mu = e^{-i\varphi_2} \sin \varphi_1$ are the components of the initial state of the incoming qubits. We will refer to this setting as the ‘XX0’ model.

In Fig. 4.10 sample trajectories are plotted on the Bloch sphere for various values of ω showing how behaviour changes qualitatively. Below we will investigate in more detail how the different patterns of behaviour may be explained.

4.4.3.1 Rate functions and spectral properties

In Ch. 6 below we discuss the Sanov theorem for quantum systems. In Fig. 4.12 we have computed the Sanov theorem level 1 and level 2 rate functions. The level 1 rate function is associated to frequencies of outcomes, while the level 2 rate function is associated to frequencies of *pairs* of outcomes. Interestingly, the level 1 rate function shows no dependency on ω , while the level 2 rate function does vary with ω . This suggests that higher level rate functions are able to detect more information than lower level rate functions, in the following sense. In this context, there are only two types of jumps: this means that the level 1 rate function is associated to the mean number of jumps of one type. The level 2 rate function can distinguish between trajectories for which this mean is the same, by detecting the different rates at which pairs of jumps occur, which is illustrated in Fig. 4.11.

Fig. 4.13 shows the spectrum of the transition operator T as a function of ω , showing that degeneracy appears at $\omega = 0$ and $\omega = \pi$. At the point $\omega = 0$ the stationary state is fully degenerate i.e. any state is a stationary state; this suggests a phase decomposition $\mathbb{C}^2 \otimes \{1\}$ with maximal multiplicity space. At $\omega = \pi$ the set of stationary states is the convex hull of the extremal stationary states $|0\rangle$ and $|1\rangle$ (that is, the vertical line joining the north and south poles of the Bloch sphere;) the phase decomposition associated to this degeneracy is $\mathbb{C} \otimes \mathbb{C}$, with a one-

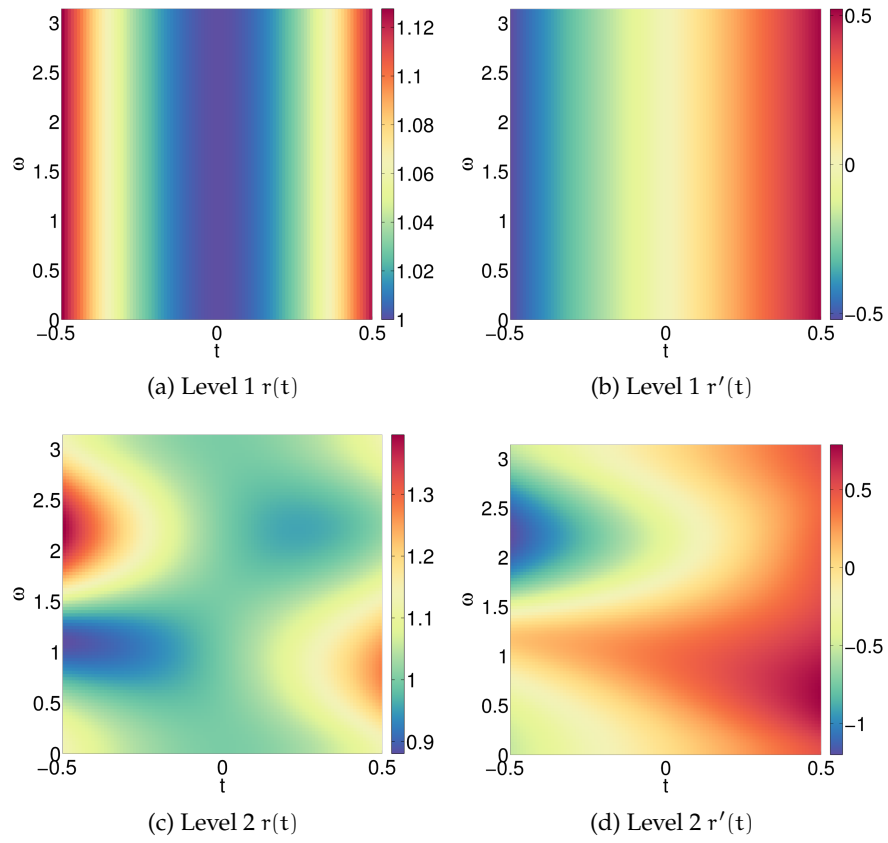


Figure 4.12: Sanov level 1 and 2 spectral radii and their derivatives for the XX0 model ($t = [t, -t]$ for level 1 and $t = [t, -t; -t, t]$ for level 2). Initial atom state angle $\pi/4$ and phase π .

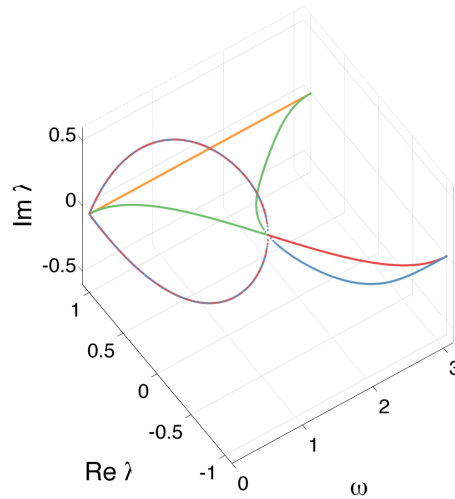


Figure 4.13: Spectrum of transition operator (real and imaginary parts) showing 4-fold degeneracy at $\omega = 0$ and 2-fold degeneracy at $\omega = \pi$

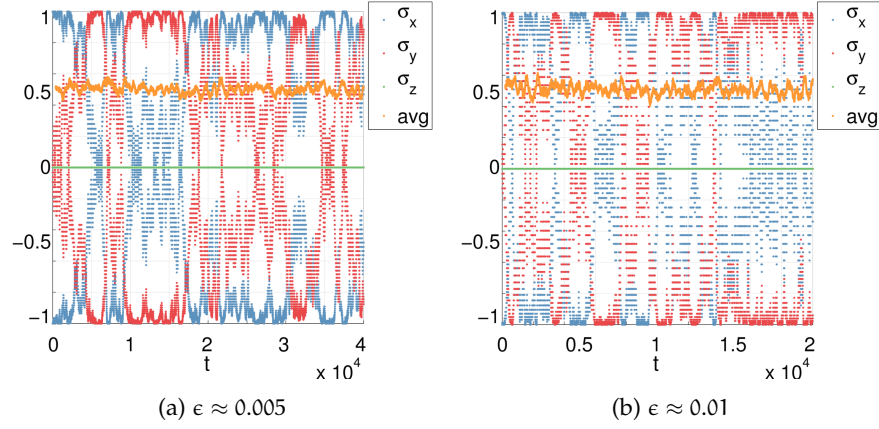


Figure 4.14: Expectations of Pauli operators σ_i in the 'XX ϵ ' model at $\omega = \pi$ critical point (note different scales)

dimensional multiplicity space. In between these critical values the decomposition may be written as $\mathbf{1} \otimes \mathbb{C}^2$, with a unique stationary state for $0 < \omega < \pi$.

4.4.3.2 Trajectories and phase transitions

This example shows an interplay between dynamical phase transitions (in s) and quantum phase transitions (in ω). We consider the trajectories of this system near the points $\omega = 0$ and $\omega = \pi$ to see how the behaviour changes near these critical points. In Figs. 4.15 and 4.14 we consider the expectation values of the Pauli operators along sample trajectories close to these critical points. We approach the critical point by choosing a very small $J_z = \epsilon$. The trajectories suggest there is some intermittency in the expectation value of σ_z , which is shown in Fig. 4.18.

The stationary state at $\omega = \pi$ depends strongly on the direction of the limit used to approach the critical point. In Fig. 4.16 we see that the limit

$$\lim_{g \rightarrow 0} \lim_{\omega \rightarrow \pi} \rho_{ss}^{(J)} \quad (4.7)$$

depends strongly on which particular line in the (ω, g) plane we choose to approach the limit $J = [\pi, \pi, 0]$. For example, we see that (following the green line)

$$\lim_{g \rightarrow 0^+} \lim_{\omega \rightarrow \pi^+} \rho_{ss}^{(J)} = |0\rangle\langle 0| \quad (4.8)$$

while

$$\lim_{g \rightarrow 0^+} \lim_{\omega \rightarrow \pi^-} \rho_{ss}^{(J)} = |1\rangle\langle 1|. \quad (4.9)$$

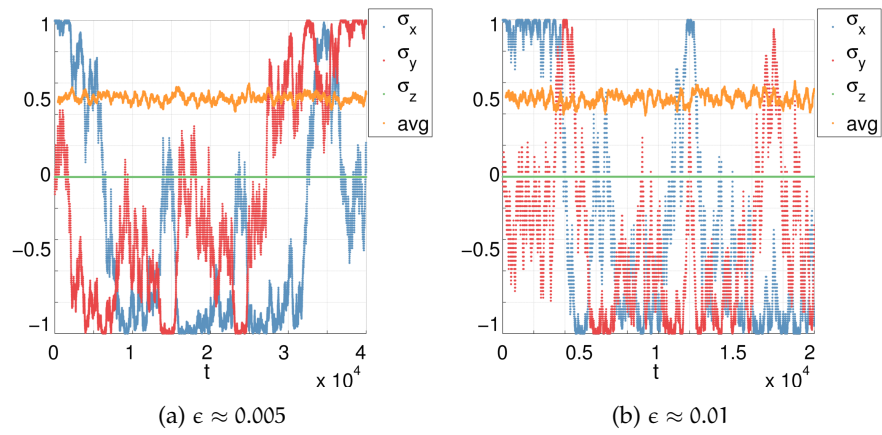


Figure 4.15: Expectations of Pauli operators σ_i in the 'XXe' model at $\omega = 0$ critical point

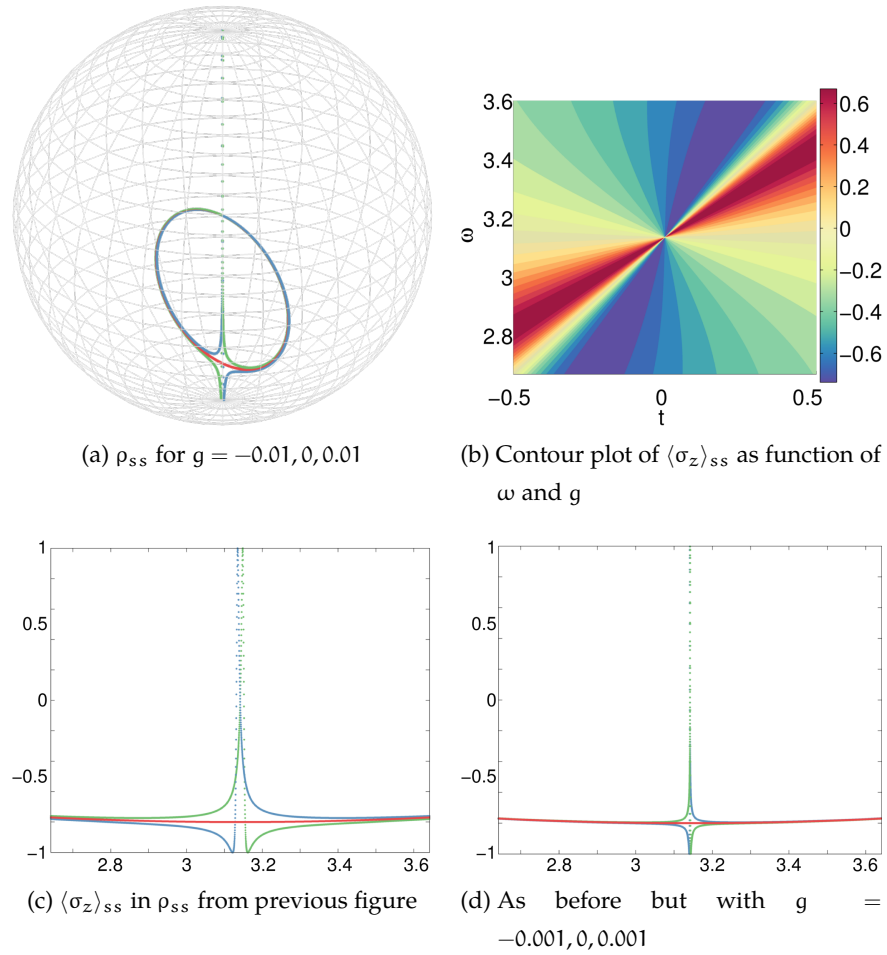


Figure 4.16: Jump in the stationary state ρ_{ss} at $\omega = \pi$ with $J = [\omega, \omega - g, 0]$

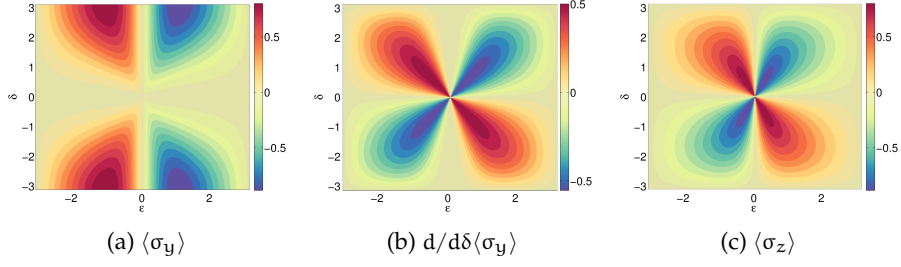


Figure 4.17: Expectation values of σ_y and σ_z with parametrisation $J = [\pi + \delta, \pi + \epsilon, 0]$ (change of coordinates from Fig. 4.16 (b).)

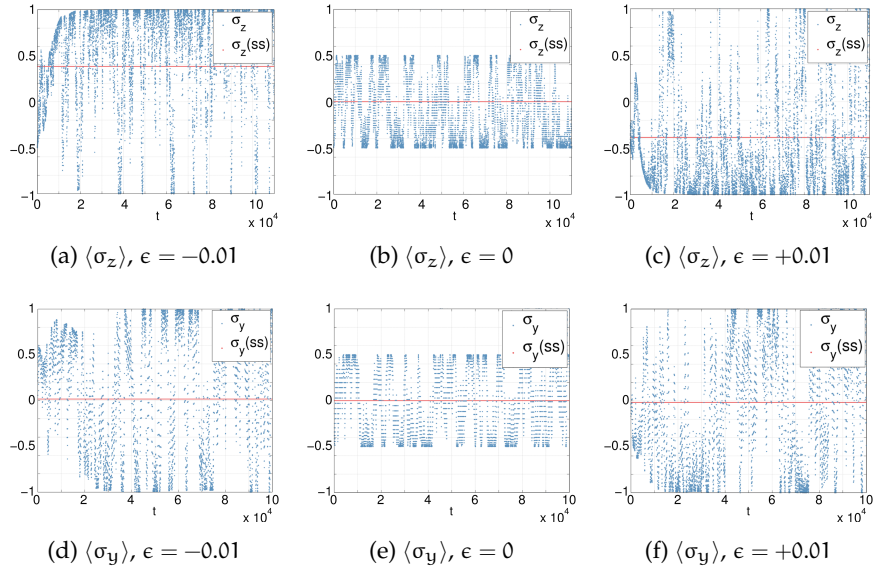


Figure 4.18: Expectation values of σ_y and σ_z along trajectories for varying ϵ in the δ, ϵ parametrisation

Differentiating the σ_y expectation value in the stationary state (Fig. 4.17) with respect to δ gives nearly exactly the same plot as the original σ_z expectation value (as in Fig. 4.17)

This is reflected in fluctuations appearing around $J = [\pi, \pi, 0]$ in the trajectory expectation values for σ_y and σ_z . Note that the sign of σ_y changes after each jump; to make the fluctuations clearer we have taken absolute values. In Fig. 4.18 we see that the average value of σ_y hardly changes with different ϵ , which is reflected in Fig. 4.17 (a) not changing rapidly around $\epsilon, \delta = 0$.

4.5 CONCLUSION

In this chapter, we have used the algebraic structure of the Kraus operators to find a decomposition for a quantum Markov process. This allowed us to clearly define the notions of phases, phase purification and phase transitions; we have also showed how large deviations comes into play in the occurrence of dynamical phase transitions in such models. Three examples served to illustrate this framework, showing evidence of dynamical phase transitions and quantum phase transitions.

As the results have been only for finite-dimensional systems, an extension to infinite-dimensional systems would be of interest. However, we anticipate this is more difficult due to the nontrivial algebraic structure of infinite-dimensional algebras of operators. In particular, the decomposition used in Eq. (4.1) does not have a straightforward infinite-dimensional counterpart.

Staying in the finite-dimensional regime, Eqs. (4.4),(4.3) characterise the set of stationary states; the exact topological structure of the state space [122, 123] is worth further study. This would allow us to relate phase transitions to changes in topological features of states, in addition to analytic features of rate functions.

CHARACTERIZATION OF DYNAMICAL PHASE TRANSITIONS IN QUANTUM JUMP TRAJECTORIES

5.1 INTRODUCTION

As we noted in Ch. 3, the occurrence of phase transitions in an open quantum system can be understood through the statistical behaviour of its jump trajectories. The main purpose of this chapter (and [2]) is to characterise dynamical phase transitions through means other than the behaviour of the stationary states of a system (i.e. through static order parameters, in the language of statistical mechanics). This static approach has been used in the analysis of quantum phase transitions in open many-body quantum systems [124, 125, 112, 126]; we will see in this chapter that the use of quantum jump trajectories provides an additional way to characterise phases and phase transitions. Furthermore, the example of glassy systems below shows that this dynamical approach may uncover phases that are not identified by the static picture.

Our approach may be outlined as follows: we first make use of a discretisation scheme introduced in [127, 128, 129] which allows for a description of the master dynamics of an open quantum system in terms of a matrix product state (MPS) [130]. This connection between the quantum jump trajectories and MPSs already hinted at in Eq. (3.6): the unravelling of the master evolution leads to the individual realisations of the dynamics as jump trajectories, which are stochastic quantities; the entire ensemble of jump trajectories is encoded in the associated MPS.

This chapter is an adapted version of [2].

The generator of the master evolution (or the *quantum master operator* (QMO)) offers a description which is in a sense dual to the trajectories point of view. Spectral properties of the QMO contain information about the phase structure. In particular, when considered as a function of a parameter of the system, non-analytic behaviour in the eigenvalues closest to 0 is characteristic of dynamical phase transitions[131, 132, 112, 133]. The reason for using trajectories as an alternative [134] approach to uncovering a phase structure is that, especially in many-body systems, calculating spectral properties of the QMO is typically too computationally involved.

Aside from this, trajectories are, by definition, directly accessible experimentally: as we explained in Sec. 3.2.3 and 3.3.4, the trajectories associated to open quantum systems exist as a consequence of measurements in their output. Although stationary behaviour is studied experimentally, as we will see later, the stationary state does not always reflect the phase transitions. As we saw in Ch. 3, large deviations plays a natural role in uncovering dynamical phase transitions in the jump trajectories framework. The examples considered in this chapter will show how dynamical phase transitions appear in trajectories as fluctuations between different regimes (illustrated in Fig. 5.2). In the thermodynamics of trajectories framework, as mentioned in Sec. 3.7, this dynamical heterogeneity is interpreted as fluctuations between different ensembles of trajectories.

After presenting the approach, we will use this formalism to study various open quantum systems, starting with a three-level system (discussed in Sec. 5.3 below), a quantum Ising model and the atom maser (in Sec. 5.4). These three examples all have dynamical phase transitions which are also reflected in the spectral properties of the QMO, and range from the simplest possible system exhibiting such behaviour, to a complex many-body system. Another model considered in Sec. 5.4 is a dissipative model of quantum glassy behaviour, which is different from the first three examples in that the dynamical phase transitions are not reflected in the behaviour of its stationary states; this final example emphasises the usefulness of the dynamical approach introduced here.

5.2 PRELIMINARIES AND FORMALISM

In Ch. 3 we introduced the time evolution of the density operator ρ of a continuous-time open quantum system; it is given by $\partial_t \rho = \mathcal{L}(\rho)$ where \mathcal{L} is the *master operator* (QMO). The master operator has the Lindblad form given in Eq. (3.9), and it is convenient to write $\mathcal{L} = \mathcal{H} + \mathcal{D}$. Here \mathcal{H} describes the Hamiltonian (or coherent) dynamics,

$$\mathcal{H}(\rho) = -i[H, \rho],$$

and \mathcal{D} describes the dissipative part of the dynamics,

$$\mathcal{D}(\rho) = \sum_{i=1}^N \left(L_i \rho L_i^* - \frac{1}{2} (L_i^* L_i \rho + \rho L_i^* L_i) \right).$$

As noted in Eq. (3.6), the ensemble of output trajectories of a discrete time quantum Markov process may be expressed[127] as an MPS. We will use this observation to relate the (dynamical) phases in quantum jump trajectories to the (static) phases of the ground state of a one-dimensional spin system. That observation is for discrete time systems; since we are looking at continuous-time quantum Markov processes, the first step is a discretisation scheme to obtain a discrete time process. The evolution of the density operator ρ on a short time interval δt , given by $T_{\delta t, *}(\rho)$, may be approximated by discrete time transition operator (see Eq. (3.1))

$$T_{\delta t, *}(\rho) = \sum_{m=0}^N V_m \rho V_m^*. \quad (5.1)$$

Here the Kraus operators are discrete-time approximations to jump events in the continuous evolution: V_0 is the event that no jumps occur

$$V_0 = e^{-i\delta t H} \left(\mathbf{1} - \delta t \sum_{k=1}^N L_k^\dagger L_k \right)^{1/2}$$

while for $m = 1, \dots, N$ the Kraus operator V_m represents the action of the jump operator L_m ,

$$V_m = e^{-i\delta t H} \sqrt{\delta t} L_m.$$

The map Eq. (5.1) is therefore a discrete-time analogue of the continuous time evolution generated by \mathcal{L} ; in particular, the state $\rho(t)$ may be approximated by

$$\rho(t) \approx T_{t/n, *}^n(\rho).$$

As in Eq. (3.6), if the initial state of the system is a pure state $|\psi_I\rangle$, the output state is the MPS

$$|\Psi_n\rangle = \sum_{i_1, \dots, i_n=0}^N \sum_{\psi_F} \langle \psi_F | V_{i_n} \cdots V_{i_1} | \psi_I \rangle \otimes |b_{i_1}, \dots, b_{i_n}\rangle$$

where the sum over ψ_F runs over a basis of final states. This MPS encodes the statistics of all possible quantum jump trajectories, in that the coefficients give the probability of a trajectory (i_1, \dots, i_n) as

$$\mathbb{P}(i_1, \dots, i_n) = \sum_{\psi_F} |\langle \psi_F | V_{i_n} \cdots V_{i_1} | \psi_I \rangle|^2.$$

Taking into consideration the physical meaning of an MPS, this means that we can represent this discretised dynamics as a chain (of length n) of $(N+1)$ -dimensional spins, the total state of which is the (unnormalised) MPS

$$|\Psi_n(F)\rangle = \sum_{i_1, \dots, i_n=0}^N \langle \psi_F | V_{i_n} \cdots V_{i_1} | \psi_I \rangle \otimes |b_{i_1}, \dots, b_{i_n}\rangle \quad (5.2)$$

(so $|\Psi_n\rangle = \sum_{\psi_F} |\Psi_n(F)\rangle$.) This formal connection between continuous-time open quantum systems and spin chains shows that dynamical phase transitions in the former (which appear in time correlations in trajectories) are reflected in spatial correlations of the latter.

The large deviations approach introduced in Ch. 2 is valid only in the asymptotic regime (i.e. as $t \rightarrow \infty$.) In terms of the spin chain representation, this is equivalent to the *thermodynamic limit*. In the thermodynamic limit, two-point correlations of any pair of observables on the output chain satisfy the following asymptotic form: suppose the observables A and B are located at positions x and $x+y$, respectively. Then as $n \rightarrow \infty$ we have [135]

$$\langle \Psi_n(F) | A^{(x)} B^{(x+y)} | \Psi_n(F) \rangle \propto \Re(\mu_2)^y = e^{-y/\xi} \cos(y\phi_2) \quad (5.3)$$

where $\Re(z)$ denotes the real part of a complex number z . The coefficients appearing on the RHS are related to spectral properties of the transition operator $T_{\delta t}$ from Eq. (5.1): the eigenvalues of $T_{\delta t}$, ordered by their absolute value, are denoted by $1 = \mu_1, \mu_2, \dots$. We write $\mu_2 = |\mu_2|e^{\pm i\phi_2}$ and let $\xi^{-1} = -\log|\mu_2|$ denote the inverse correlation length.

The spectra of $T_{\delta t}$, as $\delta t \rightarrow \infty$, and those of the continuous-time semigroup generated by \mathcal{L} , are the same; in terms of the eigenvalues of \mathcal{L} , the correlation function in Eq. (5.3) takes the form

$$\langle A(t) B(t+t') \rangle \propto \exp(-t'/\tau) \cos(\omega t').$$

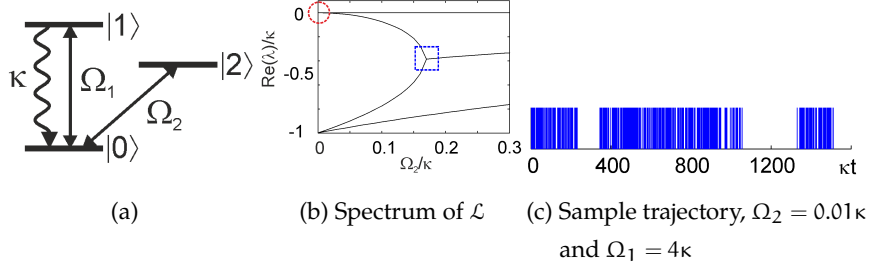


Figure 5.1: Three-level system

Here the eigenvalues of \mathcal{L} , arranged by decreasing real part, are denoted as $0 = \lambda_1, \lambda_2, \dots$; the *spectral gap* of \mathcal{L} is $\Re(\lambda_2) = -1/\tau$, and $\omega = \Im(\lambda_2)$.

This shows that the two-point correlation functions exhibit damped oscillations when μ_2 has non-zero imaginary part (which we will see in the examples below), or when $\omega \neq 0$. The spectral gap $-1/\tau$ plays an important role, as the correlation lengths diverge when this spectral gap closes; closing of the spectral gap is a feature associated to the occurrence of dynamical phase transitions, as we will see in the following examples.

5.3 THREE-LEVEL SYSTEM

The first example we consider is a three-level system [38, 57] (see diagram in Fig. 5.1a); this is a simple system which displays many of the features discussed in the previous section. The continuous-time dynamics consists of a Hamiltonian

$$H = \Omega_1 |0\rangle\langle 1| + \Omega_2 |0\rangle\langle 2| + \text{h.c.}$$

and a single jump operator $L = \sqrt{\kappa} |0\rangle\langle 1|$. This system shows a dynamical phase transition at $\Omega_2 = 0$, associated to which is a closing of the spectral gap ($\lambda_2 = 0$) visible in the circled region in Fig. (5.1b). For very small Ω_2 , this is visible in the jump trajectories in intermittent behaviour: if we take $\Omega_1 \gg \Omega_2 \approx 0$, we see strongly intermittent patterns in the photon emissions in Fig. (5.1c) [136]. This intermittency reflects the decoupling of the dynamics at $\Omega_2 = 0$ into two separate phases consisting of a driven, active two-level system and a dark, inactive level. This is seen in the spectrum of \mathcal{L} as the dominant eigenvalue $\lambda_1 = 0$ becomes degenerate at $\Omega_2 = 0$.

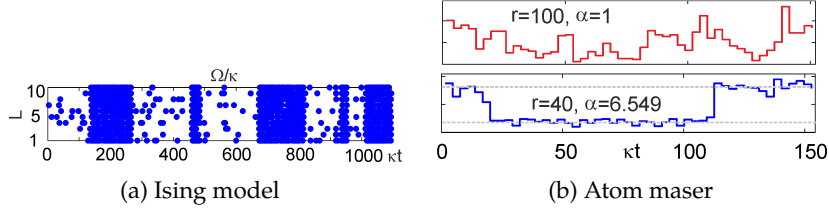


Figure 5.2: Sample jump trajectories

The phase transition at $\Omega_2 = 0$ is a first-order transition, clearly present in the trajectories by the switching between the two phases for small Ω_2 . In the language of thermodynamics of trajectories there are two ensembles of trajectories: one such ensemble is associated to the dark, inactive ('shelved') level $|2\rangle\langle 2|$, in which trajectories show no jumps at all. The other ensemble is the active subsystem with jumps occurring due to L , and the trajectories in this ensemble reflect this with a high density of jumps. Trajectories close to $\Omega_2 = 0$ fluctuate between these two ensembles, resulting in switching between periods of no jumps, and periods with many jumps in the trajectories.

Another feature shown by this model is the oscillating two-point correlations: the eigenvalue λ_2 acquires a nonzero imaginary part, which is a dynamical transition point for $\Omega_2 \neq 0$ (boxed region in Fig. 5.1b).

5.4 OTHER MODELS

5.4.1 Dissipative Ising model

The dissipative Ising model [131, 112] is a model of a quantum spin chain. In particular, the Ising model with L spins is composed of L sites, each with dimension 2. The Hamiltonian is

$$H = \Omega \sum_{k=1}^L \sigma_x^{(k)} + V \sum_{k=1}^L \sigma_z^{(k)} \sigma_z^{(k+1)}$$

where σ_x, σ_y and σ_z are the Pauli operators, and the superscript $k = 1, \dots, N+1 \equiv 1$ denotes the site index. There are N jump operators, one acting on each site, $L_k = \sqrt{\kappa} \sigma_-^{(k)}$. Acting independently of the other sites, the jump operator L_k flips the spin on the k th site i.e. $L_k |\uparrow\rangle = |\downarrow\rangle$, with rate κ .

In Fig. 5.2a a sample trajectory for the Ising model is shown, clearly illustrating the intermittent behaviour of the quantum jumps. This in-

indicates a many-body dynamical first-order phase transition with the spectral gap closing as $L \rightarrow \infty$ [2]. This intermittency is, as in the previous example, reflected in bistable static properties of the system [112].

5.4.2 Dissipative quantum glass

The next model we consider is the a model of dissipative quantum glass[126]. As the previous example, this is also a spin chain of L two-dimensional sites, but the Hamiltonian is given by

$$H = \Omega \sum_{k=1}^L \sigma_x^{(k)} f_{k+1}^2(p)$$

where the $f_k(p)$ are *kinetic constraints*, and the jump operators are $L_k = \sqrt{\kappa} \sigma_-^{(k)} f_{k+1}(p)$; this is a quantum analogue of the glassy models mentioned in Sec. 2.7. In our model, we take the constraints to be $f_k(p) = pQ_k + (1-p)\mathbf{1}$, with $0 \leq p \leq 1$, where

$$Q_k = \frac{1}{2}\mathbf{1} + \frac{\kappa}{2\omega} \sigma_z^{(k)} - \frac{2\Omega}{\omega} \sigma_y^{(k)}$$

The model displays a dynamical first-order phase transition in the parameter p . In particular, when $p = 0$ the model reduces to a noninteracting (uncorrelated) version ($V = 0$) of the previous example; in this case, the stationary state is a unique product state ρ_{ss} . On the other hand, for $p = 1$ the model is a *fully constrained* [126] quantum glass. This means that the dynamics is strongly correlated: when $p = 1$, the spin state $|\phi\rangle_k$ of site k can only change if its neighbour satisfies $Q_{k+1}|\phi\rangle_{k+1} \neq 0$.

For this reason, we would expect there to be a dynamical transition as $p \rightarrow 1$. Interestingly, the stationary state is independent of p : for any value of p , the stationary state is the uncorrelated state ρ_{ss} from the $p = 0$ case. However, the trajectories show a dramatic change in behaviour as p changes from 0 to 1: or $p \approx 1$, the jumps are extremely clustered in space and time. This is referred to as *dynamical heterogeneity*, which is a typical feature of glassy dynamics [137].

5.4.3 Atom maser

The final example we look at in this chapter is the atom maser, which we will study in detail later in this thesis; we refer to Ch. 7 for more details, and discuss here some features relevant to this chapter. The atom

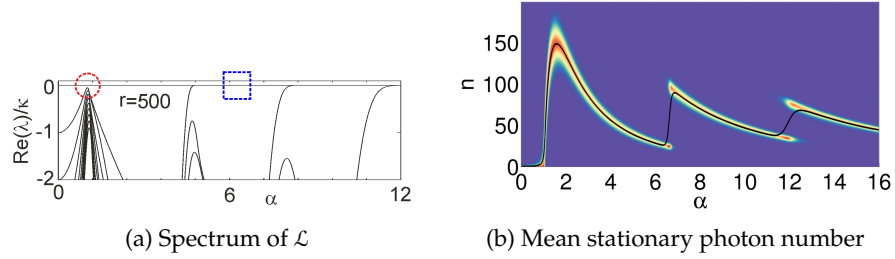


Figure 5.3: Atom maser, stationary properties

maser is a quantum Markov process on an infinite-dimensional Hilbert space, which sets it apart from the previous examples considered here. The atom maser consists of a single-mode resonant cavity which is coupled to a finite-temperature bath. Two-level atoms, identically prepared in a known state, are sent into the cavity one at a time at a constant rate r . As usual, the dynamics is represented by a master equation; see Eq. (3.23) in Ch. 7 for details.

The atom maser has a family of transition points: a second order dynamical transition, followed by a sequence of first-order transitions [138, 139, 140, 76, 4, 3]. These transition points are apparent in the spectrum of \mathcal{L} , shown in Fig. 5.3a; the second-order transition point (red circle) near $\alpha \approx 1$ shows a closing of the spectral gap, along with all other eigenvalues increasing in density. The first-order transition points (blue box) are also associated to a closing of the spectral gap, but without the other eigenvalues increasing. Near the first-order transition point the jump trajectories (associated to one of the jump operators) show fluctuations between two regimes, see Fig. 5.2b. This intermittent behaviour is related to near bistability of the stationary state for that value of α . This stands in contrast with the second-order transition point where the trajectory shows no such intermittency. As discussed in Ch. 7, these dynamical transitions are reflected in the stationary state: at each of the second-order transition points the mean photon number in the stationary state undergoes a jump [138, 139, 140, 76].

5.5 ENTANGLEMENT ENTROPY

We have considered examples which show evidence of critical behaviour in their trajectories and in their static properties; in the example of the dissipative quantum glass, only the dynamic picture was able to

exhibit the critical features. Static quantities are unable to see the transition in complex systems such as glasses and other many-body models. This is because the transitions are driven by fields which do not directly couple to obvious static quantities, but instead to time-integrated observables (for example, counting fields that arise when computing full counting statistics [141, 142, 143, 144, 145] of dynamical observables [32, 57]).

As discussed in Sec. 3.4, transitions visible in the trajectories are exhibited in the behaviour of the moment generating functions $Z_t(s)$ of the number of jump events

$$Z_t(s) = \sum_{n \geq 0} P_t(n) e^{-s n}$$

where $P_t(n)$ is the probability of observing n jumps in time t . As we have seen in Eq. (3.18), the MGF $Z_t(s)$ may be expressed as the largest eigenvalue of a deformation \mathcal{L}_s of the QMO. In the asymptotic regime, $t \rightarrow \infty$, phase transitions in the ensemble of trajectories are indicated by singular behaviour of $Z_t(s)$ at some critical value $s = s_c$ [19, 32, 57]. In this sense, the field s couples directly to the spectrum; a singularity of the MGF at s_c indicates the existence of close to degenerate dynamical states, which results in intermittency in the trajectories. By driving the field s one can single these states out; see Refs.[57, 146, 147] for details.

We may express the MGF in terms of the MPS $|\Psi\rangle$ as

$$Z_t(s) = \langle \Psi(s) | \Psi(s) \rangle,$$

where $|\Psi(s)\rangle = e^{-s\hat{J}/2}|\Psi\rangle$; here \hat{J} is an operator that counts the number of $n_{m>0}$ in a state $|n_1, \dots, n_M\rangle$. The MGF $Z_t(s)$ has a thermodynamic interpretation as a partition sum over trajectories, where s is a chemical potential which biases for, or against, quantum jumps. The biased MPS $|\Psi(s)\rangle$ is a superposition of the MPS from (5.2), where each term is weighed by a factor $e^{-s/2}$ for each jump.

As indicated previously, the largest eigenvalue of \mathcal{L}_s is related to the MGF $Z_t(s)$; the (normalised) eigenstate ρ_s corresponding to this eigenvalue satisfies $\rho_0 = \rho_{ss}$, and it is related to $|\Psi(s)\rangle$ by

$$\text{Tr}_\psi |\Psi(s)\rangle \langle \Psi(s)| = Z_t(s) \rho_s.$$

By studying counting fields at this level, they become more similar to the standard static fields which drive phase transitions; the difference is that they couple directly to the relevant order parameters which

reveal the transitions in quantum jump trajectories. This framework makes it possible to study dynamical phase transitions in systems with no obvious changes in spatial correlations, such as the strongly correlated many-body systems mentioned before.

At this level counting fields work in a similar manner to more standard static fields which drive phase transitions, but couple directly to the relevant dynamical order parameters that reveal transitions in quantum jump trajectories. This perspective should be useful in the study of dynamical phase transitions in systems where they are not obviously connected to a change in spatial correlations.

5.6 CONCLUSION

In this chapter we have discussed the results published in [2]. The main result is that features of dynamical transitions in open quantum systems, traditionally approached through the static picture, may be uncovered readily through the dynamical picture of quantum jump trajectories. We have studied several examples which served to illustrate this framework; in particular, more complicated many-body systems require this dynamical framework to see dynamical phase transitions as any static quantities do not reflect critical features.

SANOV THEOREM FOR QUANTUM MARKOV CHAINS

6.1 INTRODUCTION

In Sec. 2.2 we discussed the Sanov theorem, a fundamental result in large deviations. We now prove a large deviations principle for frequencies of arbitrary length sequences of measurement outcomes on a spin chain, which we refer to as the Sanov theorem for the empirical measure. This can be seen as an extension of the results in [87] concerning large deviations for the sample mean of measurements of finitely correlated states on the output of a quantum Markov chain.

We first discuss large deviations for the empirical measure corresponding to measurements on a spin chain. The empirical measure contains the frequencies with which measurement outcomes appear after measuring the same observable on each site of the output chain. As the number of sites increases, the empirical measure should converge by the law of large numbers. Analogous to the Cramer theorem for the sample means, the Sanov theorem states that a large deviations principle holds for the empirical measure and thus quantifies the rate of convergence.

Having gained a physical intuition for the empirical measure, we define the length m empirical measure which tracks the frequency with which sequences of length m appear in the output chain. This generalisation contains the usual empirical measure with $m = 1$. We prove that a large deviations principle holds for this length m empirical measure, using a similar approach to that employed in [87]. This involves the construction of a new level m transition operator, and showing that (using irreducibility and the Perron-Frobenius theorem) its spectral radius satisfies the Gärtner Ellis theorem, thus establishing the LDP.

6.2 BACKGROUND

We follow the argument found in [87], which is an extension to the quantum setting of the approach used in [8] (Sec. 3.1) to obtain large deviations results for finite state Markov chains. We aim to apply the Gärtner-Ellis theorem (cf. Thm. 2.4):

Theorem 6.1 (Gärtner-Ellis). Let μ_1, μ_2, \dots be a sequence of probability measures on \mathbb{R}^d . If for the sequence of moment generating functions Γ_n

$$\Gamma_n(t) = \int e^{n\langle t, x \rangle} d\mu_n(x)$$

the limit

$$F(t) = \lim_{n \rightarrow \infty} \frac{1}{n} \log \Gamma_n(t)$$

exists for all $t \in \mathbb{R}^d$ as an extended real number and is finite in a neighbourhood of 0 then (μ_n) satisfies a LDP with rate function

$$I(x) = \sup_t \{\langle t, x \rangle - F(t)\}.$$

In order to apply the Gärtner-Ellis theorem, we use the following lemma.

Lemma 6.1. ([87, Lemma C.2]). if a strictly positive operator Φ has a strictly positive eigenvector then

$$\lim_{n \rightarrow \infty} \frac{1}{n} \log \varphi(\Phi^n(x)) = \log r$$

where $r = r(\Phi)$ is the spectral radius of Φ , for any nonzero positive linear functional φ and any positive x .

The non-commutative Perron-Frobenius theory discussed in Sec. 3.5 tells us that irreducible and aperiodic operators have strictly positive eigenvectors: if $\Phi \geq 0$ is irreducible then $r(\Phi)$ is a simple eigenvalue of Φ and $\Phi(z) = rz$ for some $z > 0$. We combine Thm. 6.1 and Lem. 6.1 to obtain a desired large deviations principle as follows.

Corollary 6.1. Let $t \in \mathbb{R}^d$, suppose Φ_t is an irreducible and aperiodic positive map on M_d , and let ω be a state on M_k . Then the sequence of expectation values $\Gamma_n(t) = \omega(\Phi_t^n(x))$ satisfies a LDP on \mathbb{R}^d .

This means that, starting with a sequence of moment generating functions $\Gamma_n(t)$, we need to construct an irreducible modified transition operator $T_{e^{ta}} > 0$ such that

$$\Gamma_n(t) = \omega(T_{e^{ta}}(\mathbf{1}_B)). \quad (6.1)$$

For the length m moment generating functions, the same principle holds: we will construct a transition operator $T_{t,m}$ on a larger algebra which keeps track of previous outcomes, and which allows us to express the moment generating functions $\Gamma_n^{(m)}(t)$ in the same form.

Before we state the level m moment generating functions and the results, we will outline the setting. We are working with a discrete quantum Markov chain as discussed in Ch. 3. In the Schrödinger picture, change to the state after interaction of the cavity with a single atom (c.f. [39], Sec. 4.5.5) is described by the evolution operator

$$\begin{aligned} \mathcal{E}_* : M_d &\rightarrow M_d \otimes M_k \\ &: \rho \mapsto U(\rho \otimes \psi)U^* \end{aligned}$$

where ψ is the initial state of the atom, and the unitary operator U models the interaction via the isometry acting on pure state vectors as

$$|\varphi\rangle \mapsto U(|\varphi\rangle \otimes |\psi\rangle).$$

The Kraus operators associated to projective measurements $P_i = |i\rangle\langle i|$ are obtained by expressing the effect of \mathcal{E}_* as

$$U(|\varphi\rangle \otimes |\psi\rangle) = \sum_{i=1}^k V_i |\varphi\rangle \otimes |i\rangle.$$

Considering only pure states, the final total state $|\psi^{(n)}\rangle$ on n sites and the system[148]

$$|\psi^{(n)}\rangle = \sum_{i_1, \dots, i_n=1}^k V^{i_n} \dots V^{i_1} |\psi\rangle |i_n, \dots, i_1\rangle. \quad (6.2)$$

where $|\psi\rangle$ is the initial state of the system. For mixed states, the joint state $\rho(n)$ on the cavity and n sites, using the Markov approximation, is recursively given by

$$\rho(n) = (\mathcal{E}_* \otimes \mathcal{J}^{\otimes(n-1)})\rho(n-1),$$

where $\mathcal{J}^{\otimes n}$ denotes the identity map on $M_k^{\otimes n}$. We will be using the expression in Eq. (6.2) to compute expectation values for measurements on the output chain, and to express these in the form given in Eq. (6.1).

6.3 RESULT

Given the output state of the quantum Markov chain as computed in Eq. (6.2), we want to look at the statistics of sequences of outcomes for a given one-site observable X . For example, the simplest case would be to ask how often pairs of outcomes occur: how many times do we obtain a pair $(X_k = i, X_{k+1} = j)$? The Sanov theorem for this ‘level 2’ statistic establishes a large deviations principle for the frequencies of such pairs of outcomes.

In our main result, Thm. 6.2, we establish a Sanov theorem for all level $m \geq 1$ statistics. The result relies on first formulating the sequence of moment generating functions Γ_n associates to these outcomes; we then express these as in Eq. (6.1), in order to obtain the LDP by applying Col. (6.1).

We denote by $X^{(l)}$ the \mathbb{R}^m -valued random variable which represents the outcomes on m subsequent sites: for a sequence of outcomes $\mathbf{i} = (i_1, \dots, i_m)$ we have

$$(X^{(l)} = \mathbf{i}) \Leftrightarrow (X_l = i_1, \dots, X_{l+m-1} = i_m)$$

where X_j is the random variable associated to measurement outcomes of the observable X on site j . The moment generating function $\Gamma_n^{(m)}$ of $X^{(l)}$ is defined for $\mathbf{t} \in \mathbb{R}^m$ as

$$\Gamma_n^{(m)}(\mathbf{t}) = \mathbb{E} \left[\exp \langle \mathbf{t}, X^{(1)} + \dots + X^{(n-m+1)} \rangle \right].$$

Writing $P_{i_1}^{(1)} \dots P_{i_m}^{(l+m-1)}$ for the projection on m subsequent sites associated to a sequence of outcomes $(X^{(l)} = \mathbf{i})$, we may express this MGF as

$$\Gamma_n^{(m)}(\mathbf{t}) = \mathbb{E} \left[\exp \left(\sum_{l=1}^{n-m+1} \sum_{i_1, \dots, i_m=1}^k t_{i_1, \dots, i_m} P_{i_1}^{(l)} \dots P_{i_m}^{(l+m-1)} \right) \right].$$

Computing this expectation value in the state $|\psi^{(n)}\rangle$ from Eq. 6.2 we then get

$$\Gamma_n^{(m)}(\mathbf{t}) = \sum_{i_1, \dots, i_n=1}^k \langle \psi | V_{i_1}^* \dots V_{i_n}^* V_{i_n} \dots V_{i_1} | \psi \rangle \quad (6.3)$$

$$\times \exp \left(\sum_{l=1}^{n-m+1} t_{i_l, \dots, i_{l+m-1}} \right). \quad (6.4)$$

We introduce a transition operator $T_{t,m}$ which keeps track of the previous $m - 1$ sites; we define the map

$$T_{t,m} : M_d \otimes (\mathbb{C}^k)^{\otimes(m-1)} \rightarrow M_d \otimes (\mathbb{C}^k)^{\otimes(m-1)}, \quad (6.5)$$

$$[T_{t,m}(Y)]_{i_1, \dots, i_{m-1}} = \sum_{i_m=1}^k V_{i_1}^* [Y]_{i_2, \dots, i_m} V_{i_1} \exp(t_{i_1, \dots, i_m}) \quad (6.6)$$

where we refer to the (i_1, \dots, i_{m-1}) th block of $Y \in M_d \otimes (\mathbb{C}^k)^{\otimes(m-1)}$ using the notation $[Y]_{i_1, \dots, i_{m-1}}$. The moment generating function $\Gamma_n^{(m)}$ may then be expressed as

$$\Gamma_n^{(m)}(t) = \langle \psi | \sum_{i_1, \dots, i_{m-1}=1}^k [T_{t,m}^{n-m+1} (M^{(m)})]_{i_1, \dots, i_{m-1}} | \psi \rangle$$

where

$$[M^{(m)}]_{i_1, \dots, i_{m-1}} = V_{i_1}^* \cdots V_{i_{m-1}}^* V_{i_{m-1}} \cdots V_{i_1}.$$

Note that this expression for the moment generating functions $\Gamma_n^{(m)}(t)$ is analogous to the $m = 1$ form in Eq. 6.1; our main result is as follows.

Theorem 6.2 (Sanov theorem for quantum Markov chains). Let T be the irreducible and aperiodic transition operator for a quantum Markov chain on M_d . Then the level m empirical measure, defined in terms of the sequence of moment generating functions $\Gamma_n^{(m)}(t)$ defined in Eq. 6.3, satisfies a large deviations principle on \mathbb{R}^{m-1} . The rate function is the Legendre transform of the spectral radius $\log \rho(T_{t,m})$ where $T_{t,m}$ is the map defined in Eq. 6.5.

Proof. The proof consists of showing that $T_{t,m}$ is positive and irreducible. Since a block diagonal matrix is (strictly) positive if and only if each block is (strictly) positive, it is straightforward to verify that $T_{t,m}$ is positive.

For irreducibility, let the subspace $\mathcal{B}_m \subset M_d \otimes (\mathbb{C}^k)^{\otimes(m-1)}$ be given by

$$\mathcal{B}_m = \bigoplus_{i_1, \dots, i_{m-1}}^k Q_{i_1, \dots, i_{m-1}} M_d Q_{i_1, \dots, i_{m-1}}$$

where Q is the projection onto the support of $M^{(m)}$.

Then it remains to show that

1. $T_{t,m}$ leaves this subalgebra invariant,

2. its restriction $\tilde{T}_{t,m}$ to \mathcal{B}_m is irreducible,

1. Invariance. Denote by $\tilde{T}_{t,m}$ the restriction of $T_{t,m}$ to the subspace \mathcal{B}_m defined as

$$[\tilde{T}_{t,m}(\tilde{Y})]_{i_1, \dots, i_{m-1}} = \sum_{i_m=1}^k V_{i_1}^* [\tilde{Y}]_{i_2, \dots, i_m} V_{i_1} \exp(t_{i_1, \dots, i_m})$$

where $[\tilde{Y}]_{i_1, \dots, i_{m-1}} \in Q_{i_1, \dots, i_{m-1}} M_d Q_{i_1, \dots, i_{m-1}}$. The subspace \mathcal{B}_m is left invariant by $\tilde{T}_{t,m}$ if every block of $\tilde{T}_{t,m}(\tilde{Y})$ satisfies

$$[\tilde{T}_{t,m}(\tilde{Y})]_{i_1, \dots, i_{m-1}} \in Q_{i_1, \dots, i_{m-1}} M_d Q_{i_1, \dots, i_{m-1}}$$

for every $\tilde{Y} \in \mathcal{B}_m$. To show that this is the case, we show that

$$V_{i_1}^* [\tilde{Y}]_{i_2, \dots, i_m} V_{i_1}(u) = 0$$

for all $u \in \ker [M^{(m)}]_{i_1, \dots, i_{m-1}}$, or equivalently (since $\ker(A^*A) = \ker(A)$) all $u \in \ker(V_{i_{m-1}} \cdots V_{i_1})$. Now

$$[\tilde{Y}]_{i_2, \dots, i_m}(v) = 0 \quad \text{for all } v \in \ker(V_{i_m} \cdots V_{i_2})$$

and we either have $u \in \ker(V_{i_1})$ or $V_{i_1}(u) \in \ker(V_{i_{m-1}} \cdots V_{i_2})$ we conclude that for every $u \in \ker [\tilde{Y}]_{i_1, \dots, i_{m-1}}$ we have $u \in \ker([\tilde{T}(\tilde{Y})]_{i_1, \dots, i_{m-1}})$, proving that $\tilde{T}_{t,m}$ leaves \mathcal{B}_m invariant.

2. Irreducibility. Since, for some positive constant c we have $\tilde{T}_{t,m} > c\tilde{T}_{0,m}$ it suffices to show that $\tilde{T}_{0,m}$ is irreducible.

We prove that $\tilde{T}_{0,m}$ is irreducible by showing that there exists $n \in \mathbb{N}$ such that, for any $X \in \mathcal{B}_m$,

$$\tilde{T}_{0,m}^n(X) \geq c\mathbf{1}_{\mathcal{B}}$$

for some $c > 0$ [61]. We can assume that $n > m$, in which case

$$\begin{aligned} & [\tilde{T}_{0,m}^n(X)]_{i_1, \dots, i_m} \\ &= \sum_{i_m, \dots, i_{m+n-1}=1}^k V_{i_1}^* \cdots V_{i_n}^* [X]_{i_{n+1}, \dots, i_{m+n-1}} V_{i_n} \cdots V_{i_1} \\ &= V_{i_1}^* \cdots V_{i_{m-1}}^* \left(\sum_{i_m, \dots, i_n=1}^k V_{i_m}^* \cdots V_{i_n}^* \hat{X} V_{i_n} \cdots V_{i_m} \right) V_{i_{m-1}} \cdots V_{i_1} \end{aligned}$$

where \hat{X} is the sum of the blocks of X given by

$$\hat{X} = \sum_{i_1, \dots, i_{m-1}=1}^k [X]_{i_1, \dots, i_{m-1}}.$$

The remaining sum can be written in terms of the original transition operator T associated to the quantum Markov chain; recall that (Eq. (3.1)) for $Y \in M_d$

$$T(Y) = \sum_{i=1}^k V_i^* Y V_i$$

from which we obtain the expression

$$[\tilde{T}_{0,m}^n(X)]_{i_1, \dots, i_m} = V_{i_1}^* \cdots V_{i_{m-1}}^* T^{n-m+1}(\hat{X}) V_{i_{m-1}} \cdots V_{i_1}.$$

We assume the original Markov chain, and so T , to be irreducible and aperiodic; this means (see Sec. 3.5) that there exists $r \in \mathbb{N}$ such that $T^r(\hat{X}) \geq c \mathbf{1}$ for some $c > 0$. Therefore, with $n \geq r + m - 1$,

$$\begin{aligned} [\tilde{T}_{0,m}^n(X)]_{i_1, \dots, i_{m-1}} &\geq c V_{i_1}^* \cdots V_{i_{m-1}}^* V_{i_{m-1}} \cdots V_{i_1} \\ &\geq c Q_{i_1, \dots, i_{m-1}} \\ &= c [\mathbf{1}_{\mathcal{B}}]_{i_1, \dots, i_{m-1}}. \end{aligned}$$

Since $M^{(m)} \in \mathcal{B}_m$ we can compute the moment generating functions on this restriction i.e. $\Gamma_n(t) = \frac{1}{n} \log \varphi(\tilde{T}_{t,m}^n(V^{(m)}))$. This completes the proof of the Sanov theorem. \square

We briefly clarify why at $t = 0$ the dominant eigenvalue of our map $T_{t,m}$ is 1. The idea is that our $T_{t,m}$ is related by a similarity transformation to another transition operator which more clearly has the desired properties at $t = 0$. We define a map T_m^0 on \mathcal{B}_m which acts on each block separately as

$$[T_m^0(Y)]_{i_1, \dots, i_{m-1}} = V_{i_1}^* \cdots V_{i_{m-1}}^* Y_{i_1, \dots, i_{m-1}} V_{i_{m-1}} \cdots V_{i_1}.$$

If we define another map \bar{T}_m^0 by

$$[\bar{T}_m^0(Y)]_{i_1, \dots, i_{m-1}} = V_{i_{m-1}}^{-1} \cdots V_{i_1}^{-1} Y_{i_1, \dots, i_{m-1}} V_{i_1}^{-1*} \cdots V_{i_{m-1}}^{-1*}$$

then \bar{T}_m^0 is the inverse of T_m^0 - since we have restricted ourselves to the support of products $V_{i_1} \cdots V_{i_{m-1}}$ this is well defined. Finally, we define the map $\tilde{T}_{t,m}$ by writing

$$[\tilde{T}_{t,m}(Y)]_{i_1, \dots, i_{m-1}} = [\bar{T}_m^0 \circ T_{t,m} \circ T_m^0(Y)]_{i_1, \dots, i_{m-1}};$$

then

$$[\tilde{T}_{t,m}(Y)]_{i_1, \dots, i_{m-1}} = [T_{t,m}(Y)]_{i_1, \dots, i_{m-1}}.$$

We may conclude that $T_{t,m}$ and $\tilde{T}_{t,m}$ are identical up to a similarity transformation; the latter map is identity preserving for $t = 0$, which means the dominant eigenvalue at $t = 0$ is indeed 1.

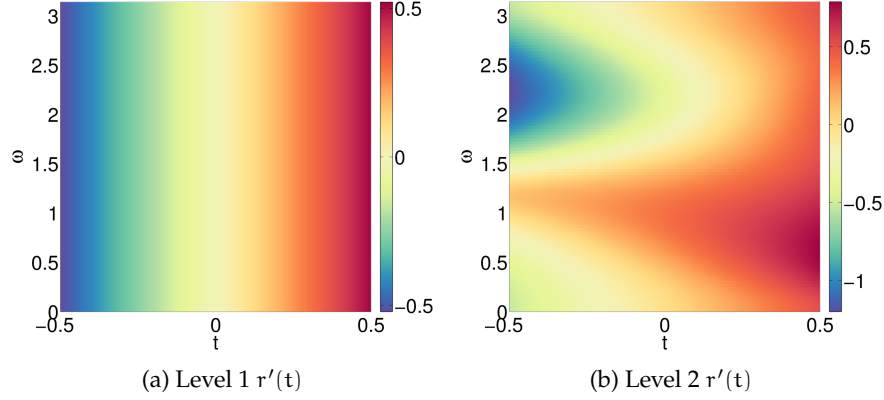


Figure 6.1: Derivatives of Sanov level 1 and 2 spectral radii for the XX0 model, see Fig. 4.12

6.4 CONCLUSION

We have shown that a large deviations principle holds for the arbitrary length empirical measure for the output of a quantum Markov chain. In studying phase transitions in models of open quantum systems, higher level rate functions, associated to such more complex measures, might be used when the ‘ordinary’ rate function does not reflect any critical behaviour. For example, in Sec. 4.4 we studied the XX0 model. As Fig. 6.1 shows, the level one spectral radius (and so the rate function) shows no dependence on the physical parameter ω , while the level two does change with ω .

If we go back to the use of large deviations in statistical mechanics, we find that higher-level rate functions from the Sanov theorem are used in Donsker-Varadhan theory in the study of phase transitions in the *Curie-Weiss-Potts model*, an extension of the Curie-Weiss model studied in Ch. 2 [9]. Furthermore, an infite-length limit of Sanov theory, called the empirical process, is employed to study the Ising model. This leads us to one possible extension of our results, which is to realise a Donsker-Varadhan theory in open quantum systems.

LARGE DEVIATIONS AND DYNAMICAL PHASE TRANSITIONS FOR THE ATOM MASER

7.1 INTRODUCTION

In this chapter we will apply the theory of large deviations introduced in Ch. 2 in order to investigate the occurrence of dynamical phase transitions in the atom maser. We introduced this model in Sec. 3.6 and we refer the reader to this section for the mathematical background and notation used in this chapter.

For certain parameters the atom maser exhibits strong intermittency in the atom detection counts, and has a bistable stationary state. Although previous numerical results suggested that the "free energy" may not be a smooth function, we show in our main result (Theorem 7.1) that the atom detection counts satisfy a large deviations principle (LDP), and therefore we deal with a phase cross-over rather than a genuine phase transition. We argue however that the latter occurs in the limit of infinite pumping rate. Such results have already been obtained in the context of discrete time quantum Markov chains with finite dimensional systems [87], but the novelty here is that we consider a continuous time Markov process with an infinite-dimensional system. As a corollary, we obtain the Central Limit Theorem for the counting process, using a result of [149].

The physical motivation lies in the new approach to the study of phase transitions for open systems developed in [53, 4] and reviewed in Sec. 3.7. Our investigation was motivated by the numerical results of [4] indicating a possible non-analytic behaviour of $\lambda(s)$. For finite

This chapter is an adapted version of [3] (see also [1]).

dimensional systems the counting process Λ_t satisfies an LDP when the Markov dynamics is mixing, i.e. irreducible and aperiodic [87]. The proof uses the Gärtner-Ellis theorem according to which it suffices to prove the convergence of the cumulant generating function to a smooth limit.

Some steps of the proof rely on a special feature of the maser dynamics which allows us to restrict the attention to the commutative invariant algebra of diagonal operators. However, the line of the proof is applicable to general infinite dimensional quantum Markov dynamics. We use an L^2 -representation [74, 73] of the semigroup generated by \mathcal{L}_s and show that the corresponding semigroup is compact. We then use the Krein-Rutman Theorem [150, 72] to establish the uniqueness and strict positivity of the eigenvector of $\lambda(s)$, and hence the existence of the spectral gap.

In Sec. 7.2 we formulate the large deviations results and give a point by point outline of the proof. The details of the proof found in Section 7.3. The results of a detailed numerical analysis are presented in Sec. 7.4, where we argue that dynamical phase transitions do occur in the thermodynamic limit of very large pumping rate.

7.2 MAIN RESULT

Our main results are the following Large Deviations and Central Limit theorems. For reader's convenience we outline the key steps of the proofs below, followed by more technical details in the next section. The LDP for the counting process Λ_t of the atom maser is obtained by applying the Gärtner-Ellis theorem, which in this context says that Λ_t satisfies an LDP if the following limit exists and is a differentiable function,

$$\lambda(s) := \lim_{t \rightarrow \infty} \frac{1}{t} \log \mathbb{E} (e^{s \Lambda_t}) = \lim_{t \rightarrow \infty} \frac{1}{t} \log \text{Tr} (\rho \mathcal{T}_s(t)(\mathbf{1})). \quad (7.1)$$

We will show that this is indeed true and $\lambda(s)$ is *spectral bound* (i.e. the eigenvalue with the largest real part) of a certain generator L_s which is closely related to \mathcal{L}_s . An essential ingredient is the Krein-Rutman theorem, a generalisation of the Perron-Frobenius Theorem to compact positive semigroups which ensures that $\lambda(s)$ is real, and under additional conditions, non-degenerate. In particular our analysis shows

that $\lambda(s)$ is smooth and its derivatives at $s = 0$ are the limiting cumulants of Λ_t

$$\lim_{t \rightarrow \infty} \frac{1}{t} C_k(\Lambda_t) = \left. \frac{d^k \lambda(s)}{ds^k} \right|_{s=0}, \quad k \geq 1,$$

the first two being the mean and the variance. Moreover the generator \mathcal{L}_s has a non-zero spectral gap; this spectral analysis is illustrated in Figure 7.1.

Theorem 7.1. The limit $\lambda(s)$ in (7.1) exists, and is a smooth function of s equal to the spectral bound of a certain semigroup generator $L_s^{(d)}$ defined below. Therefore the counting process Λ_t satisfies the large deviations principle with rate function equal to the Legendre transform of $\lambda(s)$. In particular the atom maser does not exhibit dynamical phase transitions, but rather cross-over transitions which become sharper as N_{ex} increases.

Corollary 7.1. The counting process Λ_t satisfies the Central Limit Theorem

$$\frac{1}{t}(\Lambda_t - t \cdot m) \xrightarrow{\mathcal{D}} N(0, V),$$

where \mathcal{D} denotes convergence in distribution and m and V are the mean and variance

$$m = \left. \frac{d\lambda(s)}{ds} \right|_{s=0}, \quad V = \left. \frac{d^2\lambda(s)}{ds^2} \right|_{s=0}.$$

Proof.

1. The operator

$$\mathcal{L}_s(X) = \Delta_s(X) + \mathcal{L}(X) = (e^s - 1)L_1^*XL_1 + \sum_{i=1}^4 \left(L_i^*XL_i - \frac{1}{2}\{L_i^*L_i, X\} \right).$$

is the generator of a strongly continuous semigroup $(\mathcal{T}_s(t))_{t \geq 0}$ of $*$ -weakly continuous CP maps $\mathcal{T}_s(t)$ on $\mathcal{B}(\mathfrak{h})$, and has the same domain $D(\mathcal{L})$ as \mathcal{L} . For $s = 0$ the semigroup reduces to the "physical" (master) semigroup $(\mathcal{T}(t))_{t \geq 0}$ with generator \mathcal{L} . The moment generating function of Λ_t is given by

$$\mathbb{E}(e^{s\Lambda_t}) = \text{Tr}(\rho_{in}\mathcal{T}_s(t)(\mathbf{1})).$$

where ρ_{in} is the initial state of the cavity.

2. Define the following "representation" of $(\mathcal{T}(t))_{t \geq 0}$ on $L^2(\mathfrak{h})$. Let i be the symmetric embedding

$$\begin{aligned} i : \mathcal{B}(\mathfrak{h}) &\rightarrow L^2(\mathfrak{h}) \\ X &\mapsto \rho_{ss}^{1/4} X \rho_{ss}^{1/4}. \end{aligned}$$

Then ([73], Thm. 2.3) there exists a unique strongly continuous contraction semigroup $(T(t))_{t \geq 0}$ on $L^2(\mathfrak{h})$ such that

$$T(t)(i(X)) = i(\mathcal{T}(t)(X)), \quad X \in \mathcal{B}(\mathfrak{h}).$$

For every $X \in \mathcal{D}(\mathcal{L})$ the Hilbert-Schmidt operator $i(X)$ belongs to the domain of the generator L of $(T(t))_{t \geq 0}$ ([73], Prop. 3.2) and

$$L(i(X)) = i(\mathcal{L}(X)), \quad X \in \mathcal{D}(\mathcal{L}).$$

Because we deal with a *reversible* quantum Markov process L is a self-adjoint operator on the Hilbert space $L^2(\mathfrak{h})$. Moreover the set $\mathcal{M}(\mathfrak{h})$ of finite rank operators given by finite matrices with respect to the Fock basis form a core ([73], Thm. 3.3) for L .

3. Similarly, we define the embedded version $(T_s(t))_{t \geq 0}$ of the semigroup $(\mathcal{T}_s(t))_{t \geq 0}$. This is a semigroup with generator $L_s = L + \delta_s$, with δ_s a bounded perturbation. The domain of L_s coincides with that of L and

$$L_s(i(X)) = i(\mathcal{L}_s(X)).$$

4. The moment generating function of Λ_t can be expressed in terms of the embedded semigroup as (see Lemma 7.1)

$$\mathbb{E}(e^{s\Lambda_t}) = \text{Tr}(\rho_{\text{in}} \mathcal{T}_s(t)(\mathbf{1})) = \text{Tr}(\tilde{\rho}_{\text{in}} T_s(t)(\rho_{ss}^{1/2})) = \langle \tilde{\rho}_{\text{in}}, T_s(t)(\rho_{ss}^{1/2}) \rangle_{\text{HS}},$$

where $\tilde{\rho}_{\text{in}} := \rho_{ss}^{-1/4} \rho_{\text{in}} \rho_{ss}^{-1/4}$ is assumed to belong to $L^2(\mathfrak{h})$. This holds for instance if ρ_{in} has a finite number of photons.

5. The semigroup $(T_s(t))_{t \geq 0}$ leaves invariant the subspace $L_d^2(\mathfrak{h}) \subset L^2(\mathfrak{h})$ of Hilbert-Schmidt operators which are diagonal in the Fock basis, and we denote its restriction to this subspace by $(T_s^{(d)}(t))_{t \geq 0}$, and similarly for the generator. Since $\rho_{ss} \in L_d^2(\mathfrak{h})$ the moment generating function can be expressed as

$$\mathbb{E}(e^{s\Lambda_t}) = \langle \tilde{\rho}_{\text{in}}^{(d)}, T_s^{(d)}(t)(\rho_{ss}^{1/2}) \rangle_{\text{HS}}$$

with $\tilde{\rho}_{\text{in}}^{(d)}$ denoting the diagonal of $\tilde{\rho}_{\text{in}}$. The analogous restriction of $(\mathcal{T}(t))_{t \geq 0}$ to the diagonal sub-algebra of $\mathcal{B}(\mathfrak{h})$ can be identified

with the transition semigroup of the birth-death process on \mathbb{N} with rates (3.32).

6. The restricted generator $L^{(d)}$ has compact resolvent, and $(T^{(d)}(t))_{t \geq 0}$ is immediately compact (i.e. $T^{(d)}(t)$ is compact for all $t > 0$). Moreover, the semigroup $(T_s^{(d)}(t))_{t \geq 0}$ is also immediately compact.
7. The semigroup $(T_s^{(d)}(t))_{t \geq 0}$ is strictly positive, that is $T_s^{(d)}(t)(D) > 0$ for all operators $D \geq 0$ in $L_d^2(\mathfrak{h})$ and $t \geq 0$.
8. Since $(T_s(t))_{t \geq 0}$ is compact and strictly positive, the Krein-Rutman theorem implies that the spectral radius of $T_s(t)$ is an eigenvalue with strictly positive right and left eigenvectors $r(s)$ and $l(s)$ [150, 72]. The spectral radius is equal to $e^{t\lambda(s)}$ where $\lambda(s)$ is the spectral bound of L_s , i.e. the eigenvalue with the largest real part. Using point 4. this implies that

$$\begin{aligned} \mathbb{E}(e^{s\Lambda_t}) &= \langle \tilde{\rho}_{\text{in}}, T_s(t)(\rho_{ss}^{1/2}) \rangle_{\text{HS}} \\ &= e^{t\lambda(s)} \left(\langle \tilde{\rho}_{\text{in}}, r(s) \rangle_{\text{HS}} \langle l(s), \rho_{ss}^{1/2} \rangle_{\text{HS}} + o(t) \right). \end{aligned} \quad (7.2)$$

Since $r(s), l(s) > 0$ and $\tilde{\rho}_{\text{in}}, \rho_{ss}^{1/2} \geq 0$ the inner products are non-zero and we obtain the limiting cumulant generating function

$$\lim_{t \rightarrow \infty} \frac{1}{t} \log \mathbb{E}(e^{s\Lambda_t}) = \lambda(s).$$

9. Using analytic perturbation theory, the spectral bound $\lambda(s)$ is shown to be a smooth function of s .
10. Using points 8. and 9., we apply the Gärtner-Ellis theorem to conclude that Λ_t satisfies the LD principle with rate function equal to the Legendre transform of $\lambda(s)$. In particular, the limiting cumulants of Λ_t can be computed as derivatives of $\lambda(s)$ at $s = 0$,

$$\lim_{t \rightarrow \infty} \frac{1}{t} C_k(\Lambda_t) = \left. \frac{d^k \lambda(s)}{ds^k} \right|_{s=0}.$$

11. Again by analytic perturbation theory, the spectral bound is analytic in the neighbourhood of the origin of the complex plane. By the result of [149], it follows that Λ_t satisfies the Central Limit Theorem.

7.3 DETAILS OF PROOF

Here we give point by point details on the steps of the proof.

1. The strongly continuous semigroup $(\mathcal{T}(t))_{t \geq 0}$ of w^* -continuous, identity preserving CP maps on $\mathcal{B}(\mathfrak{h})$ was analysed in [74]. Since Δ_s is a bounded perturbation, by the bounded perturbation theorem (cf. [44], Theorem III 1.3) the operator

$$\mathcal{L}_s(X) = \Delta_s(X) + \mathcal{L}(X)$$

is the generator of a strongly continuous semigroup $(\mathcal{T}_s(t))_{t \geq 0}$, and has the same domain $\mathcal{D}(\mathcal{L}_s) = \mathcal{D}(\mathcal{L})$.

2. Denote $E_{i,j} := |e_i\rangle\langle e_j|$ and $E_i := |e_i\rangle\langle e_i|$ the rank one "matrix elements". For any $X = \sum_{j,k} x_{j,k} E_{j,k}$ in the domain, the explicit action of generator is [73]

$$\begin{aligned} L(X) = & -\frac{1}{2} \sum_{j,k \geq 0} (\lambda_j^2 + \lambda_k^2 + \mu_j^2 + \mu_k^2) x_{j,k} E_{j,k} \\ & + \sum_{j,k \geq 0} \sqrt{\lambda_j \lambda_k \mu_{j+1} \mu_{k+1}} (x_{j+1,k+1} E_{j,k} + x_{j,k} E_{j+1,k+1}). \end{aligned}$$

where the coefficients λ_n, μ_n are the rates of the associated birth-and-death process (3.32). It can be directly checked that L is symmetric operator but proving its selfadjointness is non-trivial and holds only under certain assumption about λ_n, μ_n [73].

Point 4. is proved in the following lemma.

Lemma 7.1. The moment generating function of Λ_s can be expressed in terms of the embedded semigroup $(T_s(t))_{t \geq 0}$ as follows

$$\mathbb{E}(e^{s \Lambda_t}) = \text{Tr}(\rho_{\text{in}} \mathcal{T}_s(t)(\mathbf{1})) = \text{Tr}(\tilde{\rho}_{\text{in}} e^{t L_s}(\rho_{ss}^{1/2})) = \langle \tilde{\rho}_{\text{in}}, T_s(t)(\rho_{ss}^{1/2}) \rangle_{H-S},$$

where $\tilde{\rho}_{\text{in}} := \rho_{ss}^{-1/4} \rho_{\text{in}} \rho_{ss}^{-1/4} \in L^2(\mathfrak{h})$.

Proof. We first note that the linear span \mathcal{M} of the matrix units $E_{j,k}$ are analytic vectors for \mathcal{L}_s , i.e. there exists a time $T > 0$ such that for all $0 \leq t < T$, the series

$$\sum_{k \geq 0} \frac{t^k \mathcal{L}_s^k(x)}{k!}, \quad x \in \mathcal{M}.$$

converges in norm in $\mathcal{B}(\mathfrak{h})$ and the limit is $\mathcal{T}_s(t)(x)$. The proof is similar to that of Lemma 5.4 in [151] to which we refer for details. A similar statement holds for the generator L_s on $L^2(\mathfrak{h})$.

We now define the truncation

$$X_n = P_n X P_n,$$

of an arbitrary operator $X \in \mathcal{B}(\mathfrak{h})$ to the finite dimensional space defined as the span of the first n Fock basis vectors, whose orthogonal projection is P_n . Recall that the action of $T_s(t) = e^{t\mathcal{L}_s}$ and its predual semigroup are related by

$$\mathrm{Tr}(e^{t\mathcal{L}_{s*}}(\rho)X) = \mathrm{Tr}(\rho e^{t\mathcal{L}_s}(X)), \quad \rho \in L^1(\mathfrak{h}), X \in \mathcal{B}(\mathfrak{h})$$

where \mathcal{L}_{s*} is the generator of $(T_{s*}(t))_{t \geq 0}$. We want to show that

$$\mathrm{Tr}(\rho_{\mathrm{in}} e^{t\mathcal{L}_s}(\mathbf{1})) = \mathrm{Tr}(\tilde{\rho}_{\mathrm{in}} e^{tL_s}(\rho_{\mathrm{ss}}^{1/2})) \quad (7.3)$$

for all $t > 0$. Partition the time t by writing $t = t_1 + \dots + t_l$ where $t_i < T$. The main idea behind showing the above equality is by applying sequentially the analyticity of finite-rank operators and weak-* continuity to ‘move over’ each element of the semigroup $e^{t_i\mathcal{L}}$ to the trace-class operators and then the Hilbert-Schmidt operators, and repeat this until the entire semigroup lives on the other side. Using the projections P_n introduced above, we find that by weak-* continuity and the semigroup property we have

$$\mathrm{Tr}(\rho_{\mathrm{in}} e^{(t_1 + \dots + t_l)\mathcal{L}_s}(\mathbf{1})) = \lim_{n \rightarrow \infty} \mathrm{Tr}(\rho_{\mathrm{in}} e^{t_1\mathcal{L}_s} (P_n e^{(t_2 + \dots + t_l)\mathcal{L}_s}(\mathbf{1}) P_n)).$$

Let $A := e^{(t_2 + \dots + t_l)\mathcal{L}_s}(\mathbf{1}) \in \mathcal{B}(\mathfrak{h})$ and $\tilde{A} := \rho_{\mathrm{ss}}^{1/4} A \rho_{\mathrm{ss}}^{1/4} \in L^2(\mathfrak{h})$ and define the finite-rank truncations $A_n = P_n A P_n$, and $\tilde{A}_n = P_n \tilde{A} P_n$. Since A_n is an analytic vector for \mathcal{L}_s , we may express the RHS as a power series and thus we obtain

$$\lim_{n \rightarrow \infty} \mathrm{Tr} \left(\rho_{\mathrm{in}} \sum_{k \geq 0} \frac{t_1^k \mathcal{L}_s^k}{k!} (A_n) \right) = \lim_{n \rightarrow \infty} \mathrm{Tr} \left(\rho_{\mathrm{ss}}^{-1/4} \rho_{\mathrm{in}} \rho_{\mathrm{ss}}^{-1/4} \sum_{k \geq 0} \frac{t_1^k L_s^k}{k!} (\tilde{A}_n) \right)$$

by definition of the embedded generator L_s . Now \tilde{A}_n is analytic for L_s so the inner sum is equal to $e^{t_1 L_s}(\tilde{A}_n)$ and the limit may be written as

$$\begin{aligned} \lim_{n \rightarrow \infty} \mathrm{Tr}(\tilde{\rho}_{\mathrm{in}} e^{t_1 L_s}(\tilde{A}_n)) &= \lim_{n \rightarrow \infty} \langle \tilde{\rho}_{\mathrm{in}}, e^{t_1 L_s}(\tilde{A}_n) \rangle_{\mathrm{HS}} \\ &= \lim_{n \rightarrow \infty} \langle e^{t_1 L_s^*}(\tilde{\rho}_{\mathrm{in}}), \tilde{A}_n \rangle_{\mathrm{HS}} \\ &= \langle e^{t_1 L_s^*}(\tilde{\rho}_{\mathrm{in}}), \tilde{A} \rangle_{\mathrm{HS}}. \end{aligned}$$

The last equality follows from the fact that \tilde{A}_n converges weakly to \tilde{A} in $L^2(\mathfrak{h})$. Indeed for any positive $\tau \in L^2(\mathfrak{h})$ we have

$$\begin{aligned} \langle \tau, P_n \rho_{ss}^{1/4} A \rho_{ss}^{1/4} P_n \rangle_{HS} &= \text{Tr} \left(\tau P_n \rho_{ss}^{1/4} A \rho_{ss}^{1/4} P_n \right) \\ &= \text{Tr} \left(\rho_{ss}^{1/4} \tau \rho_{ss}^{1/4} P_n A P_n \right) \\ &\rightarrow \text{Tr} \left(\rho_{ss}^{1/4} \tau \rho_{ss}^{1/4} A \right); \end{aligned}$$

taking into account that $\rho_{ss}^{1/4} \tau \rho_{ss}^{1/4} \in L^1(\mathfrak{h})$ by

$$\text{Tr} \left(\rho_{ss}^{1/4} \tau \rho_{ss}^{1/4} \right) = \text{Tr} \left(\rho_{ss}^{1/2} \tau \right) = \langle \rho_{ss}^{1/2}, \tau \rangle_{HS} < \infty.$$

We now repeat the same argument for the term $e^{t_2 \mathcal{L}_s}$, by defining $B = e^{(t_3 + \dots + t_l) \mathcal{L}_s}(\mathbf{1})$, and $\tilde{B}, B_n, \tilde{B}_n$ as before. Then

$$\begin{aligned} \text{Tr}(\rho_{in} e^{t \mathcal{L}_s}(\mathbf{1})) &= \text{Tr} \left(\tilde{\rho}_{in} e^{t_1 \mathcal{L}_s} \left(\rho_{ss}^{1/4} e^{(t_2 + \dots + t_l) \mathcal{L}_s}(\mathbf{1}) \rho_{ss}^{1/4} \right) \right) \\ &= \lim_{n \rightarrow \infty} \text{Tr} \left(e^{t_1 \mathcal{L}_{s*}}(\tilde{\rho}_{in}) \rho_{ss}^{1/4} e^{t_2 \mathcal{L}_s}(P_n B P_n) \rho_{ss}^{1/4} \right) \\ &= \langle e^{(t_1 + t_2) \mathcal{L}_{s*}}(\tilde{\rho}_{in}), \tilde{B} \rangle_{HS} \end{aligned}$$

and after a finite number of steps we arrive at (7.3). This shows that the semigroup L_s on the Hilbert-Schmidt space gives rise to the desired expectation values. \square

Point 5. follows immediately from the definition of the generator \mathcal{L}_s .

Point 6. is shown in the following lemma.

Lemma 7.2. The restricted generator $L^{(d)}$ has compact resolvent, and $(T^{(d)}(t))_{t \geq 0}$ is immediately compact, i.e. $T^{(d)}(t)$ is compact for all $t > 0$. Moreover, the semigroup $(T_s^{(d)}(t))_{t \geq 0}$ is also immediately compact.

Proof. Let $L^{(d)}$ be the restriction of L to the subspace $L_d^2(\mathfrak{h})$ of diagonal Hilbert-Schmidt operators with respect to the Fock basis. Its concrete action on a diagonal operator $D = \sum_{j \geq 0} d_j E_j$ is

$$\begin{aligned} L(D) &= - \sum_{j \geq 0} (\lambda_j^2 + \mu_j^2) d_j E_j + \sum_{j \geq 0} \lambda_j \mu_{j+1} (d_{j+1} E_j + d_j E_{j+1}) \\ &:= A(D) + B(D). \end{aligned}$$

In order to establish that $L^{(d)}$ has compact resolvent, we extend a similar argument used in [152] to our setting. Note that A is a selfadjoint operator with (point) spectrum

$$\sigma_p(A) = \{a_j := -(\lambda_j^2 + \mu_j^2) : j \in \mathbb{N}\}.$$

The resolvent operator $R(z, A) = (A - z\text{Id})^{-1}$ is well defined whenever $z \notin \sigma_p(A)$ and is given by

$$(A - z\text{Id})^{-1}(X) = \sum_{j \geq 0} (a_j - z)^{-1} x_j E_j$$

Since $|a_j| \rightarrow \infty$ when $j \rightarrow \infty$, $R(z, A)(X)$ may be approximated in the L^2 -norm by its finite-rank truncations

$$R(z, A)(X) = \lim_{N \rightarrow \infty} \sum_{j=0}^N (a_j - z)^{-1} x_j E_j, \quad X \in \mathcal{N}$$

and so A has compact resolvent.

To show that $L^{(d)} = A + B$ itself has compact resolvent it is enough to show that B is a *relatively bounded* perturbation of A ([153] Thm. 3.17, p. 214). This means showing that there exists a $b > 0$ such that

$$\text{Tr}(B(X)^* B(X)) \leq b \text{Tr}(A(X)^* A(X)) \quad \text{for all } X \in L_d^2(h)$$

Using the Cauchy-Schwarz inequality in the Hilbert space $L^2(h)$ such a bound is readily found, and we may conclude that L has compact resolvent.

We now show that $T^{(d)}(t)$ is immediately compact. Since $L^{(d)}$ is self-adjoint, we find that its resolvent operator $R(z, L)$ satisfies the bound ([153] Thm. 3.16, p. 271)

$$\|R(iz, L)\| \leq |\text{Im}(z)|^{-1} \quad \text{for all } \text{Im}(z) \neq 0.$$

Therefore ([44] Thm. II 4.20 p. 115) the semigroup $(T^{(d)}(t))_{t \geq 0}$ is *immediately norm continuous*. An immediately norm continuous semigroup whose generator has compact resolvent is immediately compact ([44] Thm. 4.29, p. 119), therefore the semigroup $(T^{(d)}(t))_{t \geq 0}$ is immediately compact.

Similarly, the restriction $L_s^{(d)}$ is the perturbation of the generator $L^{(d)}$

$$\begin{aligned} L_s^{(d)}(D) &= L^{(d)}(D) + \delta_s(D), \\ \delta_s(D) &= (e^s - 1) N_{\text{ex}} \sum_{j \geq 0} \sin^2(\phi \sqrt{j+1}) \frac{\mu_{j+1}}{\lambda_j} d_{j+1} E_j \end{aligned}$$

Since δ_s is bounded, the semigroup $(T_s^{(d)}(t))_{t \geq 0}$ is also immediately compact, cf. [44] Thm. III.1.16.

□

Point 7. We show first that the unperturbed semigroup $(T(t))_{t \geq 0}$ on $L_d^2(\mathfrak{h})$ is strictly positive. Since any positive $D \in L_d^2(\mathfrak{h})$ is of the form $D = \sum_k d_k E_k$ with $d_k \geq 0$, it is enough to show that $T^{(d)}(t)(E_i) > 0$. This is equivalent to

$$\langle E_j, T^{(d)}(t)(E_i) \rangle_{HS} > 0, \quad i, j \in \mathbb{N}.$$

By using the technique of Lemma 7.1 we find

$$\langle E_j, T^{(d)}(t)(E_i) \rangle_{HS} = \text{Tr}(E_j \mathcal{T}^{(d)}(t)(E_i)) = \text{Tr}(E_i \mathcal{T}_*^{(d)}(t)(E_j))$$

where the right side is the probability $\mathbb{P}_{j,i}(t)$ of going from state j to i in time t , for the associated birth and death process. This probability can be unravelled as

$$\mathbb{P}_t(j, i) = \sum_{k \geq 0} \sum_{i_1, \dots, i_k=1}^4 \int_{0 \leq t_1 \leq \dots \leq t_k \leq t} \dots \int p_{j,i}(t; t_1, i_1, \dots, t_k, i_k) dt_1 \dots dt_k$$

where

$$p_{j,i}(t; t_1, i_1, \dots, t_k, i_k) := \text{Tr} \left(E_j \cdot e^{(t-t_k)\mathcal{L}_0} \mathcal{J}_{i_k} \dots \mathcal{J}_{i_1} e^{t_1 \mathcal{L}_0} (E_i) \right),$$

is the probability density for the trajectory consisting of jumps of type i_1, \dots, i_k occurring at times $0 \leq t_1 \leq \dots \leq t_k \leq t$, respectively. To show strict positivity, we can restrict our attention to trajectories which exhibit only jumps of type 3 and 4 and connect the states j and i . Since the jump rates are strictly positive, the probability of such a trajectory is strictly positive and therefore $\mathcal{T}^{(d)}(t)$ and $T^{(d)}(t)$ are strictly positive. The same argument can be repeated for the semigroup $(T_s^{(d)}(t))_{t \geq 0}$ whose unravelling is

$$\langle E_j, T_s^{(d)}(t)(E_i) \rangle_{HS} = \sum_{k \geq 0} \sum_{i_1, \dots, i_k=1}^4 \int_{0 \leq t_1 \leq \dots \leq t_k \leq t} \dots \int p_{j,i}^{(s)}(t; t_1, i_1, \dots, t_k, i_k) dt_1 \dots dt_k$$

where

$$p_{j,i}^{(s)}(t; t_1, i_1, \dots, t_k, i_k) = e^{sn(1)} p_{j,i}(t; t_1, i_1, \dots, t_k, i_k),$$

with $n(1)$ equal to the number of jumps of type 1.

Point 8. Recall that to establish the LDP for the counting process Λ_t it is enough to show that the limit

$$\lim_{t \rightarrow \infty} \frac{1}{t} \log \mathbb{E} (e^{s \Lambda_t}) = \lim_{t \rightarrow \infty} \frac{1}{t} \log \text{Tr}(\tilde{\rho}_{in} e^{t L_s} (\rho_{ss}^{1/2}))$$

exists and is a smooth function of s .

Since $(T_s^{(d)}(t))$ is an immediately compact semigroup, we have ([44], Col. IV.3.12) a spectral mapping theorem of the form

$$e^{t\sigma(L_s^{(d)})} = \sigma(T_s^{(d)}(t)) \setminus \{0\}, \quad t > 0;$$

in particular, the *spectral radius* of $T_s^{(d)}(t)$ is given by

$$r_s(t) := r(T_s^{(d)}(t)) = e^{t\lambda(s)}.$$

where $\lambda(s)$ is the *spectral bound* of $L_s^{(d)}$, i.e. the real part of the eigenvalue with the largest real part. Since $T_s^{(d)}(t)$ is compact and strictly positive, the Krein-Rutman Theorem implies that $\lambda(s)$ is a real eigenvalue with unique strictly positive right and left eigenvectors $r(s)$ and $l(s)$ such that $\langle l(s)|r(s) \rangle = 1$. In particular L_s has a spectral gap $g(s) = \lambda(s) - \text{Re}\lambda_1(s)$ and

$$T_s^{(d)}(t)(D) = e^{t\lambda(s)}|r(s)\rangle\langle l(s)| + R(t)$$

where the reminder term satisfies $\|R(t)\| \leq Ce^{t(\lambda(s)-g+\epsilon)}$ for some constant C and $\epsilon < g$. Therefore (7.2) holds.

Point 9. To complete the proof we need to show that $\lambda(s)$ is a differentiable function of s . This follows from analytic perturbation theory for the generator $L_s^{(d)}$, cf. [154] (Prop. 3.25, p. 141); any isolated eigenvalue (of finite multiplicity) and its associated eigenprojection are analytic functions of s in some disc around $s = 0$. Applied to the family of perturbations

$$L_s^{(d)} = L^{(d)} + \delta_s,$$

we find that the spectral bound of $\lambda(s)$ is an analytic function of s , and remains isolated as a function of s .

7.4 DYNAMICAL PHASE TRANSITIONS

The existence of a "phase transition" in the atom maser has been discussed in several theoretical physics papers [139, 76, 138, 140, 4]. There is a general agreement that if N_{ex} is sufficiently large (for instance $N_{\text{ex}} \approx 150$), then "for all practical purposes" we can consider that the mean photon number of the stationary state has a jump at $\alpha \approx 6.66$ (see Figure 3.3) which matches up with a jump between the left and right derivatives of $\lambda(s)$ at $s = 0$, in the dynamical scenario (see Figure 7.1).

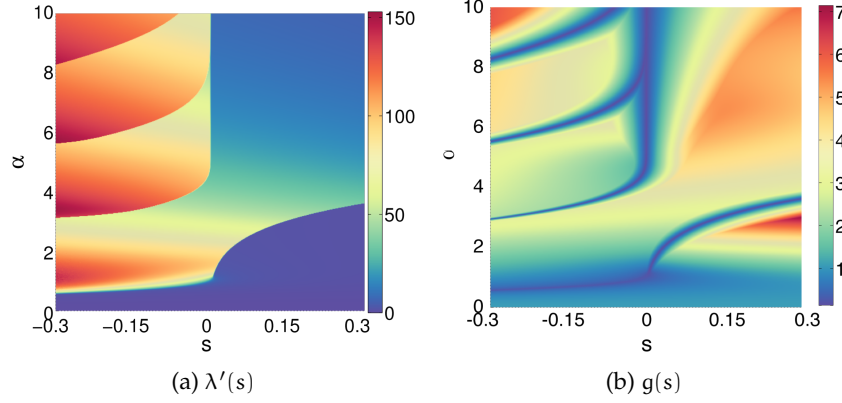


Figure 7.1: $\lambda'(s)$ and the spectral gap $g(s)$ of L_s as functions of s and $\alpha = \phi/\sqrt{N_{\text{ex}}}$ (after Fig. 3 in [4]).

However, the question whether we are dealing with a "true" (dynamical) phase transition or rather a steep but smooth cross-over was left open, and motivated this investigation. Having proved that the latter is the case, we would like to briefly put the result in the context of a numerical analysis.

As the proof shows, dynamical phase transitions are intimately connected with the closing of the spectral gap of the semigroup generator. Figure 7.1 shows the close match between the behaviour of the first derivative of $\lambda(s)$ and the spectral gap $g(s) := \lambda(s) - \text{Re}\lambda_1(s)$. In particular, at first sight it would appear that for $\alpha \geq 4.6$ (the point where the stationary state becomes bistable), the entire $s = 0$ line is a phase separation line. However, by zooming in a vertical strip of size 10^{-7} in this region (see Figure 7.2), we find that the line separating the phases is not perfectly vertical but crosses $s = 0$ at $\alpha \approx 6.6$ which corresponds roughly to the transition point for the stationary state. Moreover, on this scale it is clear that we deal with a steep but smooth transition between phases.

Figure 7.2 shows that the phase separation lines become sharper with larger N_{ex} , and a "true" phase transition emerges in infinite pumping rate limit. A similar conclusion can be drawn by plotting the rescaled stationary mean $\langle N \rangle / N_{\text{ex}}$, cf. Figure 7.3. This can be intuitively understood by appealing to the effective potential (3.33). As N_{ex} increases the potential barrier becomes larger and two stable phases appear at the point where the local minima are equal. Indeed, Figure 3.5 shows the plot of the rescaled potential U/N_{ex} as a function of the res-

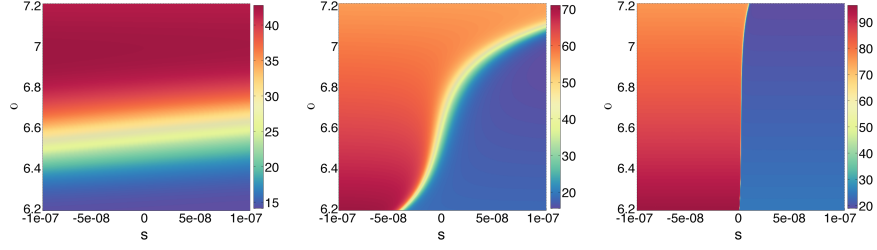


Figure 7.2: Phase boundaries at the $s = 0, \alpha \approx 6.66$ crossover with $N_{ex} = 75, 100$ and 125 .

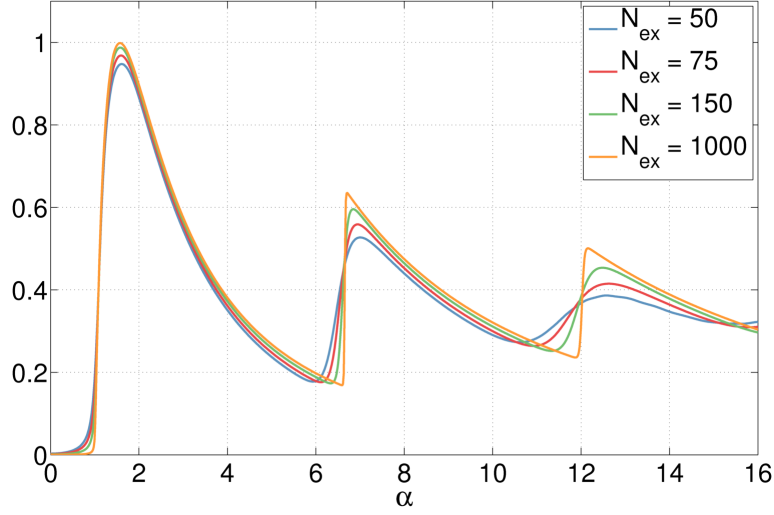
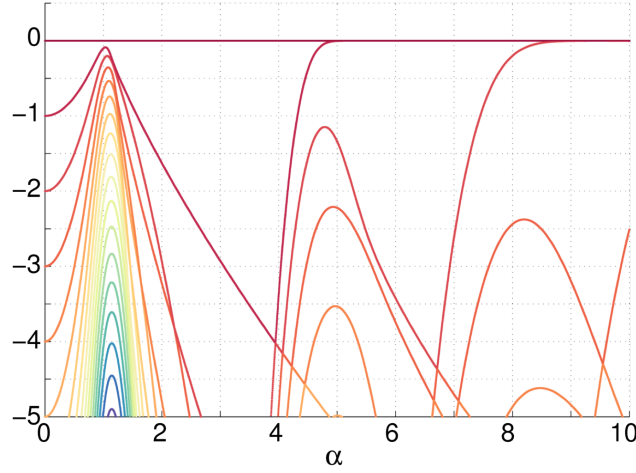


Figure 7.3: Rescaled stationary state mean photon numbers, $\langle \rho_{ss} \rangle / N_{ex}$ for increasing N_{ex} , showing phase transition becomes sharp as $N_{ex} \rightarrow \infty$.

caled variable $\chi = n/N_{ex}$, which approaches the (N_{ex} independent) limit

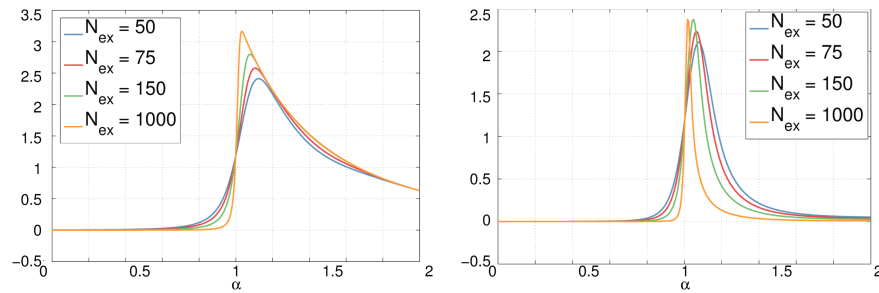
$$v(\chi) = - \int_0^\chi \log[(v + \sin^2(\alpha\sqrt{y})) / (v + 1)] dy$$

as it can be deduced from the formulas (3.28) and (3.33). Therefore, in the limit of large pumping rate we deal with a particle in a fixed potential $v(\chi)$ at inverse temperature $1/kT = N_{ex}$. At $\alpha \approx 1$ the dependence of the mean on N_{ex} switches from constant to linear behaviour as the minimum of the potential $v(\chi)$ moves away from zero. When the two minima are at different heights, the lower one becomes the stable and other one is metastable. Communication between the phases becomes increasingly unlikely, with probability decreasing exponentially with N_{ex} . When the two minima are equal, we have two stable states, and the corresponding value of α is the phase transition point for the mean photon number.

Figure 7.4: Spectrum of semigroup generator for $N_{ex} = 150$

More information about the dynamical phase transitions may be obtained from the rest of the spectrum of the semigroup generator, shown in Figure 7.4. We note several points of interest: firstly, at all "transition points" the spectral gap closes; but at the second order transition point $\alpha \approx 1$ the gap closes considerably more slowly than at the other transition points $\alpha \approx 6.66, \dots$. Secondly, at $\alpha \approx 1$ the spectrum becomes increasingly dense, in the sense that a fixed interval contains an increasing number of eigenvalues as N_{ex} increases.

Although the mean of the counting process Λ_t coincides with the mean of the stationary state photon number distribution, as we show in Figure 7.5, this is not the case with the respective variances. The critical point $\alpha \approx 1$, associated with an increasing density of the spectrum of the generator and closing of the spectral gap, also exhibits a change in the scaling of the cumulants with N_{ex} .

Figure 7.5: Variance of stationary state (left) and variance of counting process (right), rescaled by factors of N_{ex}^{-1} and $N_{ex}^{-1.6}$, respectively

7.5 CONCLUSION

We have studied the counting process associated to the measurement of the outgoing atoms in the atom maser, and shown that this process satisfies the large deviations principle. In particular, this means that the cross-over behaviour observed in numerical simulations is not associated with the non-analyticity of the limiting log-moment generating function, as one would expect for a genuine phase transition. The rescaled counting process Λ_t/N_{ex} does exhibit such a transition in the limit of infinite rate N_{ex} , as argued in the previous section using the potential model, and illustrated in Figures 3.5, 7.2, and 7.3. In particular, the transitions occurring at $\alpha \approx 1$ and $\alpha \approx 6.66$ are of different types, as seen in the scaling of the moments as well as the behaviour of the spectrum at these points.

As a corollary, we have showed that the counting process satisfies the central limit theorem, which can be used to develop the statistical estimation theory of local asymptotic normality [1].

The model we have investigated has the property that the stationary state is diagonal in the Fock basis and all the jump operators leave the set of diagonal states invariant. The large deviations problem could then be considered in the framework of "classical" probability, as a property of the birth-death process associated to the cavity dynamics. Indeed, at one point our proof relies on the restriction to the diagonal algebra for proving the strict positivity of the dynamical semigroup. However, the steps of the proof are formulated in the language of non-commutative probability theory and offer a general recipe for other settings where no classical reduction is possible. An example would be the atom maser where the outgoing atoms are measured in a different basis than the standard one, thus breaking the invariance of the diagonal algebra. In this case, using analytic perturbation theory one can show that the limiting log-moment generating function $\lambda(s)$ is smooth in a neighbourhood of $s = 0$ but we were not able to extend this to all s .

The compactness of the Markov semigroup makes our model tractable as it becomes essentially finite dimensional, as the bath decay dominates the absorption due to the atom interaction. An interesting problem would be to explore more general classes of infinite dimensional systems (e.g. continuous variables or infinite spin chains) where a

similar phenomenon holds. Another issue is the general relation between the "static" transitions which refer to non-analytic properties of the stationary state, and dynamic transitions which characterise properties of the measurement process. As shown in [2] one can construct examples where the stationary state does not change while the system undergoes a dynamical phase transition.

Finally, a more general large deviations setup can be considered which takes into account the correlations between the detection events rather than the total number of counts (see Ch. 4).

CONCLUSION

8.1 SUMMARY

In Chs. 2 and 3 we presented an introduction to the theory of large deviations and quantum Markov processes, respectively. The two topics are connected through the framework of thermodynamics of quantum trajectories; a point of view which, as we explained, is useful in uncovering phase transitions in open quantum systems.

We followed these introductory chapters with a presentation of several results which are all part of a promising and new approach to the dynamics of open quantum systems. What all these results have in common is that they use the statistical properties of quantum jump trajectories as indicators of critical dynamical features such as phase transitions, while in the individual chapters we have considered different aspects of this approach. This may be summarised as follows: Ch. 4 considered phase decompositions and purification, followed by Ch. 5, where we argued that the trajectories serve as indicators of critical features. This was followed by Ch. 6 where more subtle statistical properties of trajectories was studied, while Ch. 7 served as a case study in the application of this approach to a particular model.

In Ch. 4 we established a decomposition for quantum Markov processes into phases; we used this structure to define phase purification and phase transitions, with large deviations rate functions serving as an indicator of both these critical features. The examples we discussed served to illustrate this result.

In Ch. 5 we have discussed the results published in [2]. The important message in this chapter is that features of dynamical transitions in open quantum systems may be uncovered readily through the dynamical picture of quantum jump trajectories, rather than solely through the

static properties such as the stationary state; several examples illustrated this framework.

We stated and proved a Sanov theorem for the output of quantum Markov chains in Ch. 6. This result allows us to define higher-level rate functions, which in turn may be used to distinguish critical behaviour in systems for which the usual rate function does not show any features.

Finally, in Ch. 7 we established a large deviations principle for the counting process on the output of a particular quantum Markov process, the atom maser. We discussed the cross-over behaviour of numerical simulations and concluded that these features are not associated to any non-analytic behaviour of the large deviations rate function. We argue that the counting process does exhibit critical behaviour in the limit of infinite pumping rate.

8.2 OUTLOOK

In general, future directions involve building on the research presented in this thesis. This means exploiting the developed mathematical framework to investigate physical models of dynamical phase transitions, and exploring metastability in quantum non-equilibrium dynamics and its applications in quantum control theory.

The phase structure, discussed in Ch. 4, could be extended to infinite-dimensional systems (such as the atom maser, or the many-body systems from Ch. 5); however, since infinite-dimensional operator algebras have a more complicated structure, this would be more mathematically involved. Aside from this, another further direction is to more deeply examine the topological structure of the space of stationary states. This would allow for phase transitions to be considered as a topological, as well as analytic, phenomenon.

The results in Ch. 5 may be extended in the development of a purely quantum theory of large deviations by exploiting the connection with matrix product states, which generalises the results on “classical” LD for measurement trajectories. After this, a future direction is to compute the parent Hamiltonian of physically relevant interacting spin models and explore their relevance for this large deviation theory.

The Sanov theorem for the output of a quantum Markov chain in Ch. 6 has a natural extension to the empirical process. This essentially

means taking the infinite limit of the length of the sequence in the Sanov theorem; this leads us to one possible extension of our results, which is to realise a Donsker-Varadhan theory in open quantum systems.

Our study of the atom maser in Ch. 7 was limited to the case where the choice of measurement (the counting process) led to a commutative restriction of the dynamics, which somewhat simplified a few of the steps required in the proof. As the majority of the proof is formulated in the language of non-commutative probability theory it offers a general recipe for other settings where no classical reduction is possible. For example, if the output atoms of the atom maser are measured in a different basis than the standard one, this breaks the invariance of the commutative algebra. In this case, using analytic perturbation theory one can show that the limiting log-moment generating function $\lambda(s)$ is smooth in a neighbourhood of $s = 0$ but we were not able to extend this to all s . A key mathematical property is compactness of the semigroup; another interesting problem would be to explore more general classes of infinite dimensional systems (e.g. continuous variables or infinite spin chains) where a similar phenomenon holds. Finally, a more general large deviations setup can be considered which takes into account the correlations between the detection events rather than the total number of counts.

A topic not presented in this thesis is the possible role played by large deviations in quantum random walks, which we have only studied numerically so far by extending the four-level model from Ch. 4. We would like to develop numerical and theoretical methods for a systematic study of dynamical transitions in quantum random walks; the obtained insights may be used to attack open problems related to the quantum jump (stochastic Schrödinger) evolution of open systems observed from the environment.

BIBLIOGRAPHY

- [1] C. Catana, M. van Horssen, and M. Guta, “Asymptotic inference in system identification for the atom maser,” *Philosophical transactions. Series A, Mathematical, physical, and engineering sciences* **370** no. 1979, (Nov., 2012) 5308–23, [arXiv:arXiv:1112.2080v1](#). (Cited on pages [iv](#), [99](#), and [113](#).)
- [2] I. Lesanovsky, M. van Horssen, M. Guta, and J. P. Garrahan, “Characterization of Dynamical Phase Transitions in Quantum Jump Trajectories Beyond the Properties of the Stationary State,” *Physical Review Letters* **110** no. 15, (Apr., 2013) 150401. (Cited on pages [iv](#), [81](#), [87](#), [90](#), [114](#), and [115](#).)
- [3] M. van Horssen and M. Guta, “Large Deviations, Central Limit and dynamical phase transitions in the atom maser,” [arXiv:1206.4956](#). (Cited on pages [iv](#), [88](#), and [99](#).)
- [4] J. P. Garrahan, A. Armour, and I. Lesanovsky, “Quantum trajectory phase transitions in the micromaser,” *Physical Review E* **84** no. 2, (Aug., 2011), [arXiv:1103.0919](#). (Cited on pages [xii](#), [51](#), [52](#), [88](#), [99](#), [109](#), and [110](#).)
- [5] F. den Hollander, *Large Deviations*. Fields Institute Monographs. American Mathematical Society, Providence, Rhode Island, 2000. (Cited on pages [4](#), [5](#), and [7](#).)
- [6] S. Karlin and H. M. Taylor, *A First Course in Stochastic Processes*. Academic Press, second ed., 1975. (Cited on page [5](#).)
- [7] S. Varadhan, *Large Deviations and Applications*. Regional Conference Series in Applied Mathematics. SIAM, Philadelphia, 1984. (Cited on page [5](#).)
- [8] A. Dembo and O. Zeitouni, *Large Deviations Techniques and Applications*, vol. 38 of *Stochastic Modelling and Applied Probability*. Springer Berlin Heidelberg, Berlin, Heidelberg, 2010. (Cited on pages [5](#), [11](#), [12](#), [13](#), [14](#), [15](#), and [92](#).)

- [9] R. S. Ellis, “An Overview of the Theory of Large Deviations and Applications to Statistical Mechanics,” *Scand. Actuarial. J.* no. 1, (1995) 97–142. (Cited on pages [9](#), [12](#), [17](#), [18](#), [19](#), and [98](#).)
- [10] R. S. Ellis, “The Theory of Large Deviations: from Boltzmann’s 1877 calculation to equilibrium macrostates in 2D turbulence,” *Physica D* **133** (1999) 106–136. (Cited on page [11](#).)
- [11] H. Schneider, “The concepts of irreducibility and full indecomposability of a matrix in the works of Frobenius, König and Markov,” *Linear Algebra and its Applications* **18** no. 2, (Jan., 1977) 139–162. (Cited on page [13](#).)
- [12] C. D. Meyer, *Matrix Analysis and Applied Linear Algebra*. SIAM, 2001. (Cited on page [13](#).)
- [13] A. Berman and R. J. Plemmons, *Nonnegative Matrices in the Mathematical Sciences*. Computer Science and Applied Mathematics. Academic Press, New York, 1979. (Cited on page [13](#).)
- [14] I. H. Dinwoodie, “Identifying a Large Deviation Rate Function,” *The Annals of Probability* **21** no. 1, (1993) 216–231. (Cited on page [15](#).)
- [15] D. Chandler, *Introduction to Modern Statistical Mechanics*. Oxford University Press, Oxford, UK, 1987. (Cited on page [17](#).)
- [16] H. Touchette, “The large deviation approach to statistical mechanics,” *Physics Reports* **478** no. 1-3, (July, 2009) 1–69. (Cited on page [20](#).)
- [17] R. L. Jack and P. Sollich, “Large deviations and ensembles of trajectories in stochastic models,” [arXiv:0911.0211](#). (Cited on page [21](#).)
- [18] V. Lecomte, F. van Wijland, and C. Appert-Rolland, “Chaotic Properties of Systems with Markov Dynamics,” *Physical Review Letters* **95** no. 010601, (2005) 1–65, [arXiv:0606211v2 \[arXiv:cond-mat\]](#). (Cited on page [21](#).)
- [19] V. Lecomte, C. Appert-Rolland, and F. van Wijland, “Thermodynamic formalism for systems with Markov

- dynamics," *J. Stat. Phys.* **127** no. 1, (Apr., 2007) 51–106. (Cited on pages 21, 38, and 89.)
- [20] B. Derrida, "Non-equilibrium steady states: fluctuations and large deviations of the density and of the current," *Journal of Statistical Mechanics: Theory and Experiment* **2007** no. 07, (July, 2007) P07023–P07023. (Cited on page 21.)
- [21] T. Bodineau and B. Derrida, "Distribution of current in nonequilibrium diffusive systems and phase transitions," *Physical Review E* **72** no. 6, (Dec., 2005) 1–8. (Cited on page 21.)
- [22] J.-P. Eckmann and D. Ruelle, "Ergodic theory of chaos and strange attractors," *Reviews of Modern Physics* **57** no. 3, (July, 1985) 617–656. (Cited on page 21.)
- [23] J. L. Lebowitz and H. Spohn, "A Gallavotti-Cohen Type Symmetry in the Large Deviation Functional for Stochastic Dynamics," *Journal of Statistical Physics* **95** (1999) 333–365, [arXiv:9811220v1 \[arXiv:cond-mat\]](#). (Cited on page 21.)
- [24] B. Gaveau and L. S. Schulman, "Theory of nonequilibrium first-order phase transitions for stochastic dynamics," *Journal of Mathematical Physics* **39** no. 3, (1998) 1517–1533. (Cited on page 21.)
- [25] F. Ritort and P. Sollich, "Glassy dynamics of kinetically constrained models," *Advances in Physics* **52** no. 4, (June, 2003) 219–342. (Cited on page 22.)
- [26] S. Whitelam and J. P. Garrahan, "Geometrical Picture of Dynamical Facilitation," *The Journal of Physical Chemistry B* **108** no. 21, (May, 2004) 6611–6615. (Cited on page 22.)
- [27] J. P. Garrahan and D. Chandler, "Geometrical Explanation and Scaling of Dynamical Heterogeneities in Glass Forming Systems," *Physical Review Letters* **89** no. 3, (July, 2002) 3–6. (Cited on page 22.)
- [28] M. Merolle, J. P. Garrahan, and D. Chandler, "Space-time thermodynamics of the glass transition.," *Proceedings of the National Academy of Sciences of the United States of America* **102** no. 31, (Aug., 2005) 10837–40. (Cited on page 22.)

- [29] J. P. Garrahan and D. Chandler, “Coarse-grained microscopic model of glass formers,” *Proceedings of the National Academy of Sciences of the United States of America* **100** no. 17, (Aug., 2003) 9710–4. (Cited on page 22.)
- [30] Y. Jung, J. P. Garrahan, and D. Chandler, “Excitation lines and the breakdown of Stokes-Einstein relations in supercooled liquids,” *Physical Review E* **69** no. 6, (June, 2004) 1–7. (Cited on page 22.)
- [31] R. L. Jack, J. P. Garrahan, and D. Chandler, “Space-time thermodynamics and subsystem observables in a kinetically constrained model of glassy materials,” *The Journal of chemical physics* **125** no. 18, (Nov., 2006) 184509. (Cited on page 22.)
- [32] J. P. Garrahan, R. L. Jack, V. Lecomte, E. Pitard, K. van Duijvendijk, and F. van Wijland, “Dynamical first-order phase transition in kinetically constrained models of glasses,” *Phys. Rev. Lett.* **98** (2007) 195702. (Cited on pages 22, 38, 51, and 89.)
- [33] J. P. Garrahan, R. L. Jack, V. Lecomte, E. Pitard, K. van Duijvendijk, and F. van Wijland, “First-order dynamical phase transition in models of glasses: an approach based on ensembles of histories,” *Journal of Physics A: Mathematical and Theoretical* **42** no. 7, (Feb., 2009) 075007. (Cited on pages 22 and 51.)
- [34] L. O. Hedges, R. L. Jack, J. P. Garrahan, and D. Chandler, “Dynamic order-disorder in atomistic models of structural glass formers,” *Science* **323** no. 5919, (Mar., 2009) 1309–13. (Cited on pages 22 and 51.)
- [35] C. W. Gardiner and P. Zoller, *Quantum Noise*. Springer Series in Synergetics. Springer, Berlin Heidelberg New York, 3 ed., 2004. (Cited on pages 23 and 34.)
- [36] K. Parthasarathy, *An Introduction to Quantum Stochastic Calculus*. Monographs in Mathematics. Birkhäuser, Basel Boston Berlin, 1992. (Cited on pages 23 and 31.)
- [37] V. P. Belavkin, “Nondemolition measurements, nonlinear filtering and dynamic programming of quantum stochastic

- processes*," in *Modeling and Control of Systems SE - 15*, A. Blaqui re, ed., vol. 121 of *Lecture Notes in Control and Information Sciences*, pp. 245–265. Springer Berlin Heidelberg, 1989. (Cited on page 23.)
- [38] M. B. Plenio and P. L. Knight, "The quantum-jump approach to dissipative dynamics in quantum optics," *Rev. Mod. Phys.* **70** no. 1, (Jan., 1998) 101–144. (Cited on pages 23, 51, 52, and 85.)
- [39] B. K mmerer, "*Quantum Markov Processes*," in *Coherent Evolution in Noisy Environments*, vol. 611 of *Lecture Notes in Physics*, ch. 4, pp. 139–198. Springer, Berlin Heidelberg, 2002. (Cited on pages 23 and 93.)
- [40] F. Strocchi, *An Introduction to the Mathematical Structure of Quantum Mechanics*. Advanced Series in Mathematical Physics. World Scientific, Singapore, second ed., 2008. (Cited on page 23.)
- [41] B. K mmerer, "*Quantum Markov Processes and Applications in Physics*," in *Quantum Independent Increment Processes II*, M. Sch uermann and U. Franz, eds., vol. 330 of *Lecture Notes in Mathematics*, pp. 259–330. Springer-Verlag, Berlin Heidelberg, 2006. (Cited on pages 25 and 27.)
- [42] G. Lindblad, "On the generators of quantum dynamical semigroups," *Communications in Mathematical Physics* **48** no. 2, (June, 1976) 119–130. (Cited on page 30.)
- [43] V. Gorini, A. Kossakowski, and E. C. G. Sudarshan, "Completely positive dynamical semigroups of N-level systems," *Journal of Mathematical Physics* **17** no. 5, (1976) 821. (Cited on page 30.)
- [44] K.-J. Engel and R. Nagel, *One-parameter semigroups for linear evolution equations*. Graduate Text in Mathematics. Springer-Verlag, New York, June, 2000. (Cited on pages 30, 104, 107, and 109.)
- [45] V. P. Belavkin, "Non-Demolition Measurement and Control in Quantum Dynamical Systems," in *Proceedings of CISM, Udine*, A. Blacquiere, S. Diner, and G. Lochak, eds., Information complexity and control in quantum physics, pp. 331–336. Springer-Verlag, Wien-New York, 1987. (Cited on page 31.)

- [46] V. P. Belavkin, "Quantum stochastic calculus and quantum nonlinear filtering," *Journal of Multivariate Analysis* no. 42, (1992) 171–201. (Cited on page 31.)
- [47] V. P. Belavkin, "Measurement, filtering and control in quantum open dynamical systems," *Rep. Math. Phys* no. 43, (1999) 405–425. (Cited on page 31.)
- [48] L. Bouten, R. Van Handel, and M. R. James, "An Introduction to Quantum Filtering," *SIAM Journal on Control and Optimization* **46** no. 6, (2007) 2199. (Cited on pages 32, 34, and 36.)
- [49] E. B. Davies, *Quantum Theory of Open Systems*. Academic Press, London, 1976. (Cited on page 35.)
- [50] H. Carmichael, *An Open Systems Approach to Quantum Optics*, vol. 18 of *Lecture Notes in Physics Monographs*. Springer Berlin Heidelberg, Berlin, Heidelberg, 1993. (Cited on page 35.)
- [51] C.-A. Pillet, "Quantum Dynamical Systems," in *Open Quantum Systems I*, no. Umr 6207 in *Lecture Notes in Mathematics*, pp. 107–182. Berlin / Heidelberg, 2006. (Cited on page 36.)
- [52] S. Sachdev, *Quantum Phase Transitions*. Cambridge University Press, Cambridge, 2nd ed., 2011. (Cited on page 37.)
- [53] J. P. Garrahan and I. Lesanovsky, "Thermodynamics of Quantum Jump Trajectories," *Physical Review Letters* **104** no. 16, (Apr., 2010) 5, [arXiv:0911.0556](#). (Cited on pages 37, 51, 52, and 99.)
- [54] J. D. Cresser, "Ergodicity of Quantum Trajectory Detection Records," in *Directions in Quantum Optics*, *Lecture Notes in Physics*, pp. 358–369. 2001. (Cited on page 37.)
- [55] B. Kümmerer and H. Maassen, "An ergodic theorem for quantum counting processes," *Journal of Physics A: Mathematical and General* **36** no. 8, (Feb., 2003) 2155–2161. (Cited on page 37.)
- [56] B. Kümmerer and H. Maassen, "A pathwise ergodic theorem for quantum trajectories," *Journal of Physics A: Mathematical and General* **37** no. 49, (Dec., 2004) 11889–11896. (Cited on page 37.)

- [57] J. P. Garrahan and I. Lesanovsky, “Thermodynamics of Quantum Jump Trajectories,” *Phys. Rev. Lett.* **104** no. 16, (Apr., 2010) 160601. (Cited on pages 38, 85, and 89.)
- [58] T. Wellens and A. Buchleitner, “Bistability and stochastic resonance in an open quantum system,” *Chemical Physics* **268** no. 1-3, (June, 2001) 131–149. (Cited on page 40.)
- [59] C. Carr, R. Ritter, C. G. Wade, C. S. Adams, and K. J. Weatherill, “Nonequilibrium Phase Transition in a Dilute Rydberg Ensemble,” *Physical Review Letters* **111** no. 11, (Sept., 2013) 113901. (Cited on page 40.)
- [60] N. Malossi, M. M. Valado, S. Scotto, P. Huillery, P. Pillet, D. Ciampini, E. Arimondo, and O. Morsch, “Full counting statistics and phase diagram of a dissipative Rydberg gas,” *arXiv:1308.1854v1*. (Cited on page 40.)
- [61] D. E. Evans and R. Høegh Krohn, “Spectral Properties of Positive Maps on C^* -Algebras,” *Journal of the London Mathematical Society* **s2-17** no. 2, (Apr., 1978) 345–355. (Cited on pages 40, 41, 56, and 96.)
- [62] A. Frigerio and M. Verri, “Long-Time Asymptotic Properties of Dynamical Semigroups on W^* -algebras,” *Mathematische Zeitschrift* **180** (1982) 275–286. (Cited on page 41.)
- [63] F. Fagnola and R. Pellicer, “Irreducible and Periodic Positive Maps,” *Communications on Stochastic Analysis* **3** no. 3, (2009) 407–418. (Cited on page 41.)
- [64] S. Albeverio and R. Høegh Krohn, “Frobenius theory for positive maps of von Neumann algebras,” *Communications in Mathematical Physics* **64** no. 1, (Dec., 1978) 83–94. (Cited on page 41.)
- [65] U. Groh, “The peripheral point spectrum of schwarz operators on C^* -algebras,” *Mathematische Zeitschrift* **176** no. 3, (Sept., 1981) 311–318. (Cited on page 41.)
- [66] R. Schrader, “Perron-Frobenius Theory for Positive Maps on Trace Ideals,” *arXiv:0007020 [math-ph]*. (Cited on page 41.)

- [67] W. Arveson, “Asymptotic Stability I: Completely Positive Maps,” [arXiv:0304488 \[math\]](#). (Cited on page [41](#).)
- [68] A. Luczak, “The eigenvectors of semigroups of positive maps on von Neumann algebras,” [arXiv:0911.4434](#). (Cited on page [41](#).)
- [69] A. Bátkai, U. Groh, D. Kunszenti-Kovács, and M. Schreiber, “Decomposition of operator semigroups on W^* -algebras,” *Semigroup Forum* **84** no. 1, (Dec., 2011) 8–24, [arXiv:1106.0287](#). (Cited on page [41](#).)
- [70] V. Paulsen, *Completely Bounded Maps and Operator Algebras*. Cambridge Studies in Advanced Mathematics. Cambridge University Press, Cambridge, 2003. (Cited on page [41](#).)
- [71] B.-S. Tam, “A cone-theoretic approach to the spectral theory of positive linear operators: the finite dimensional case,” *Taiwanese Journal of Mathematics* **5** no. 2, (2001) 207–277. (Cited on page [42](#).)
- [72] Y. Du, *Order Structure And Topological Methods in Nonlinear Partial Differential Equations*, vol. 1 of *Series on Partial Differential Equations and Applications*. World Scientific, Singapore, 2006. (Cited on pages [42](#), [100](#), and [103](#).)
- [73] R. Carbone and F. Fagnola, “Exponential L^2 -convergence of quantum Markov semigroups on $B(H)$,” *Mathematical Notes* **68** no. 4, (Oct., 2000) 452–463. (Cited on pages [43](#), [100](#), [102](#), and [104](#).)
- [74] F. Fagnola, R. Rebolledo, and C. Saavedra, “Quantum flows associated to master equations in quantum optics,” *Journal of Mathematical Physics* **35** no. 1, (1994) 1. (Cited on pages [43](#), [100](#), and [104](#).)
- [75] B.-G. Englert and G. Morigi, “Five Lectures on Dissipative Master Equations,” in *Coherent Evolution in Noisy Environments*, A. Buchleitner and K. Hornberger, eds., vol. 2 of *Lecture Notes in Physics*, ch. 2, pp. 55–106. Springer, Berlin Heidelberg New York, 2002. (Cited on page [43](#).)

- [76] B.-G. Englert, “Elements of Micromaser Physics,” [arXiv:0203052 \[quant-ph\]](#). (Cited on pages 45, 48, 88, and 109.)
- [77] F. Fagnola and R. Rebolledo, “On the existence of stationary states for quantum dynamical semigroups,” *Journal of Mathematical Physics* **42** no. 3, (2001) 1296. (Cited on page 46.)
- [78] S. Haroche and J.-M. Raimond, *Exploring the Quantum*. Oxford University Press, Oxford, UK, 2006. (Cited on page 49.)
- [79] H. Nagaoka and T. Ogawa, “Strong converse and Stein’s lemma in quantum hypothesis testing,” *IEEE Transactions on Information Theory* **46** no. 7, (2000) 2428–2433. (Cited on page 51.)
- [80] F. Hiai, M. Mosonyi, and T. Ogawa, “Error exponents in hypothesis testing for correlated states on a spin chain,” *Journal of Mathematical Physics* **49** no. 3, (2008) 032112. (Cited on page 51.)
- [81] V. Jakšić, Y. Ogata, C.-A. Pillet, and R. Seiringer, “Quantum hypothesis testing and non-equilibrium statistical mechanics,” *Reviews in Mathematical Physics* **24** no. 06, (July, 2012) 1230002. (Cited on page 51.)
- [82] M. Hayashi, “Two quantum analogues of Fisher information from a large deviation viewpoint of quantum estimation,” [arXiv:0202003 \[quant-ph\]](#). (Cited on page 51.)
- [83] R. Nagaoka, “Two quantum analogues of the large deviation Cramer-Rao inequality,” in *Proceedings of 1994 IEEE International Symposium on Information Theory*, no. 6, p. 118. IEEE, 1991. (Cited on page 51.)
- [84] I. Bjelaković, J.-d. Deuschel, T. Krüger, R. Seiler, R. Siegmund-Schultze, and A. Szkořca, “Typical Support and Sanov Large Deviations of Correlated States,” *Communications in Mathematical Physics* **279** no. 2, (Feb., 2008) 559–584. (Cited on page 51.)
- [85] I. Bjelaković, J.-d. Deuschel, T. Krüger, R. Seiler, R. Siegmund-Schultze, and A. Szkořca, “A quantum version

- of Sanov's theorem," [arXiv:0412157 \[quant-ph\]](#). (Cited on page 51.)
- [86] R. Ahlswede and V. M. Blinovsky, "Large Deviations in Quantum Information Theory," *Problems of Information Transmission* **39** no. 4, (Oct., 2003) 373–379. (Cited on page 51.)
- [87] F. Hiai, M. Mosonyi, and T. Ogawa, "Large deviations and Chernoff bound for certain correlated states on a spin chain," *Journal of Mathematical Physics* **48** no. 12, (2007) 123301. (Cited on pages 51, 91, 92, 99, and 100.)
- [88] F. Hiai, M. Mosonyi, H. Ohno, and D. Petz, "Free Energy Density for Mean Field Perturbation of States of a One-Dimensional Spin Chain," *Reviews in Mathematical Physics* **20** no. 03, (Apr., 2008) 335–365. (Cited on page 51.)
- [89] Y. Ogata, "Large Deviations in Quantum Spin Chains," *Communications in Mathematical Physics* **296** no. 1, (Feb., 2010) 35–68. (Cited on page 51.)
- [90] Y. Ogata and L. Rey-Bellet, "Ruelle-Lanford functions for quantum spin systems," [arXiv:1009.4491](#). (Cited on page 51.)
- [91] V. Jakšić, Y. Ogata, Y. Pautrat, and C.-A. Pillet, "Entropic fluctuations in quantum statistical mechanics. An Introduction," in *Les Houches Summer School Proceedings*. 2011. (Cited on page 51.)
- [92] J. L. Lebowitz, M. Lenci, and H. Spohn, "Large deviations for ideal quantum systems," *Journal of Mathematical Physics* **41** no. 3, (2000) 1224. (Cited on page 51.)
- [93] M. Lenci and L. Rey-Bellet, "Large Deviations in Quantum Lattice Systems: One-Phase Region," *Journal of Statistical Physics* **119** no. 3-4, (May, 2005) 715–746. (Cited on page 51.)
- [94] K. Netočný and F. Redig, "Large Deviations for Quantum Spin Systems," *Journal of Statistical Physics* **117** no. 3-4, (Nov., 2004) 521–547. (Cited on page 51.)
- [95] V. Jakšić, B. Landon, and C.-A. Pillet, "Entropic fluctuations in XY chains and reflectionless Jacobi matrices," [arXiv:1209.3675](#). (Cited on page 51.)

- [96] V. Jakšić and C.-A. Pillet, “Entropic Functionals in Quantum Statistical Mechanics,” [arXiv:1301.3332](#). (Cited on page 51.)
- [97] W. De Roeck, C. Maes, K. Netočný, and L. Rey-Bellet, “A note on the non-commutative Laplace-Varadhan integral lemma,” *Reviews in Mathematical Physics* **22** no. 07, (Aug., 2010) 839–858. (Cited on page 51.)
- [98] W. De Roeck, C. Maes, and K. Netočný, “Quantum Macrostates, Equivalence of Ensembles and an H-Theorem,” [arXiv:0601027 \[math-ph\]](#). (Cited on page 51.)
- [99] W. De Roeck, “Large deviation generating function for energy transport in the Pauli-Fierz model,” [arXiv:0704.3400](#). (Cited on page 51.)
- [100] G. Gallavotti, J. L. Lebowitz, and V. Mastropietro, “Large Deviations in Rarefied Quantum Gases,” *Journal of Statistical Physics* **108** no. 5-6, (2002) 831–861. (Cited on page 51.)
- [101] Z. S. Szewczak, “Large deviations in operator form,” *Positivity* **12** no. 4, (Oct., 2008) 631–641. (Cited on page 51.)
- [102] H. Comman, “Large Deviations for Quantum Markov Semigroups on the 2×2 -Matrix Algebra,” *Annales Henri Poincaré* **9** no. 5, (Aug., 2008) 979–1003. (Cited on page 51.)
- [103] M. R. Evans, S. Franz, C. Godreche, and D. Mukamel, “Focus issue on Dynamics of Non-Equilibrium Systems,” *Journal of Statistical Mechanics: Theory and Experiment* (2007) P07001–P07024. (Cited on page 51.)
- [104] D. Andrieux, “Quantum trajectories face a transition,” *Physics* **3** no. 34, (Apr., 2010) . (Cited on pages 51 and 52.)
- [105] A. Budini, “Thermodynamics of quantum jump trajectories in systems driven by classical fluctuations,” *Physical Review E* **82** no. 6, (Dec., 2010) 12, [arXiv:1012.0776](#). (Cited on pages 51 and 52.)
- [106] L. Bruneau and C.-a. Pillet, “Thermal Relaxation of a QED Cavity,” *Journal of Statistical Physics* **134** no. 5-6, (Dec., 2008) 1071–1095. (Cited on page 51.)

- [107] F. Hiai and D. Petz, “The proper formula for relative entropy and its asymptotics in quantum probability,” *Communications in Mathematical Physics* **143** no. 1, (Dec., 1991) 99–114. (Cited on page 51.)
- [108] J. Dereziński, W. De Roeck, and C. Maes, “Fluctuations of Quantum Currents and Unravelings of Master Equations,” *Journal of Statistical Physics* **131** no. 2, (Feb., 2008) 341–356. (Cited on page 51.)
- [109] P. Zoller, M. Marte, and D. Walls, “Quantum jumps in atomic systems,” *Physical Review A* **35** no. 1, (Jan., 1987) 198–207. (Cited on page 51.)
- [110] E. Barkai, Y. Jung, and R. Silbey, “Theory of single-molecule spectroscopy: beyond the ensemble average,” *Annual review of physical chemistry* **55** (Jan., 2004) 457–507. (Cited on page 52.)
- [111] J. M. Hickey, S. Genway, I. Lesanovsky, and J. P. Garrahan, “Thermodynamics of Quadrature Trajectories in Open Quantum Systems,” [arXiv:1206.5719](#). (Cited on page 52.)
- [112] C. Ates, B. Olmos, J. P. Garrahan, and I. Lesanovsky, “Dynamical phases and intermittency of the dissipative quantum Ising model,” *Physical Review A* **85** no. 4, (Apr., 2012) 1–8. (Cited on pages 52, 81, 82, 86, and 87.)
- [113] S. Genway, J. P. Garrahan, I. Lesanovsky, and A. Armour, “Phase transitions in trajectories of a superconducting single-electron transistor coupled to a resonator,” *Physical Review E* **85** no. 5, (May, 2012) 1–12. (Cited on page 52.)
- [114] A. Budini, “Large deviations of ergodic counting processes: A statistical mechanics approach,” *Physical Review E* **84** no. 1, (July, 2011) 1–11. (Cited on page 52.)
- [115] S. Garnerone, “Thermodynamic formalism for dissipative quantum walks,” [arXiv:1205.5744](#). (Cited on page 52.)
- [116] B. Baumgartner and H. Narnhofer, “Analysis of quantum semigroups with GKS-Lindblad generators: II. General,” *Journal of Physics A: Mathematical and Theoretical* **41** no. 39, (Oct., 2008) 395303. (Cited on pages 55, 56, 57, and 65.)

- [117] J. Dixmier, *Von Neumann Algebras*. North Holland, 1981. (Cited on page 57.)
- [118] R. Alicki, “Controlled Quantum Open Systems,” in *Irreversible Quantum Dynamics*, no. 0, pp. 121–139. Springer Berlin Heidelberg, 2003. (Cited on page 57.)
- [119] M. Guta and J. Kiukas, “Equivalence classes and local asymptotic normality in system identification for quantum Markov chains,” *In preparation* (2014) . (Cited on pages 58 and 61.)
- [120] B. Baumgartner, H. Narnhofer, and W. Thirring, “Analysis of quantum semigroups with GKS-Lindblad generators: I. Simple generators,” *Journal of Physics A: Mathematical and Theoretical* **41** no. 6, (Feb., 2008) 065201. (Cited on page 65.)
- [121] B. Baumgartner and H. Narnhofer, “The Structures Of State Space Concerning Quantum Dynamical Semigroups,” *Reviews in Mathematical Physics* **24** no. 02, (Mar., 2012) 1250001. (Cited on page 65.)
- [122] I. Bengtsson and K. Życzkowski, *Geometry of Quantum States: An Introduction to Quantum Entanglement*. Cambridge University Press, Cambridge, 2006. (Cited on page 80.)
- [123] D. Cavalcanti, F. G. S. L. Brandão, and M. O. T. Cunha, “Geometric Phase Transition: direct measurement of a mathematical abstraction,” *arXiv:0510068 [quant-ph]*. (Cited on page 80.)
- [124] G. Konya, D. Nagy, G. Szirmai, and P. Domokos, “Finite-size scaling in the quantum phase transition of the open-system Dicke-model,” *arXiv:1206.5131*. (Cited on page 81.)
- [125] S. Diehl, A. Tomadin, A. Micheli, R. Fazio, and P. Zoller, “Dynamical Phase Transitions and Instabilities in Open Atomic Many-Body Systems,” *Physical Review Letters* **105** no. 1, (July, 2010) 1–5, *arXiv:1003.2071*. (Cited on page 81.)
- [126] B. Olmos, I. Lesanovsky, and J. P. Garrahan, “Facilitated Spin Models of Dissipative Quantum Glasses,” *Physical Review*

- Letters* **109** no. 2, (July, 2012) 020403, [arXiv:1203.6585](#). (Cited on pages [81](#) and [87](#).)
- [127] C. Schön, E. Solano, F. Verstraete, J. I. Cirac, and M. M. Wolf, “Sequential Generation of Entangled Multiqubit States,” *Physical Review Letters* **95** no. 11, (Sept., 2005) 1–4. (Cited on pages [81](#) and [83](#).)
- [128] F. Verstraete and J. I. Cirac, “Continuous Matrix Product States for Quantum Fields,” *Physical Review Letters* **104** no. 19, (May, 2010) 1–4. (Cited on page [81](#).)
- [129] T. J. Osborne, J. Eisert, and F. Verstraete, “Holographic quantum states,” [arXiv:1005.1268](#). (Cited on page [81](#).)
- [130] M. Fannes, B. Nachtergaele, and R. F. Werner, “Finitely correlated states on quantum spin chains,” *Communications in Mathematical Physics* **144** no. 3, (1992) 443–490. (Cited on page [81](#).)
- [131] T. E. Lee, H. Häffner, and M. C. Cross, “Collective Quantum Jumps of Rydberg Atoms,” *Phys. Rev. Lett.* **108** no. 2, (Jan., 2012) 23602. (Cited on pages [82](#) and [86](#).)
- [132] M. Foss-Feig, K. R. A. Hazzard, J. J. Bollinger, and A. M. Rey, “Non-equilibrium dynamics of Ising models with decoherence: an exact solution,” *preprint* (2012) [arXiv:1209.5795](#). (Cited on page [82](#).)
- [133] E. M. Kessler, G. Giedke, A. Imamoglu, S. F. Yelin, M. D. Lukin, and J. I. Cirac, “Dissipative phase transition in a central spin system,” *Phys. Rev. A* **86** no. 1, (July, 2012) 12116. (Cited on page [82](#).)
- [134] R. Hübener, A. Mari, and J. Eisert, “Wick’s Theorem for Matrix Product States,” *Phys. Rev. Lett.* **110** (2013) 40401. (Cited on page [82](#).)
- [135] U. Schollwöck, “The density-matrix renormalization group,” *Reviews of Modern Physics* **77** no. 1, (Apr., 2005) 259–315. (Cited on page [84](#).)
- [136] I. Marzoli, J. I. Cirac, R. Blatt, and P. Zoller, “Laser cooling of trapped three-level ions: Designing two-level systems for

- sideband cooling," *Phys. Rev. A* **49** no. 4, (Apr., 1994) 2771–2779. (Cited on page 85.)
- [137] M. D. Ediger, "Spatially heterogeneous dynamics in supercooled liquids," *Annu. Rev. Phys. Chem.* **51** (2000) 99–128. (Cited on page 87.)
- [138] O. Benson, G. Raithel, and H. Walther, "Quantum jumps of the micromaser field: Dynamic behavior close to phase transition points," *Physical Review Letters* **72** no. 22, (May, 1994) 3506–3509. (Cited on pages 88 and 109.)
- [139] H.-J. Briegel, B.-G. Englert, N. Sterpi, and H. Walther, "One-atom maser: Statistics of detector clicks," *Physical Review A* **49** no. 4, (Apr., 1994) 2962–2985. (Cited on pages 88 and 109.)
- [140] G. Rempe and H. Walther, "Sub-Poissonian atomic statistics in a micromaser," *Physical Review A* **42** no. 3, (Aug., 1990) 1650–1655. (Cited on pages 88 and 109.)
- [141] L. S. Levitov, H. Lee, and G. B. Lesovik, "Electron counting statistics and coherent states of electric current," *J. Mat. Phys.* **37** no. 10, (Oct., 1996) 4845–4866. (Cited on page 89.)
- [142] D. A. Bagrets and Y. V. Nazarov, "Full counting statistics of charge transfer in Coulomb blockade systems," *Phys. Rev. B* **67** no. 8, (Feb., 2003) 85316. (Cited on page 89.)
- [143] S. Pilgram, A. N. Jordan, E. V. Sukhorukov, and M. Büttiker, "Stochastic Path Integral Formulation of Full Counting Statistics," *Phys. Rev. Lett.* **90** (2003) 206801. (Cited on page 89.)
- [144] C. Flindt, T. Novotný, A. Braggio, M. Sassetti, and A.-P. Jauho, "Counting Statistics of Non-Markovian Quantum Stochastic Processes," *Phys. Rev. Lett.* **100** (2008) 150601. (Cited on page 89.)
- [145] M. Esposito, U. Harbola, and S. Mukamel, "Nonequilibrium fluctuations, fluctuation theorems, and counting statistics in quantum systems," *Rev. Mod. Phys.* **81** no. 4, (2009) 1665. (Cited on page 89.)

- [146] J. P. Garrahan, A. D. Armour, and I. Lesanovsky, “Quantum trajectory phase transitions in the micromaser,” *Phys. Rev. E* **84** no. 2, (Aug., 2011) 21115. (Cited on page 89.)
- [147] C. Ates, B. Olmos, J. P. Garrahan, and I. Lesanovsky, “Dynamical phases and intermittency of the dissipative quantum Ising model,” *Phys. Rev. A* **85** no. 4, (Apr., 2012) 43620. (Cited on page 89.)
- [148] C. Schön, K. Hammerer, M. M. Wolf, J. I. Cirac, and E. Solano, “Sequential Generation of Matrix-Product States in Cavity QED,” [arXiv:0612101 \[quant-ph\]](#). (Cited on page 93.)
- [149] W. Bryc, “A remark on the connection between the large deviation principle and the central limit theorem,” *Statistics & Probability Letters* **18** (1993) 253–256. (Cited on pages 99 and 103.)
- [150] M. G. Krein and M. A. Rutman, “Linear operators leaving invariant a cone in a Banach Space,” *Amer. Math. Soc. Translation* **26** (1950) . (Cited on pages 100 and 103.)
- [151] F. Cipriani, F. Fagnola, and J. M. Lindsay, “Spectral Analysis and Feller Property for Quantum Ornstein-Uhlenbeck Semigroups,” *Communications in Mathematical Physics* **210** no. 1, (Mar., 2000) 85–105. (Cited on page 104.)
- [152] J. Janas and S. Naboko, “Multithreshold Spectral Phase Transitions for a Class of Jacobi Matrices,” in *Recent Advances in Operator Theory: The Israel Gohberg Anniversary Volume*, vol. 124 of *Operator Theory: Advances and Applications*, pp. 267–285. Birkhäuser Verlag, Basel Boston Berlin, 2001. (Cited on page 106.)
- [153] T. Kato, *Perturbation Theory for Linear Operators*. Springer-Verlag, Berlin Heidelberg New York, 2nd ed., 1976. (Cited on page 107.)
- [154] F. Chatelin, *Spectral Approximation of Linear Operators*. Computer Science and Applied Mathematics. Academic Press, London, 1983. (Cited on page 109.)